

APPLICATIONS OF THE DA BASED NORMAL FORM ALGORITHM ON
PARAMETER-DEPENDENT PERTURBATIONS

By

Adrian Weisskopf

A THESIS

Submitted
to Michigan State University
in partial fulfillment of the requirements
for the degree of

Physics – Master of Science

2016

ABSTRACT

APPLICATIONS OF THE DA BASED NORMAL FORM ALGORITHM ON PARAMETER-DEPENDENT PERTURBATIONS

By

Adrian Weisskopf

Many advanced models in physics use a simpler system as the foundation upon which problem-specific perturbation terms are added. There are many mathematical methods in perturbation theory which attempt to solve or at least approximate the solution for the advanced model based on the solution of the unperturbed system. The analytical approaches have the advantage that their approximation is an algebraic expression relating all involved quantities in the calculated solution up to a certain order. However, the complexity of the calculation often increases drastically with the number of iterations, variables, and parameters considered. On the other hand, the computer-based numerical approaches are fast once implemented, but their results are only numerical approximations without a symbolic form. A numerical integrator, for example, takes the initial values and integrates the ordinary differential equation up to the requested final state and yields the result as specific numbers. Therefore, no algebraic expression, much less a parameter dependence within the solution is given. The method presented in this work is based on the differential algebra (DA) framework, which was first developed to its current extent by Martin Berz *et. al* [3, 4, 5]. The used DA Normal Form Algorithm is an advancement by Martin Berz from the first arbitrary order algorithm by Forest, Berz, and Irwin [13], which was based on an DA-Lie approach. Both structures are already implemented in COSY INFINITY [18] documented in [7, 16, 17]. The result of the presented method is a numerically calculated algebraic expression of the solution up to an arbitrary truncation order. This method combines the effectiveness and automatic calculation of a computer-based numerical approximation and the algebraic relation between the involved quantities.

ACKNOWLEDGEMENTS

First of all, I would like to thank my academic advisor Professor Martin Berz for his continuous support, patience and helpful guidance in my research.

Furthermore, I particularly appreciated the discussions with David Tarazona, Robert Hipple, Erika Kazantseva, and Ravi Jagasia during my work and would like to thank all of them.

I also shall not forget Scott Pratt, Wade Fisher and Kyoko Makino for being so kind and agreeing to be on my thesis committee.

The last year has been a great experience which was only possible due to the generous scholarship by the Studienstiftung des deutschen Volkes and further financial support by Michigan State University for my studies and research here. I am very thankful for this opportunity and all the great memories that came along with it during the year.

Last but not least, I would like to recognize Kim Crosslan, who was always there if questions or problems of any kind arose.

TABLE OF CONTENTS

LIST OF TABLES	vi
LIST OF FIGURES	viii
CHAPTER 1 INTRODUCTION	1
1.1 Motivation	1
1.2 Basic concepts	4
1.2.1 Floating Point numbers	4
1.2.2 Truncated Polynomial Expansion	6
1.2.3 Differential Algebra	7
1.2.4 Diagonalization	10
1.2.5 Action-Angle coordinates	14
1.2.6 The Flow Operator	16
1.2.6.1 Example of symmetrically perturbed Hamiltonian	17
CHAPTER 2 INTEGRATORS	20
2.1 Flow Integrator	20
2.2 Fourth-Order Runge-Kutta integrator	23
2.3 Fixed point Integrator	24
2.4 Error vs step-size for RK4 integrator	26
2.5 Integrator comparison	29
CHAPTER 3 THE NORMAL FORM ALGORITHM	32
3.1 The DA Normal Form Algorithm	32
3.1.1 Diagonalization	34
3.1.1.1 Diagonalization transformation of the linear part	34
3.1.1.2 Diagonalization transformation of the non-linear parts	36
3.1.2 The non-linear transformation	39
3.1.3 Transformation to Normal Form coordinates	44
CHAPTER 4 PROTRACTING CALCULATIONS IN PERTURBATION THEORY	48
4.1 Variation of parameters	48
4.2 Example of an analytical perturbation theory approach	49
4.2.1 Symmetric perturbed harmonic oscillator example	49
4.2.2 Asymmetric perturbation	55
CHAPTER 5 PERTURBED HARMONIC OSCILLATOR	57
5.1 The Pendulum	57
5.1.1 Introduction to the Problem	57
5.1.2 Unperturbed case	59
5.1.3 Pendulum transformation	62
5.2 Normal Form Uniqueness	69

5.3	Comparison to Lie Transform perturbation Theory	71
5.4	Solving perturbed Harmonic oscillator with perharmosc.fox	79
CHAPTER 6	CONCLUSION	83
APPENDIX	85
BIBLIOGRAPHY	88

LIST OF TABLES

Table 2.1	The table represents the q-component of the transfer map of the initial state from $t = 0$ to t in the Pendulum vector field from equation 5.26 up to the 11 th order. The transfer map was calculated with one step via the three different DA base integrators. The columns with bold order numbers indicate terms of $\mathcal{O}(t^5)$, which are the first error affected terms of the RK4 integrator, which supports the theory discussed in section 2.4. Furthermore, the results of fixed point integration and Flow integration are identical, which also agrees with the theory.	30
Table 2.2	The table shows the p-component equivalent to Table 2.1.	31
Table 5.1	Coefficients of the COSY result up to order 10 in r for the Pendulum tunes $\omega_{l'}(r)$ shown in equation 5.28 with corresponding fraction representation and maximal error in the representation.	65
Table 5.2	Coefficients of the COSY result for the Pendulum Period $T_{l'}(q, p)$ shown in equation 5.33 with corresponding fraction representation and maximal error in the representation.	67
Table 5.3	Coefficients of the COSY result for the tunes $\omega_{l'}(q_1, p_1)$ shown in equation 5.59 with corresponding fraction representation and maximal error in the representation. A table with coefficients to equation 5.59 up to order 10 in (q_1, p_1) are listed in the appendix in table 5.4.	74
Table 5.4	COSY coefficients of $\omega_{l'}(q_1, p_1)$ up to order 14 for the calculation in equation 5.59.	75
Table 5.5	The table reveals the terms and related coefficients of $\omega_{l'}(q', p)$ for the oscillation around the fixed point $(q'_0, p_0) = \left(\sqrt{\frac{3}{2} + \frac{\sqrt{3}}{2}}, 0 \right)$ of the Hamiltonian in equation 5.39 with the parameters $(\omega_0, \varepsilon, a) = (1, 2, 2/9)$ and $q' = q - q_0$	79
Table 5.6	The table illustrates an example output of COSY for the period T in the (q_1, p_1) -coordinates up to 5 th order in (q_1, p_1) . The column 'I' denotes the row-counter. The columns under 'EXPONENTS' each represent one variable. The first two are the (q_1, p_1) -coordinates. Each additional column denotes a parameter d_k, e_l or g_i starting with the parameter associated with the first perturbation term entered to the program. The number in the respective column denotes the exponent of the variable/parameter. The column 'ORDER' sums up all the exponents and presents the total order of the term. The second column 'COEFFICIENT' yields the COSY Taylor expansion coefficient regarding the associated term.	82

Table A.1	COSY coefficients of $r^2(q_1, p_1)$ up to order 10 in (q_1, p_1) for the Pendulum calculation.	86
Table A.2	COSY coefficients of $\omega_{t'}(q_1, p_1)$ up to order 10 in (q_1, p_1) for the Pendulum calculation.	87
Table A.3	COSY coefficients of $\omega_{t'}(q, p)$ up to order 10 in (q, p) for the Pendulum calculation.	87

LIST OF FIGURES

Figure 1.1	The plot shows the classic RK4-tracking of the Pendulum-ODE (eq. 5.4) from the (-1,1)-initial state until $t = \pi/4$. All parameters had to be given specific values and were set to 1.	2
Figure 1.2	The purple area represents a section of the initial state set in phase space $(q_0, p_0) = ([-1.3, 1.3], [-1.3, 1.3])$. The green area denotes the transfer map $\mathcal{M}(q_0, p_0)$ of the initial state set in the Pendulum vector field (eq. 5.4) at time $t = 0.5, 1, 2$ and π , respectively. The DA based RK4 method with a step-size of $h = 0.01$ was used for the integration to algebraically connect the whole initial state set up to order m with the final state. The state set is normally extended over more dimensions which also involves the parameter-space. For the 2D-illustration the parameters are set to 1.	3
Figure 1.3	Illustration of phase space coordinate transformation to Action-Angle coordinates.	15
Figure 2.1	The graph illustrates how the total error of a DA based RK4-integration drops $\sim h^4$ until a certain critical step size is reached. From this step-size onwards, more steps do not result in more precise results since the maximum precision, determined by the floating point calculation errors, is reached. For this example, the critical step-size is approximately $2^{-10}h_0 \approx 10^{-4}h_0$. The error is estimated by calculating the difference of the result from the step-size $2^{-k}h_0$ to the result from the step-size $2^{-12}h_0$, which is considered the 'exact' solution. The difference is then normalized to the respective result of the 2^0h_0 -step-size-calculation. The different plots/colors represent the coefficients of different terms of the $t = 2h_0$ map of the Pendulum ODE (eq. 5.4) after the integration from the $t = h_0$ map using a different number of steps according to the step-size.	27
Figure 2.2	The graph illustrates how the single-step error of a DA based RK4-integration step drops $\sim h^5$ with h being the step-size. The error is estimated by calculating the difference of the result from the step-size $2^{-k}h_0$ to the result from the step-size $2^{-9}h_0$, which is considered the exact solution in this case. The difference is then normalized to the respective result of the $2^{-1}h_0$ -step-size-calculation. The different plots represent the coefficients of different terms of the $t = h_0 + h$ map of the Pendulum ODE (eq. 5.4) after the integration from the $t = h_0$ map using one step of step-size h . The additional factor of 2^5 in the error to 1/step-size ratio originates from normalization with respect to the $2^{-1}h_0$ -step-size-calculation.	28
Figure 5.1	Illustration shows mathematical Pendulum of length l with point mass m in a gravitational field of strength g [10].	58

Figure 5.2	The figure shows the phase space curves of the Pendulum oscillation according to the transfer map at $t' = 1$, which was generated by integrating equation 5.4 with the DA based RK4 in 1000 steps of step-size $h = 0.001$. For the illustration, all parameters were set to 1. The transfer map was tracked for 1000 iterations. The different curves represent the following initial conditions, listed from inner to outer curve: $q = .3, .6, .9, 1.2, \dots, 3.0$; $p = 0$. Details regarding the seemingly closed and fragmented curves can be found in section 5.2.	63
Figure 5.3	The figure shows the phase space curves of the Pendulum oscillation according to the transfer map at $t = 1$, which was generated by integrating equation 5.4 with the DA based RK4 in 1000 steps of step-size $h = 0.001$ with order truncation 20. For the illustration, all parameters are set to 1. The transfer map at $t = 1$ was transformed to Normal form coordinates and tracked for 1000 iterations. The different curves represent the following initial conditions, listed from inner to outer curve: $q = .3, .6, .9, 1.2, \dots, 3.0$; $p = 0$. The curves show circular motion and the separation in the fragmented curves has a constant distance in contrast to figure 5.2. Details regarding this are in section 5.2.	64
Figure 5.4	The graph illustrates the amplitude θ_0 dependence of the relative period-error for different amplitude shifts $\Delta\theta$	68
Figure 5.5	The phase space curves originate from the same map used in figure 5.2. The different curves consist of 'low' period fixed points, which represent the specific resonances of the curve. The distance between the single resonance points illustrates how the frequency changes along the curve.	70
Figure 5.6	The phase space curves originate from the same map used in figure 5.3. The different curves consist of 'low' period fixed points, which represent the specific resonances of the curve. In the Normal Form, the distance between the single resonance points is constant along one curve, which means that the frequency does not change along the curve. The Normal Form coordinates are unique in this property.	70
Figure 5.7	The graph shows the potential $V = \frac{q^2}{2} - \frac{q^4}{2} + \frac{q^6}{9}$ of the Hamiltonian in equation 5.39 for the parameters $(\omega_0, \varepsilon, a) = (1, 2, 2/9)$. There are three stable stationary points at the origin and $q = \pm\sqrt{\frac{3}{2} + \frac{\sqrt{3}}{2}}$. The two unstable stationary points are at $q = \pm\sqrt{\frac{3}{2} - \frac{\sqrt{3}}{2}}$. The potential allows oscillation in each of the three valleys as well as a global oscillation over large p	76

Figure 5.8 The transfer map of the ODE in equation 5.57 was calculated using the RK4 with 100 steps of step-size $h = 0.001$ until $t = 0.1$. The illustration shows the phase space tracking of 1000 iterations using the parameters $(\omega_0, \varepsilon, a) = (1, 2, 2/9)$. The curves around the origin are similar to the one in the Pendulum example in figure 5.2. For larger $|q|$ and small p the phase space curve oscillates around a different fixed point at approximately $(\pm 1.5, 0)$. For large q and p the phase space curve oscillates around all three fixed points. Figure 5.7 makes this behavior apparent. 77

Figure 5.9 Tracking of 1000 iterations using the parameters $(\omega_0, \varepsilon, a) = (1, 2, 2/9)$ of the transfer map used in figure 5.8 in Normal Form. In comparison to figure 5.8 only the curves around the origin are preserved, which illustrates how perturbation theory only works in the direct surrounding of the considered fixed point. 78

Figure 5.10 Tracking picture of the same transfer map used in figure 5.8 only with a shifted reference point for the perturbation. 78

CHAPTER 1

INTRODUCTION

1.1 Motivation

Many detailed models in physics are based on a simpler model - an ideal case - where the exact solution to the problem is known. The mathematical methods of perturbation theory can subsequently be used to approximate the solution to the advanced problem from the exact solution of the ideal case. Examples of realistic systems are the Pendulum oscillation or the energy states of a hydrogen atom in an electric field. Both can be approximated or even solved with perturbation theory due to the established solutions of the ideal cases, namely the simple harmonic oscillator or the unperturbed hydrogen atom, respectively. Methods are constantly being advanced to cope with the variety of perturbed systems that may require specific approaches and methods to be solved effectively. Choosing an approach fundamentally determines the form of the result. An analytical approach yields an algebraic expression, which could involve parameter dependencies, but requires great efforts in the calculation. A computer-based numerical approach, which automatically yields a result, lacks any possibility to relate the result algebraically to parameters or the initial conditions.

This thesis, however, is concerned with a hybrid method of analytical and numerical calculations. It uses a differential algebra (DA) based numerical approximation of solutions to perturbed periodic systems. The DA framework was first developed to its current extent by Martin Berz *et. al* [3, 4, 5]. It allows for the algebraic structure to be stored in so-called DA vectors which are used as the elements of the numerical calculation. The approach consists of three main steps. First, the ordinary differential equation (ODE) as a result of Hamilton equations is transformed to coordinates which make them suitable for the third step. The ODE is then integrated, in the second step, to create a transfer map. Due to the DA framework this map relates the final state to the initial state and ODE inherent parameters algebraically. In the last step, the transfer map is transformed

to 'Normal Form' coordinates. In Normal Form coordinates the map represents circular motion in phase space with only amplitude dependent frequencies. These frequencies are the key quantities to determine the behavior of periodic systems. For this step the DA Normal Form Algorithm [6] is used, which is an advancement by Martin Berz from the first arbitrary order algorithm that was based on an DA-Lie approach by Forest, Berz, and Irwin [13]. The whole method is implemented in COSY INFINITY [18], which is already equipped with the DA framework and the DA Normal Form Algorithm documented in [7, 16, 17].

The great advantage of this method is that it combines analytical and numerical calculations and is not limited to the order to which the calculations can be done. The computer-based DA calculation allows the manipulation of polynomial transfer maps up to the floating point accuracy of the computer. Therefore it is precise and effective at the same time. To introduce the advantage of the DA based calculation, the result of a fourth-order Runge-Kutta (RK4) shall be presented in the original and the DA based configuration. In the classic calculation (fig. 1.1) the solution is traced from the initial state along the vector field of the ODE.

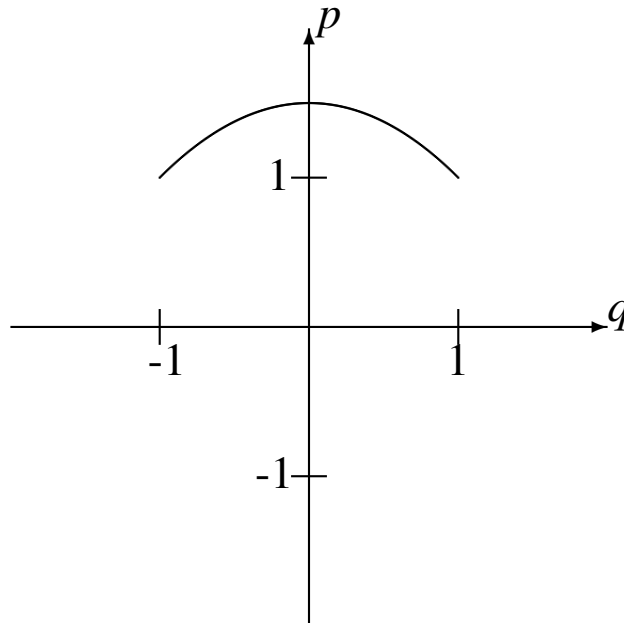


Figure 1.1 The plot shows the classic RK4-tracking of the Pendulum-ODE (eq. 5.4) from the $(-1,1)$ -initial state until $t = \pi/4$. All parameters had to be given specific values and were set to 1.

In the DA based version (fig. 1.2) the whole initial state set \vec{z}_{ini} in the vector field is represented by the map \mathcal{M}_{ini} in the form of $\vec{z}_{ini} = \mathcal{M}_{ini} = (q, p)$ and then integrated with respect to time. The resulting transfer map $\mathcal{M}(q, p) = \vec{z}_f$ relates the initial state set \vec{z}_{ini} to its final state \vec{z}_f including vector field inherent parameters. The two dimensional state space in figure 1.2 representing q and p coordinate, could even be expanded by further dimension for the involved parameters.

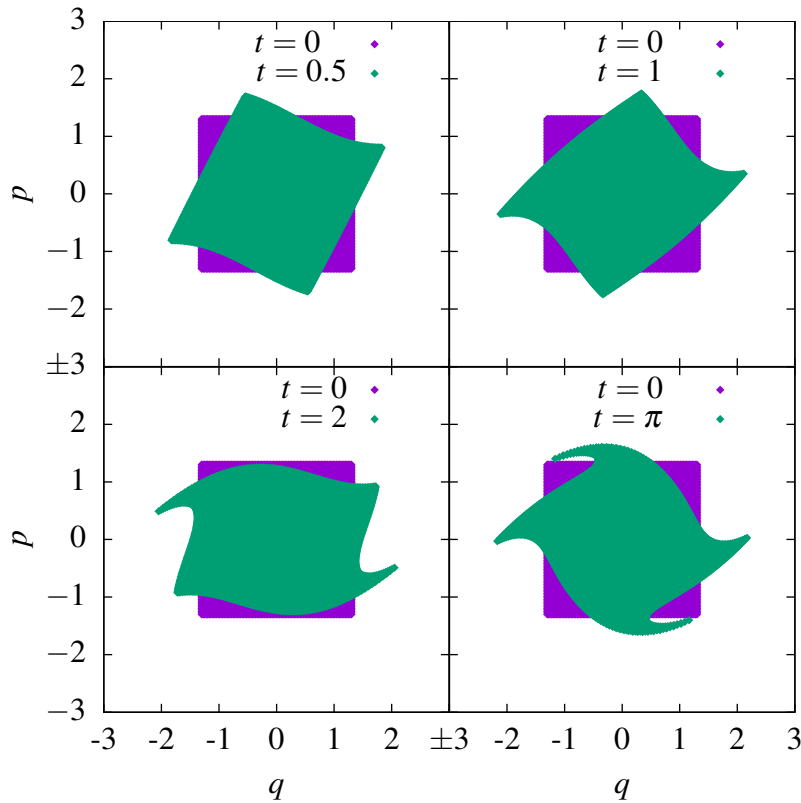


Figure 1.2 The purple area represents a section of the initial state set in phase space $(q_0, p_0) = ([-1.3, 1.3], [-1.3, 1.3])$. The green area denotes the transfer map $\mathcal{M}(q_0, p_0)$ of the initial state set in the Pendulum vector field (eq. 5.4) at time $t = 0.5, 1, 2$ and π , respectively. The DA based RK4 method with a step-size of $h = 0.01$ was used for the integration to algebraically connect the whole initial state set up to order m with the final state. The state set is normally extended over more dimensions which also involves the parameter-space. For the 2D-illustration the parameters are set to 1.

1.2 Basic concepts

The following section introduces essential concepts which are used in this thesis and are indispensable to understanding certain steps or arguments later on. First of all, the issues of approximating potentially infinitely long real numbers in the floating point representation to make them suitable for the computer-based calculations are presented. Before giving a brief introduction to the DA framework, the approximation of analytical functions using Truncated Polynomial Series is discussed. The main process of diagonalization which is important for the decoupling of the linear parts of the transfer maps later on is then presented. A strong focus is on the calculation of the two dimensional case using the Twiss parameters [12]. Subsequently, the key characteristics of Action-Angle coordinates are summarized and related to the Normal Form coordinates. Lastly, the Flow Operator and its way of time-expanding observables are introduced.

1.2.1 Floating Point numbers

Floating point numbers (\mathbb{F}) are used in science to approximate real numbers (\mathbb{R}) to their significant part up to a certain precision. A real number can potentially require an infinite amount of digits to be represented, depending on the base of the numeral system used. The floating point representation uses the most significant¹ digits and scales them by an exponent to the appropriate range. In most cases, including the IEEE 754 standard [21] which will be discussed in more detail below, a fixed base is used and the significand and the exponent are adjusted to approximate the number:

$$\pm \text{significand} \times \text{base}^{\text{exponent}}. \quad (1.1)$$

In contrast to the fixed point number representation, the point can flow between the decimal places, due to appropriate adjustment of the exponent. Therefore, the floating point representation has the advantage of a range based precision. While the 'scientific notation' of floating point numbers uses a base₁₀ representation, computing, in contrast to that, uses a base₂ representation due to the binary system.

¹most significant: all digits allowed by the current precision of the floating point representation.

It might not be obvious at first glance, but there are various ways to define operations on floating point numbers, especially concerning the rounding. Let \oplus, \ominus, \odot and \oslash be the operations on \mathbb{F} corresponding to $+, -, \cdot$ and $/$ in \mathbb{R} . The following example shows the evaluation of $\left(\frac{1}{x+2}\right)^2$ at $x = 4$ in \mathbb{R} and \mathbb{F} with 3 significant decimal digits (precision $p = 3$) in base₁₀, while rounding half up after each calculation in \mathbb{F} :

$$\begin{array}{rcccccc}
 \mathbb{R} : & 4 & \xrightarrow{x_0+2} & 6 & \xrightarrow{1/x_1} & \frac{1}{6} & \xrightarrow{x_2^2} & \frac{1}{36} \\
 & = & & = & & \approx & & \approx \\
 \mathbb{F}_3 : & 4 & \xrightarrow{x_0\oplus 2} & 6 & \xrightarrow{1\oslash x_1} & 0.167 & \xrightarrow{x_2\odot x_2} & 0.279 \times 10^{-3}
 \end{array} \tag{1.2}$$

Note that $\mathbb{F}_3\left(\frac{1}{36}\right) = 0.278 \times 10^{-3} \neq 0.279 \times 10^{-3}$, which shows the main problem of operations on floating point numbers. Not only does the error of the initial approximation of the real numbers occur, but those errors also tend to grow due to operations. To keep them as small as possible and to make results comparable between computations on different machines, the IEEE 754 standard [21] was introduced. It defines the floating point number representation and arithmetic, which ensures that all machines produce the same output for the same floating point operations. It also defines another operation, which can be a source of additional errors - the base-conversion. While the computer calculates in base₂, the result is given in a base₁₀-expression most of the time.

To state which digits of the \mathbb{F} -calculation-result are actually significant, the study of the propagation of those errors is critically important. Calculations, proofs and other important information on floating-point arithmetic can be found in [14]. COSY INFINITY, the computation program used in this thesis, adopts the double precision representation, which is a 64-bit (1-bit sign + 11-bit exponent + 52-bit significand) system, yielding a precision of ~ 14 significant decimal digits. Most results of calculations within this work, are accurate up to 10^{-14} , depending on the complexity of the previous calculation and the associated rounding error propagation.

1.2.2 Truncated Polynomial Expansion

Similar to the way floating point numbers approximate a potentially infinitely long real number to its significant digits, truncated polynomials can approximate a Taylor polynomial expansion of an analytical function f at \vec{a} up to the significant order m_{max} :

$$\vec{f}(\vec{a} + \vec{h}) = \sum_{n=0}^{\infty} \frac{[(\vec{h}\vec{\nabla}_{\vec{x}})^n \vec{f}(\vec{x})]_{\vec{x}=\vec{a}}}{n!} \approx \sum_{i=0}^{m_{max}} \frac{[(\vec{h}\vec{\nabla}_{\vec{x}})^n \vec{f}(\vec{x})]_{\vec{x}=\vec{a}}}{n!}. \quad (1.3)$$

Consider the following three analytical functions $f_i \in C^\infty(\mathbb{R})$:

$$f_1(x) = \exp(x) \quad f_2(x) = 2 + \sin(x) - \cos(x) + \frac{x^3}{3} \quad f_3(x) = 1 + x + \frac{x^2}{2} + \frac{x^3}{6}. \quad (1.4)$$

The approximation of those functions with truncated Taylor expansions around $x = 0$ up to 3rd order can all be represented by the same function f_3 :

$$\mathcal{T}_{f_1}(x) =_3 \mathcal{T}_{f_2}(x) =_3 \mathcal{T}_{f_3}(x) = 1 + x + \frac{x^2}{2} + \frac{x^3}{6} = f_3(x). \quad (1.5)$$

The following definition of the equivalence classes and its properties is according to the definition in [6, p.91]. The notation ' $=_m$ ' indicates that the expressions on both sides are equivalent up to order m . In general, this means that the equivalence relation $f =_m g$ between two functions $f, g \in C^\infty(\mathbb{R}^v)$, is given when $f(\vec{0}) = g(\vec{0})$ and $\partial_i^k f(\vec{x})|_{\vec{x}=\vec{0}} = \partial_i^k g(\vec{x})|_{\vec{x}=\vec{0}}$ for all $0 \leq i \leq v$ and all $k \leq m$. This allows for the definition of an equivalence class $[f]_m$ that represents all elements f of the vector space of infinitely differential functions $C^\infty(\mathbb{R}^v)$ with v real variables that have identical derivatives at the origin up to order m . The point zero is chosen out of convenience and without loss of generality, meaning that any other point may be selected as well. Since \mathcal{T}_f , the truncated Taylor expansion of f is always equivalent to f itself up to order m , this small theorem is apparent

$$[f]_m = [\mathcal{T}_f]_m \quad (1.6)$$

where \mathcal{T}_f is the expansion at 0. \mathcal{T}_f can be used as the equivalence class representative. Hence, relation 1.5 can be summarized to: $f_1, f_2 \in [f_3]_3 = \left[1 + x + \frac{x^2}{2} + \frac{x^3}{6}\right]$. All equivalence classes $[]_n$ are denoted as $_n D_v$ [6] where v represents the number of variables. To make $_n D_v$ a differential algebra it requires the definition of certain operations which will be introduced in the next section.

1.2.3 Differential Algebra

The following brief overview of the DA definitions and arithmetic largely draws from [6], where Berz summarizes the DA framework and its techniques from his earlier work [3, 4, 5]; please refer to those references for further information. $_mD_v$ denotes the DA for v variables and differentiation up to m^{th} order. To introduce the DA framework, Berz illustrates the simplest case $_1D_1$ in [6]. Similar to complex numbers which have a real and imaginary basis with $i = (0, 1)_{\mathbb{C}}$, the $_1D_1$ can be represented in a constant and differential basis with the differential unit $d \stackrel{def}{=} (0, 1)$ [6]. While the square property of the imaginary unit is known to be $i^2 = (0, 1)_{\mathbb{C}} \cdot (0, 1)_{\mathbb{C}} = (-1, 0)_{\mathbb{C}}$ the square of the differential unit d has the special property of vanishing with $d^2 = (0, 1) \cdot (0, 1) = (0, 0)$ [6].

In the following part the $_2D_1$ shall be discussed, where the operations that form the algebra with the tuples (x_0, x_1, x_2) can be defined as follows:

$$(x_0, x_1, x_2) + (y_0, y_1, y_2) = (x_0 + y_0, x_1 + y_1, x_2 + y_2) \quad (1.7)$$

$$c \cdot (x_0, x_1, x_2) = (c \cdot x_0, c \cdot x_1, c \cdot x_2) \quad (1.8)$$

$$(x_0, x_1, x_2) \cdot (y_0, y_1, y_2) = (x_0 \cdot y_0, x_0 \cdot y_1 + x_1 \cdot y_0, x_0 \cdot y_2 + x_1 \cdot y_1 + x_2 \cdot y_0). \quad (1.9)$$

Similar to above we can calculate d^2 in $_2D_1$:

$$d^2 = (0, 1, 0) \cdot (0, 1, 0) = (0, 0, 1). \quad (1.10)$$

Therefore, any tuple can be represented by

$$(x_0, x_1, x_2) = x_0 + x_1 \cdot d + x_2 \cdot d^2. \quad (1.11)$$

Just like in $_1D_1$, the operations allow the definition of a total order that is compatible with its algebraic operations [6]. From the order, the name for d being infinitesimal or differential becomes apparent, since it is smaller than any real number

$$0 = (0, 0, 0) = d^3 < (0, 0, 1) = d^2 < (0, 1, 0) = d < (x_0, 0) = x_0. \quad (1.12)$$

In fact, d it is in general so small that the $(m-1)^{th}$ power of d in $_mD_v$ vanishes which is also called the nilpotent element of $_mD_v$. The three operations and the tuples of real numbers form a ring

algebra, but not a field, since there is not a multiplicative inverse in ${}_2D_1$ for every $(x_0, x_1, x_2) \in {}_2D_1$. As a matter of fact, only tuples (x_0, x_1, x_2) with $x_0 \neq 0$ have a multiplicative inverse $(y_0, y_1, y_2) \in {}_2D_1$ with

$$\begin{aligned} (x_0, x_1, x_2) \cdot (y_0, y_1, y_2) &\stackrel{(1.9)}{=} (x_0 \cdot y_0, x_0 \cdot y_1 + x_1 \cdot y_0, x_0 \cdot y_2 + x_1 \cdot y_1 + x_2 \cdot y_0) \stackrel{!}{=} (1, 0, 0) \\ \Rightarrow y_0 &= \frac{1}{x_0} & y_1 &= \frac{-x_1}{x_0^2} & y_2 &= \frac{x_1^2}{x_0^3} - \frac{x_2}{x_0^2}. \end{aligned} \quad (1.13)$$

Introducing the endomorphism (structure-preserving map from ${}_2D_1$ into itself) called derivation ∂ , makes $({}_2D_1, \partial)$ a differential algebra.

$$\partial : {}_2D_1 \rightarrow {}_2D_1 \quad (1.14)$$

$$(x_0, x_1, x_2) \mapsto \partial(x_0, x_1, x_2) = (0, x_1, 2x_2). \quad (1.15)$$

The operations behave as follows under the derivation map for $u_1, u_2 \in {}_2D_1$:

$$\partial(u_1 + u_2) = \partial u_1 + \partial u_2 \quad (1.16)$$

$$\partial(c \cdot u_1) = c \cdot \partial u_1 \quad (1.17)$$

$$\partial(u_1 \cdot u_2) = (\partial u_1) \cdot u_2 + u_1 \cdot (\partial u_2). \quad (1.18)$$

While equation 1.16 and 1.17 are rather trivial, equation 1.18 requires a small derivation:

$$\begin{aligned} (\partial u_1) \cdot u_2 + u_1 \cdot (\partial u_2) &= (0, x_1, 2x_2) \cdot (y_0, y_1, y_2) + (x_0, x_1, x_2) \cdot (0, y_1, 2y_2) \\ &= (0, x_1 \cdot y_0, x_1 \cdot y_1 + 2x_2 \cdot y_0) + (0, x_0 \cdot y_1, x_0 \cdot 2y_2 + x_1 \cdot y_1) \\ &= (0, x_0 \cdot y_1 + x_1 \cdot y_0, 2(x_0 \cdot y_2 + x_1 \cdot y_1 + x_2 \cdot y_0)) \\ &= \partial(u_1 \cdot u_2). \end{aligned} \quad (1.19)$$

According to [6] the DA arithmetic can generally be expanded to the equivalence classes $[f]_n$ which are denoted by ${}_nD_v$, with $d_i = [x_i] \quad \forall i \leq v$ and the following operations:

$$[f]_n + [g]_n = [f + g]_n \quad (1.20)$$

$$c \cdot [f]_n = [c \cdot f]_n \quad (1.21)$$

$$[f]_n \cdot [g]_n = [f \cdot g]_n \quad (1.22)$$

which define the algebra on ${}_nD_V$ and are equivalent to the operations on $C^\infty(\mathbb{R}^V)$ up to order m .
Introducing the endomorphism derivation ∂ :

$$\partial_V[f]_n = [x_V \partial_V f]_n \quad (1.23)$$

makes it a differential algebra, since the following small theorem is generally also satisfied similar to the derivation in equation 1.19

$$\partial_V([f]_n \cdot [g]_n) = [f]_n \cdot \partial_V[g]_n + [g]_n \cdot \partial_V[f]_n. \quad (1.24)$$

Operations like the division are only defined if the divisor $[f]_m$ has a non-zero constant part which is due to the fact that ${}_nD_V$ is only a ring and not a field (see above). The composition of two functions or maps $f, g \in {}_nD_V$

$$[f([g]_n)]_n = [f(g)]_n \quad (1.25)$$

is only possible if g has no constant part [2].

In general $[f]_n$ can be defined by its truncated Taylor expansion as follows [6, 2.42+43]:

$$[f]_n = \sum_{\sum_{i=1}^V k_i \leq n} a_{k_1, \dots, k_V} \cdot d_1^{k_1} \cdot \dots \cdot d_V^{k_V} \quad (1.26)$$

$$\text{with } a_{k_1, \dots, k_V} = \frac{1}{\prod_{j=1}^V k_j!} \frac{\partial^{\sum_{i=1}^V k_i} f}{\prod_{j=1}^V \partial x_j^{k_j}}. \quad (1.27)$$

Hence, a_{k_1, \dots, k_V} represents the Taylor expansion coefficients of f and $d_1^{k_1} \cdot \dots \cdot d_V^{k_V}$ may be used as the basis of a DA vector, which stores the coefficients accordingly. In this way it is possible to approximate any $f \in C^\infty(\mathbb{R}^V)$ by a truncated polynomial series which is then represented with its Taylor expansion coefficients a_{k_1, \dots, k_V} up to order m in a DA vector. The implementation and specific operations of the DA vectors in COSY INFINITY based on the framework above are explained in [18, 6, 5].

1.2.4 Diagonalization

The goal of diagonalization is to transform a matrix \hat{L} to its diagonal form. The diagonal form has entries only on the diagonal and therefore requires \hat{L} to be a quadratic matrix. Furthermore, not every quadratic $n \times n$ matrix can be diagonalized, but only matrices that are **similar** to a diagonal matrix $\hat{\Lambda}$.

Two matrices \hat{A} and \hat{B} are **similar** if and only if (following: *iff*) there exists a similarity transformation matrix \hat{T} and its inverse \hat{T}^{-1} , such that $\hat{B} = \hat{T}\hat{A}\hat{T}^{-1}$.

An $n \times n$ matrix \hat{T} has an inverse \hat{T}^{-1} with $\hat{T}^{-1}\hat{T} = \hat{T}\hat{T}^{-1} = \mathcal{I}$, where \mathcal{I} is the identity *iff* all columns of \hat{T} are linearly independent. To find those matching linearly independent component-vectors, the eigenvectors and eigenvalues of \hat{L} are relevant. The eigenvalues λ_i and the corresponding eigenvectors \vec{v}_i of a quadratic $n \times n$ matrix \hat{L} are determined by the eigenvalue equation: $\hat{L}\vec{v}_i = \lambda_i\vec{v}_i$. To solve the eigenvalue equation, only the nontrivial solutions of the eigenvalue problem $(\hat{L} - \lambda_i\mathcal{I})\vec{v}_i = \vec{0}$ are of interest. In this case, nontrivial solutions are any $\vec{v}_i \neq \vec{0}$. Therefore, solving

$$\text{Det}(\hat{L} - \lambda\mathcal{I}) = 0 \quad (1.28)$$

yields the nontrivial solutions of the eigenvalue problem. The characteristic polynomial $p(\lambda)$ of an $n \times n$ matrix \hat{L} is introduced in this context. It is the determinant of the eigenvalue problem matrix and is therefore related to its eigenvalues λ_i as follows:

$$p_{\hat{L}}(\lambda) = \text{Det}(\hat{L} - \lambda\mathcal{I}) = \prod_{i=1}^n (\lambda - \lambda_i). \quad (1.29)$$

The important property of the characteristic polynomial of a matrix \hat{L} in the context of diagonalization is that it has the same roots and has therefore the same eigenvalues λ_i as the corresponding eigenvectors \vec{v}_i , as the characteristic polynomials of all matrices **similar** to \hat{L} . This property can be shown in this short proof:

$$\lambda_i \left(\hat{T}^{-1} \vec{v}_i^B \right) = \hat{T}^{-1} \lambda_i \vec{v}_i^B = \hat{T}^{-1} \hat{B} \vec{v}_i^B = \hat{T}^{-1} \hat{T} \hat{A} \hat{T}^{-1} \vec{v}_i^B = \hat{A} \left(\hat{T}^{-1} \vec{v}_i^B \right) \quad (1.30)$$

which shows that $\hat{T}^{-1}\vec{v}_i^B = \vec{v}_i^A$ with eigenvalue λ_i . $\hat{T}\vec{v}_i^A = \vec{v}_i^B$ and \hat{T} is the transformation matrix between the two similar matrices \hat{A} and \hat{B} . Finally, an $n \times n$ matrix \hat{L} with eigenvalues λ_i is diagonalizable *iff* all n corresponding eigenvectors \vec{v}_i^L are linearly independent. The following proof of this theorem will also reveal the transformation matrix \hat{T} for the diagonalization:

Define $\hat{T}^{-1} = (\vec{v}_1^L, \vec{v}_2^L, \dots, \vec{v}_n^L)$ and $\hat{\Lambda}$ a diagonal matrix with entry $\Lambda_{ii} = \lambda_i$. Now,

$$L\hat{T}^{-1} = \hat{A} \begin{pmatrix} \vec{v}_1^L \\ \vec{v}_2^L \\ \dots \\ \vec{v}_n^L \end{pmatrix} = \begin{pmatrix} \hat{L}\vec{v}_1^L \\ \hat{L}\vec{v}_2^L \\ \dots \\ \hat{L}\vec{v}_n^L \end{pmatrix} = \begin{pmatrix} \lambda_1\vec{v}_1^L \\ \lambda_2\vec{v}_2^L \\ \dots \\ \lambda_n\vec{v}_n^L \end{pmatrix} = \hat{T}^{-1}\hat{\Lambda} \quad (1.31)$$

iff all eigenvectors \vec{v}_i^L are linearly independent, then there is a matrix \hat{T} , which is inverse to \hat{T}^{-1} and thus

$$\hat{T}\hat{A}\hat{T}^{-1} = \hat{\Lambda}. \quad (1.32)$$

In this thesis, 2×2 matrices are a key element since matrices of higher dimensions of the form $2\nu \times 2\nu$ can be simplified to a diagonal block matrix, which has 2×2 -submatrices on its diagonal. For this reason, the 2-dimensional case shall be investigated in more detail. The following diagonalizable real 2×2 matrix \hat{L} is considered:

$$\hat{L} = \begin{pmatrix} a & b \\ c & d \end{pmatrix}. \quad (1.33)$$

According to equation 1.29 the characteristic polynomial is given by

$$\text{Det} \begin{pmatrix} a - \lambda & b \\ c & d - \lambda \end{pmatrix} = (a - \lambda)(d - \lambda) - cb = \lambda^2 - \text{Tr}(\hat{L})\lambda + \text{Det}(\hat{L}) = 0. \quad (1.34)$$

The eigenvalues can be obtained by solving the quadratic equation from above:

$$\lambda^\pm = \frac{\text{Tr}(\hat{L})}{2} \pm \sqrt{\underbrace{\frac{\text{Tr}(\hat{L})^2}{4} - \text{Det}(\hat{L})}_{\delta}}. \quad (1.35)$$

Depending on the discriminant δ , the eigenvalues are either real, complex, or degenerate. For $\delta > 0$ the eigenvalues are real, as well as their corresponding eigenvectors. For $\delta = 0$ the eigenvalues will be real and degenerate $\lambda^\pm = \frac{Tr(\hat{\mathcal{L}})}{2}$. The interesting case is $\delta < 0$ where the eigenvalues and the corresponding eigenvectors are complex conjugate pairs. It is useful to write the eigenvalues in the $re^{\pm i\mu}$ -notation, where magnitude r and phase μ can be derived from the real and imaginary part of the eigenvalue pair as follows:

$$\Re(\lambda^\pm) = \frac{Tr(\hat{\mathcal{L}})}{2} \quad \Im(\lambda^\pm) = \pm \sqrt{Det(\hat{\mathcal{L}}) - \frac{Tr(\hat{\mathcal{L}})^2}{4}} \quad (1.36)$$

$$r = \sqrt{\Re(\lambda^\pm)^2 + \Im(\lambda^\pm)^2} = \sqrt{Det(\hat{\mathcal{L}})} \quad (1.37)$$

$$\mu = \arccos\left(\frac{\Re(\lambda^\pm)}{r}\right) = \arccos\left(\frac{Tr(\hat{\mathcal{L}})}{2\sqrt{Det(\hat{\mathcal{L}})}}\right). \quad (1.38)$$

Since the arccos-function is symmetric, with $\arccos(x) = -\arccos(x)$, the sign of μ must be defined.

A common definition [6] is using $\text{sign}(b)$, which results in

$$\mu = \text{sign}(b) \arccos\left(\frac{Tr(\hat{\mathcal{L}})}{2\sqrt{Det(\hat{\mathcal{L}})}}\right). \quad (1.39)$$

Courant and Snyder introduced the Twiss parameters [12], which are a set of parameters concerning 2×2 matrices with complex conjugate eigenvectors. Considering the matrix $\hat{\mathcal{L}}$ from equation 1.33, the Twiss parameters are defined as follows [12]:

$$\alpha = \frac{a-d}{2r \sin \mu} \quad (1.40)$$

$$\beta = \frac{b}{r \sin \mu} \quad (1.41)$$

$$\gamma = \frac{-c}{r \sin \mu}. \quad (1.42)$$

Note that the sign definition of μ using b assures that β is always positive. The Twiss parameters

are not independent of each other, but satisfy

$$\begin{aligned}
\beta\gamma - \alpha^2 &= \frac{-4bc + (a-d)^2}{4r^2 \sin^2 \mu} \\
&= \frac{4(ad - bc) + (a+d)^2}{4\mathbb{I}m^2(\lambda^\pm)} \\
&= \frac{4\text{Det}(\hat{\mathcal{L}}) - \text{Tr}^2(\hat{\mathcal{L}})}{4\text{Det}(\hat{\mathcal{L}}) - \text{Tr}^2(\hat{\mathcal{L}})} = 1.
\end{aligned} \tag{1.43}$$

Rewriting $\hat{\mathcal{L}}$ in terms of the Twiss parameters yields

$$\hat{\mathcal{L}} = r \begin{pmatrix} \cos \mu + \alpha \sin \mu & \beta \sin \mu \\ -\gamma \sin \mu & \cos \mu - \alpha \sin \mu \end{pmatrix}. \tag{1.44}$$

The eigenvectors \vec{v}^\pm to the eigenvalue $\lambda^\pm = \exp(\pm i\mu)$ are therefore given as follows:

$$\begin{aligned}
&\left(\begin{pmatrix} \cos \mu + \alpha \sin \mu & \beta \sin \mu \\ -\gamma \sin \mu & \cos \mu - \alpha \sin \mu \end{pmatrix} - \begin{pmatrix} e^{\pm i\mu} & 0 \\ 0 & e^{\pm i\mu} \end{pmatrix} \right) \begin{pmatrix} x \\ y \end{pmatrix} = \begin{pmatrix} 0 \\ 0 \end{pmatrix} \\
&\begin{pmatrix} x(\alpha \pm i) \sin \mu + y\beta \sin \mu \\ -x\gamma \sin \mu + y(-\alpha \pm i) \sin \mu \end{pmatrix} = \begin{pmatrix} x(\alpha \pm i) + y\beta \\ -x\gamma + y(-\alpha \pm i) \end{pmatrix} = \begin{pmatrix} 0 \\ 0 \end{pmatrix}
\end{aligned} \tag{1.45}$$

where $\exp(\pm i\mu) = \cos \mu \pm i \sin \mu$. Equation 1.45 is satisfied for $x = -\beta$ and the corresponding $y = \alpha \pm i$, which compose the complex conjugate eigenvector pair

$$\vec{v}^\pm = \begin{pmatrix} -\beta \\ \alpha \pm i \end{pmatrix}. \tag{1.46}$$

In the case of $b = 0$ and therefore $\beta = 0$, an equivalent complex conjugated eigenvector pair can be derived to

$$\vec{v}^\pm = \begin{pmatrix} -\alpha \pm i \\ \gamma \end{pmatrix} \tag{1.47}$$

using equation 1.45 with $y = \gamma$ and $x = -\alpha \pm i$. For the trivial case where $\beta = 0 \wedge \gamma = 0$, the original matrix is already in diagonal form and no transformation is required.

In general, the eigenvectors can be scaled by a complex number k . However, to preserve the complex conjugate property of the eigenvector pairs, the vectors will only be scaled by real numbers in this work. The matrix \hat{L} can then be diagonalized to $\hat{\Lambda}$ with the transformation matrix $\hat{T}^{-1} = k(\vec{v}^+, \vec{v}^-)$ and its inverse, which are given in detail as follows:

$$\hat{\Lambda} = r \begin{pmatrix} e^{i\mu} & 0 \\ 0 & e^{-i\mu} \end{pmatrix} = \hat{T} \hat{L} \hat{T}^{-1} \quad (1.48)$$

$$\hat{T}^{-1} = k \begin{pmatrix} -\beta & -\beta \\ \alpha + i & \alpha - i \end{pmatrix} \quad (1.49)$$

$$\hat{T} = \frac{1}{\text{Det}(\hat{T}^{-1})} \begin{pmatrix} \alpha - i & \beta \\ -\alpha - i & -\beta \end{pmatrix} \quad (1.50)$$

where k is an additional scaling factor which can be used to scale the matrix, such that the magnitude of the determinate of the transformation matrix is 1. This scaling is essential for the transformation of nonlinear terms, since it ensures a scaling-neutral transformation.

1.2.5 Action-Angle coordinates

Action-Angle variables are a special set of phase space coordinates (J, θ) , which define a momentum J called action that is constant and unique for each phase space curve. Each point on the phase space curve is associated with the coordinate θ called action angle. Any Hamiltonian that can be canonically transformed to those coordinates is called integrable. In the case of a one degree of freedom problem, the new Hamiltonian K in the new phase space coordinate system then only

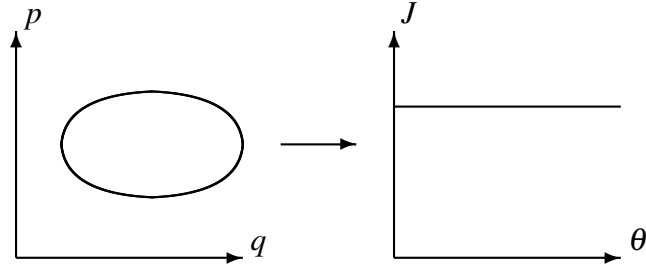


Figure 1.3 Illustration of phase space coordinate transformation to Action-Angle coordinates.

depends upon the new momentum J (fig. 1.3). Thus, the Hamilton equations yield

$$\dot{J} = -\frac{\partial K}{\partial \theta} = 0 \quad (1.51)$$

$$\dot{\theta} = \frac{\partial K}{\partial J} = \omega(J) = \text{const.} \quad (1.52)$$

Having K as a function of J alone assures that the action J is constant following the Hamilton equation 1.51 for each phase space curve. Hence, $\dot{\theta} = \omega$ from equation 1.52 is also constant and therefore $\theta(t) = \theta(0) + \omega(J)t$. Action-angle coordinates are mainly used when the Hamiltonian of the system is not explicitly time-dependent, which results in the conservation of H . The generalized momentum, which resembles the action for each original generalized coordinate can then be defined as:

$$J(E_0) = \frac{1}{2\pi} \oint p(E_0, q) dq \quad (1.53)$$

where the 2π is conventional depending on whether ω (frequency for norm period = 2π) or ν (frequency for norm period = 1) is used. J is hence the phase space area swept out in one period/ 2π .

In general, it does not follow that if H and (p, q) satisfy the Hamilton equation, the new phase space coordinates (J, θ) and the new Hamiltonian K will too. This is only the case if the transformation is canonical, which means there must be a generating function of the second type $F_2(q, J) = S(q, J)$ of old coordinate q and new momentum J . This function is then a solution of the Hamilton-Jacobi equation [1]

$$K(J) = \left[q, \frac{\partial S(q, J)}{\partial q} \right] \quad (1.54)$$

which yields the following relations:

$$p = \frac{\partial S}{\partial q} \text{ and } \theta = \frac{\partial S}{\partial J}. \quad (1.55)$$

The exact derivation and further information on canonical transformations can be found in [22, 1]. The concept of Action-Angle variables (J, θ) resembles the basic idea of the Normal Form coordinates (t^+, t^-) in 2D which are later introduced in detail. Both systems possess a constant of the phase space curve of the system: $J \sim r^2 = (t^+)^2 + (t^-)^2$ and the frequency is only dependent on that constant of the curve $\omega(J) \sim \omega(r^2)$.

1.2.6 The Flow Operator

Since this work deals with coupled first order differential equations, it is useful to discuss possible methods to investigate the time evolution of a certain observable $\mathcal{O}(\vec{r}, t)$ of a system. It is assumed that the first time derivatives $\dot{\vec{r}}$ of the system's coordinates are given by the function $\vec{f}(\vec{r}, t)$. The first time derivative of the observable \mathcal{O} is therefore:

$$\frac{d}{dt} \mathcal{O}(\vec{r}, t) = \frac{\partial \mathcal{O}}{\partial t} + \frac{d\vec{r}}{dt} \frac{d\mathcal{O}}{d\vec{r}} = \left(\partial_t + \vec{f} \cdot \vec{\nabla} \right) \mathcal{O} = L_{\vec{f}} \mathcal{O}(\vec{r}, t) \quad (1.56)$$

Applying the Flow Operator $L_{\vec{f}} = \partial_t + \sum_{i=1}^n \dot{r}_i \partial_i$ is equivalent to taking the first time derivative [6]. $L_{\vec{f}}$ is also referred to as the derivative operator [19] and represents the vector field of \vec{f} .

For the time evolution, the Taylor expansion of $\mathcal{O}_{t_0}(\vec{r}, t)$ at $t_0 = 0$ is considered [2]:

$$\mathcal{O}(\vec{r}, t) = \sum_{n=0}^{\infty} \frac{t^n}{n!} \left(\frac{d^n}{dt^n} \mathcal{O} \right) (\vec{r}, 0) = \sum_{n=0}^{\infty} \frac{t^n}{n!} \left(L_{\vec{f}}^n \mathcal{O} \right) (\vec{r}, 0) = \exp \left(t L_{\vec{f}} \right) \mathcal{O}(\vec{r}, 0) \quad (1.57)$$

For a one-dimensional Hamiltonian system $H(q, p, t)$, the function $\vec{f}(\vec{r}, t)$ can be derived from the Hamilton equations:

$$\vec{f}(\vec{r}, t) = \dot{\vec{r}} = \begin{pmatrix} \dot{q} \\ \dot{p} \end{pmatrix} = \begin{pmatrix} \frac{\partial H}{\partial p} \\ -\frac{\partial H}{\partial q} \end{pmatrix} \quad (1.58)$$

The Flow Operator can then be written as:

$$L_{\vec{f}} = \left(\partial_t + \vec{f} \cdot \vec{\nabla} \right) = \left(\partial_t + \dot{q} \partial_q + \dot{p} \partial_p \right) = \left(\partial_t + \frac{\partial H}{\partial p} \partial_q - \frac{\partial H}{\partial q} \partial_p \right) \quad (1.59)$$

This work only deals with the time evolution of the trivial observable $\vec{r} = \mathcal{I}$ in an autonomous and origin preserving system, which yields the following first terms relevant for the expansion:

$$L_{\vec{f}}^0 \vec{r} = \vec{r} \quad L_{\vec{f}}^1 \vec{r} = \vec{f} \quad L_{\vec{f}}^2 \vec{r} = L_{\vec{f}}^1 \vec{f}. \quad (1.60)$$

The time expansion at t_0 is therefore given as follows:

$$\vec{r}_{t_0}(t) = \exp \left((t - t_0) L_{\vec{f}_{t_0}} \right) \mathcal{I} \quad (1.61)$$

1.2.6.1 Example of symmetrically perturbed Hamiltonian

In the example of the symmetrically perturbed Hamiltonian, the time evolution shall be examined using the Flow Operator. The following Hamiltonian is considered:

$$H = \frac{p^2}{2} + \frac{q^2}{2} + \frac{\alpha}{4} (p^2 + q^2)^2 \quad (1.62)$$

For the time evolution of \vec{r} , the vector field consisting of the first time derivative $\dot{\vec{r}}$ is needed, which can be derived from the Hamilton equations:

$$\dot{\vec{r}} = \begin{pmatrix} \dot{q} \\ \dot{p} \end{pmatrix} = \begin{pmatrix} p(1 + \alpha(p^2 + q^2)) \\ -q(1 + \alpha(p^2 + q^2)) \end{pmatrix} = \vec{f}(\vec{r}) \quad (1.63)$$

The special time-independent property of H makes it a constant of the motion. But since $H = \frac{r^2}{2} + \frac{\alpha r^4}{4} = \text{const.}$ with $r^2 = q^2 + p^2$, this means that r^2 is also a constant of the motion. Therefore, $\vec{f}(\vec{r})$ can be rewritten to

$$\vec{f}(\vec{r}) = \begin{pmatrix} \dot{q} \\ \dot{p} \end{pmatrix} = (1 + \alpha r^2) \begin{pmatrix} 0 & -1 \\ 1 & 0 \end{pmatrix} \begin{pmatrix} p \\ q \end{pmatrix} = \begin{pmatrix} p(1 + \alpha r^2) \\ -q(1 + \alpha r^2) \end{pmatrix} \quad (1.64)$$

From equation 1.60 the first terms of the time evolution $\vec{r}_f(t) = \exp(tL_{\vec{f}})\mathcal{I}$ are given as follows:

$$L_{\vec{f}}^0 \vec{r} = \begin{pmatrix} q \\ p \end{pmatrix} \quad L_{\vec{f}}^1 \vec{r} = \begin{pmatrix} p \\ -q \end{pmatrix} (1 + \alpha r^2) \quad (1.65)$$

$$L_{\vec{f}}^2 \vec{r} = (\dot{q}\partial_q + \dot{p}\partial_p) \begin{pmatrix} p \\ -q \end{pmatrix} (1 + \alpha r^2) \quad (1.66)$$

$$= \begin{pmatrix} -q \\ -p \end{pmatrix} (1 + \alpha r^2)^2 \quad (1.67)$$

$$L_{\vec{f}}^3 \vec{r} = (\dot{q}\partial_q + \dot{p}\partial_p) \begin{pmatrix} -q \\ -p \end{pmatrix} (1 + \alpha r^2)^2 \quad (1.68)$$

$$= \begin{pmatrix} -p \\ q \end{pmatrix} (1 + \alpha r^2)^3 \quad (1.69)$$

$$L_{\vec{f}}^4 \vec{r} = (\dot{q}\partial_q + \dot{p}\partial_p) \begin{pmatrix} -p \\ q \end{pmatrix} (1 + \alpha r^2)^3 \quad (1.70)$$

$$= \begin{pmatrix} q \\ p \end{pmatrix} (1 + \alpha r^2)^4 = L_{\vec{f}}^0 \vec{r} (1 + \alpha r^2)^4 \quad (1.71)$$

Collecting the terms for the Taylor expansion according to the equation 1.57 yields the following time evolution:

$$\vec{r}(t) = \left(L_{\vec{f}}^0 + tL_{\vec{f}}^1 + \frac{t^2 L_{\vec{f}}^2}{2} + \frac{t^3 L_{\vec{f}}^3}{6} + \frac{t^4 L_{\vec{f}}^4}{24} + \dots \right) \vec{r} \quad (1.72)$$

$$= \begin{pmatrix} q \\ p \end{pmatrix} \left(1 - \frac{t^2 (1 + \alpha r^2)^2}{2} + \frac{t^4 (1 + \alpha r^2)^4}{24} - \dots \right) \quad (1.73)$$

$$+ \begin{pmatrix} p \\ -q \end{pmatrix} \left(t (1 + \alpha r^2) - \frac{t^3 (1 + \alpha r^2)^3}{6} + \dots \right) \quad (1.74)$$

$$= \begin{pmatrix} q \\ p \end{pmatrix} \cos \left((1 + \alpha r^2) t \right) + \begin{pmatrix} p \\ -q \end{pmatrix} \sin \left((1 + \alpha r^2) t \right) \quad (1.75)$$

$$= \begin{pmatrix} \cos \left((1 + \alpha r^2) t \right) & \sin \left((1 + \alpha r^2) t \right) \\ -\sin \left((1 + \alpha r^2) t \right) & \cos \left((1 + \alpha r^2) t \right) \end{pmatrix} \begin{pmatrix} q \\ p \end{pmatrix} \quad (1.76)$$

This result is very similar to the commonly known solution of the simple harmonic oscillator. Both represent a circular motion in phase space with the only difference being that the frequency is the radius/amplitude dependent. In beam physics, the frequency of the linearized unperturbed system is referred to as **tune** which is ω and unity in this case. The **tune shifts** are identified as the amplitude dependent frequency changes from the tune due to the perturbation. Solutions in this specific set of coordinates, which, in this case, coincides with the original coordinates will later be introduced as Normal Form coordinates, which is one reason for selecting this example specifically.

CHAPTER 2

INTEGRATORS

There are various ways to approximate solutions to ordinary differential equations (ODE) numerically. In the following section, three different integrators shall be introduced that may be used to track the phase space curve from the initial state to the final state. In contrast to common integration, where the integration is done along one phase-space curve, the DA framework allows the computation of transfer maps at each step of the integration; relating an arbitrary initial state vector \vec{r}_i to the state vector at that particular time of the step algebraically $\vec{r}_f = \mathcal{M}(\vec{r}_i)$. The first integrator is based on a Taylor expansion, which uses the Flow Operator from 1.2.6. The commonly known and used RK4 integrator, which simulates the Taylor-expansion of 4th-Order is introduced afterwards. The last integrator uses the fixed point theorem and the contracting properties of anti-derivation operation in the DA framework to approximate the solution. All integrators work for time dependent as well as time-independent systems.

2.1 Flow Integrator

The Flow Integrator operates via a time-wise step by step integration. The basic principle of a single step is a Taylor expansion in time of $\vec{r}_n = \mathcal{I}_n = (q_n, p_n)$ at t_n by using the Flow Operator (1.2.6) and then evaluating $\vec{r}_n(t = t_n + h) = \vec{r}_{n+1}(t_{n+1})$ [2]. Afterwards, the coordinates of \vec{r}_{n+1} are rewritten in terms of the original coordinates $\vec{r}_0 = (q_0, p_0)$. The approach of using the Flow Operator is known from publications such as [11], but since the multiple application of the Flow Operator $L_{\vec{f}}$ can become very extensive for even slightly complex functions, it is not very practical. However, the differential algebras ${}_n D_{v+1}$ with v position variables and one time variable implemented in COSY INFINITY, allow for the automatic differentiation which makes the calculation very efficient. The Flow Integrator is implemented as follows:

$$\mathcal{M}_{(n+1)}(\vec{r}_0, t_{n+1}) = \exp\left(hL_{\vec{f}}\Big|_{t_n=t_0+nh}\right)\mathcal{I}\Big|_{t_0=0} \circ \mathcal{M}_n(\vec{r}_0) \quad (2.1)$$

where \mathcal{M}_n is the map at time $t_n = nh$ and therefore $\mathcal{M}_0 = \vec{r}_0 = \mathcal{I}$. In the case of a not explicitly time-dependent system, where $\partial_t \vec{f} = 0$ it follows that:

$$\exp\left(hL_{\vec{f}_{t_n=t_0+nh}}\right)\mathcal{I}\Big|_{t_0=0} = \mathcal{M}_1 \quad \forall n \quad (2.2)$$

where \mathcal{M}_1 is the initial flow from $t = 0$ to $t = h$, therefore equation 2.1 can be rewritten to:

$$\mathcal{M}_{(n+1)}(\vec{r}_0) = \mathcal{M}_1 \circ \mathcal{M}_1^n(\vec{r}_0) = \mathcal{M}_1^{n+1}(\vec{r}_0) \quad (2.3)$$

The order m to which the process is done can be chosen arbitrarily. Therefore, it is apparent that the truncation error of a step is $\sim \mathcal{O}(h^{m+1})$, while the global truncation error is $\sim \mathcal{O}(h^m)$ [19].

To illustrate the process of a two step iteration, the following example is calculated, with

$$\vec{f} = \begin{pmatrix} \dot{q} \\ \dot{p} \end{pmatrix} = \begin{pmatrix} p \\ t \end{pmatrix}. \quad (2.4)$$

The time-expansion at t_0 is derived as follows:

$$\begin{pmatrix} q \\ p \end{pmatrix} = \begin{pmatrix} q|_{t_0} \\ p|_{t_0} \end{pmatrix} + \begin{pmatrix} \dot{q}|_{t_0} \\ \dot{p}|_{t_0} \end{pmatrix} (t-t_0) + \begin{pmatrix} L_{\vec{f}}\dot{q}|_{t_0} \\ L_{\vec{f}}\dot{p}|_{t_0} \end{pmatrix} \frac{(t-t_0)^2}{2} + \begin{pmatrix} L_{\vec{f}}^2\dot{q}|_{t_0} \\ L_{\vec{f}}^2\dot{p}|_{t_0} \end{pmatrix} \frac{(t-t_0)^3}{6} \dots \quad (2.5)$$

$$= \begin{pmatrix} q_{t_0} \\ p_{t_0} \end{pmatrix} + \begin{pmatrix} p_{t_0} \\ t_0 \end{pmatrix} (t-t_0) + \begin{pmatrix} t_0 \\ 1 \end{pmatrix} \frac{(t-t_0)^2}{2} + \begin{pmatrix} 1 \\ 0 \end{pmatrix} \frac{(t-t_0)^3}{6} \quad (2.6)$$

Equation 2.6 shows that the expansion already terminates after the 3rd order in t . Therefore, the entire time evolution can be represented by this finite expansion and the 2-step approach, which is usually done for a higher precision, is not needed. However, for illustration purposes a two-step integration with step size $h = 1$ is presented. The final map can be already terminated by using equation 2.6 with $t = 2$ and $t_0 = 0$, yielding the following map:

$$\mathcal{M}_2(q_0, p_0) = \begin{pmatrix} q_2 \\ p_2 \end{pmatrix} = \begin{pmatrix} q_0 + 2p_0 + \frac{4}{3} \\ p_0 + 2 \end{pmatrix} \quad (2.7)$$

For the step by step integration, the first step is achieved by using the same equation as above (2.6) for $t_0 = 0$ and $t = t - t_0 = h = 1$, yielding the following map:

$$\mathcal{M}_1(q_0, p_0) = \begin{pmatrix} q_1 \\ p_1 \end{pmatrix} = \begin{pmatrix} q_0 + p_0 + \frac{1}{6} \\ p_0 + \frac{1}{2} \end{pmatrix} \quad (2.8)$$

The next step in the expansion is performed at $t_1 = t_0 + h = 1$ and again, $t - t_1 = h = 1$:

$$\mathcal{M}_2(q_1, p_1) = \begin{pmatrix} q_2 \\ p_2 \end{pmatrix} = \begin{pmatrix} q_1 + p_1 + 1 + \frac{1}{6} \\ p_1 + 1 + \frac{1}{2} \end{pmatrix} \quad (2.9)$$

$$\mathcal{M}_2(q_0, p_0) = \begin{pmatrix} \left(q_0 + p_0 + \frac{1}{6}\right) + \left(p_0 + \frac{1}{2}\right) + 1 + \frac{1}{6} \\ \left(p_0 + \frac{1}{2}\right) + 1 + \frac{1}{2} \end{pmatrix} = \begin{pmatrix} q_0 + 2p_0 + \frac{4}{3} \\ p_0 + 2 \end{pmatrix} \quad (2.10)$$

The result in equation 2.10 agrees with the expected result from equation 2.7. Note that in equation 2.10 $\mathcal{M}_2(q_1, p_1) = \mathcal{M}_{1 \rightarrow 2}$ and that $\mathcal{M}_2(q_0, p_0) = \mathcal{M}_{1 \rightarrow 2} \circ \mathcal{M}_1(q_0, p_0)$ with $\mathcal{M}_{1 \rightarrow 2} \neq \mathcal{M}_1$, due to the explicit time dependence of \vec{f} . Since the system is explicitly time dependent, the evaluation of each step is needed.

$$\mathcal{M}_1^2(q_0, p_0) = \begin{pmatrix} \left(q_0 + p_0 + \frac{1}{6}\right) + \left(p_0 + \frac{1}{2}\right) + \frac{1}{6} \\ \left(p_0 + \frac{1}{2}\right) + \frac{1}{2} \end{pmatrix} \neq \begin{pmatrix} q_0 + 2p_0 + \frac{4}{3} \\ p_0 + 2 \end{pmatrix} = \mathcal{M}_2(q_0, p_0) \quad (2.11)$$

2.2 Fourth-Order Runge-Kutta integrator

The fourth-order Runge-Kutta method (RK4) simulates the accuracy of the Taylor series method of order $m = 4$ [19]. It is one of the most commonly used since it is stable, quite accurate, and easy to implement. It was first developed by the German mathematicians Carl Runge and Martin Kutta in 1901. It consists of a step-wise integration of the independent variable t . Given a set of initial conditions $\vec{r}_n = \vec{r}(t_i)$, one step of the Runge-Kutta method yields an approximation for $\vec{r}_{n+1} = \vec{r}(t_f = t_i + h)$, where h is the step-size of the integration. In the simplest form of the method, the step-size will be constant throughout the integration. More advanced integrators use an adaptive step-size [15]. A series of Runge-Kutta steps make it possible to trace the trajectory \vec{r} from the set of initial conditions to the final state $\vec{r}_f(t_f)$ in steps of h . This work uses a 4th-Order Runge-Kutta method (RK4) with a constant step size h , where \vec{r}_{n+1} at $t_{n+1} = t_n + h$ is calculated as follows:

$$\vec{r}_{n+1} = \vec{r}_n + \frac{h}{6} (\vec{a}_n + 2\vec{b}_n + 2\vec{c}_n + \vec{d}_n) \quad (2.12)$$

$$\text{with} \quad \vec{a}_n = \vec{f}(\vec{r}_n, t_n) \quad (2.13)$$

$$\vec{b}_n = \vec{f}\left(\vec{r}_n + \frac{h}{2}\vec{a}_n, t_n + \frac{h}{2}\right) \quad (2.14)$$

$$\vec{c}_n = \vec{f}\left(\vec{r}_n + \frac{h}{2}\vec{b}_n, t_n + \frac{h}{2}\right) \quad (2.15)$$

$$\vec{d}_n = \vec{f}(\vec{r}_n + h\vec{c}_n, t_n + h) \quad (2.16)$$

The derivation of the coefficients $\vec{a}_n, \vec{b}_n, \vec{c}_n$ and \vec{d}_n can be found in [8]. Due to the DA based implementation the calculation yields a transfer map that relates the initial state to the final state. However, the ordinary method (not DA based) can only be used for element-by-element tracking, yielding only a numerical relation between the initial and final value.

2.3 Fixed point Integrator

The fixed point Integrator turns an ordinary differential equation (ODE) into a fixed point problem which it solves through iteration. Hence, the following short introduction to fixed point problems is given.

A function F has a fixed point x_0 if $F(x_0) = x_0$ is satisfied. Assuming that $F(x)$ has a fixed point x_0 , the question arises under what conditions can the fixed point be approximated through the iteration

$$x_{n+1} = F(x_n). \quad (2.17)$$

It is apparent that the fixed point must be attractive for the starting value of the iteration. Therefore $F(x)$ must be contracting. A map $F : M \rightarrow M$ on a metric space (M, d) with a metric d is contracting, if $\forall x, y \in M$

$$d(F(x), F(y)) < kd(x, y) \quad (2.18)$$

where k is a real number $0 \leq k < 1$ which is called a Lipschitz constant. M therefore defines the space of contraction of F . Furthermore, if

$$kd(x_n, y_n) > d(F(x_n), F(y_n)) = d(x_{n+1}, y_{n+1}) \xrightarrow{n \rightarrow \infty} d(x_0, x_0) = 0 \quad (2.19)$$

then F is contracting on M with the fixed point x_0 and the iteration process which will yield the fixed point. Considering the example of $F(x) = x^2$, one fixed point is trivially $x_0 = 0$ and is attractive for the range of $|x| < 1$. The other fixed point is at $x_1 = 1$, which has a range of zero and is therefore not attractive. On the other hand, $G(x) = \sqrt{x}$ has a fixed point at $x_0 = 1$, which is attractive for all $x \in \mathbb{R}^+$, which is every value of the domain of G except for the only other fixed point $x_1 = 0$.

According to [2] the integrator solves the fixed point problem for the function $\vec{R}(\vec{r}(t), t)$ with

$$\vec{R}(\vec{r}(t), t) = \vec{r}(0) + \int_0^t \vec{f}(\vec{r}(t'), t) dt', \quad (2.20)$$

where $\vec{f} = \dot{\vec{r}}$ and $\vec{r}(0) = \mathcal{I}$. The fixed point of $\vec{R}(\vec{r}(t), t)$ is obviously $\vec{r}(t)$, which shall be approximated by fixed point iteration (eq. 2.17). The integration, which is represented by an anti-

differentiation operation ∂^{-1} in the DA framework, is contracting with respect to the depth (first non-vanishing derivative) [6]. The fixed point problem

$$\vec{r}(t) = \mathcal{I} + \int_0^t \vec{f}(\vec{r}(t'), t') dt', \quad (2.21)$$

can therefore be approximated, order by order, through the iteration:

$$\vec{r}_{n+1}(t) = \mathcal{I} + \int_0^t \vec{f}(\vec{r}_n(t'), t') dt', \quad (2.22)$$

with $\vec{r}_0(t) = \vec{0}$. So, with each step of the iteration the following is valid for m being at least n .

$$\vec{r}(t) =_m \vec{r}_n(t) \quad (2.23)$$

As an illustrative example the same ODE introduced previously for the Flow Integrator is approximated with the fixed point method:

$$r_0(t) = \mathcal{I} + \int_0^t \vec{f}(\vec{0}, t') dt' = r(0) = \begin{pmatrix} q \\ p \end{pmatrix} \quad (2.24)$$

$$r_1(t) = \mathcal{I} + \int_0^t \vec{f}(r_0, t') dt' = \begin{pmatrix} q \\ p \end{pmatrix} + \begin{pmatrix} pt \\ \frac{t^2}{2} \end{pmatrix} \quad (2.25)$$

$$r_2(t) = \mathcal{I} + \int_0^t \vec{f}(r_2, t') dt' = \begin{pmatrix} q \\ p \end{pmatrix} + \begin{pmatrix} pt \\ \frac{t^2}{2} \end{pmatrix} + \begin{pmatrix} \frac{t^3}{6} \\ 0 \end{pmatrix} \quad (2.26)$$

and $\forall n > 2$ $r_n(t) = r_2(t)$. In this example, the iteration terminates after the 3rd order. The algorithm can be implemented in COSY INFINITY in a very efficient way, by constraining the order of each step to the necessary minimum, which is the order of the iteration itself. So the second iteration (eq. 2.25) would be restrained to 2nd order and so on; this avoids unnecessary calculations of higher orders in each step, which become drastically even more time consuming with each additional order.

2.4 Error vs step-size for RK4 integrator

The following section investigates the error in the RK4 integration. In general, the errors are distinguished in single-step and multi-step errors, each of which is determined by the difference of the RK4-calculated result to the exact solution. For the RK4, the single-step error depends on the step size h with $\mathcal{O}(h^5)$ [19]. The multi-step error, which is the total error from all the single steps combined, depends on the step-size with $\mathcal{O}(h^4)$ [19]. This property can be shown in the following example using the Hamilton equations resulting from the Pendulum oscillation, which is discussed in detail in section 5.1:

$$\begin{pmatrix} 0 & -1 \\ 1 & 0 \end{pmatrix} \begin{pmatrix} p_1 \\ q_1 \end{pmatrix} + \begin{pmatrix} \frac{aq_1^3}{3!} - \frac{a^2q_1^5}{5!} + \frac{a^3q_1^7}{7!} - \frac{a^4q_1^9}{9!} + \dots \\ 0 \end{pmatrix} \quad (2.27)$$

The ODE is integrated using a single-RK4-step from $t = 0$ to $t = h_0$. The resulting map yields the starting point for the following test: To show that the multi-step error, which is also called the global truncation error, is of order $\mathcal{O}(h^4)$, the integration to $t = 2h_0$ is done in multiple ways: 1, 2, 4, ..., 32768 steps are done with the corresponding step-sizes of $h_0, \frac{h_0}{2}, \frac{h_0}{4}, \dots, \frac{h_0}{32768}$. The result of the smallest step size is considered the exact result. Hence, the error is the difference of the result from the respective step-size to the 'exact' result. The error is plotted against the number of steps used and shown in a log-log scaling in figure 2.1. Alternatively, the reciprocal relative step size can be used, which is equivalent to the used steps in this example. The linear correlation yields an h^4 -dependency, which confirms the expected result. Note that for very small step-sizes the constant error that originates from the floating point number approximations (see sec. 1.2.1) becomes the dominant part of the total error. Accordingly, the step-size can potentially be chosen ineffectively small, where an increase in steps, and therefore computation time, does not result in more precise results. In this example, the critical step-sizes is approximately $h_0/1024 \approx 10^{-4}h_0$. The other test concerns a single step of the RK4 method, whereby the error equivalently defined as above, is supposed to be of the order $\mathcal{O}(h^5)$ [19]. Again, the map for $t = h_0$ is used as the starting point from which one step of the different step-sizes $h_0/2, h_0/4, h_0/8, \dots, h_0/256$ is done.

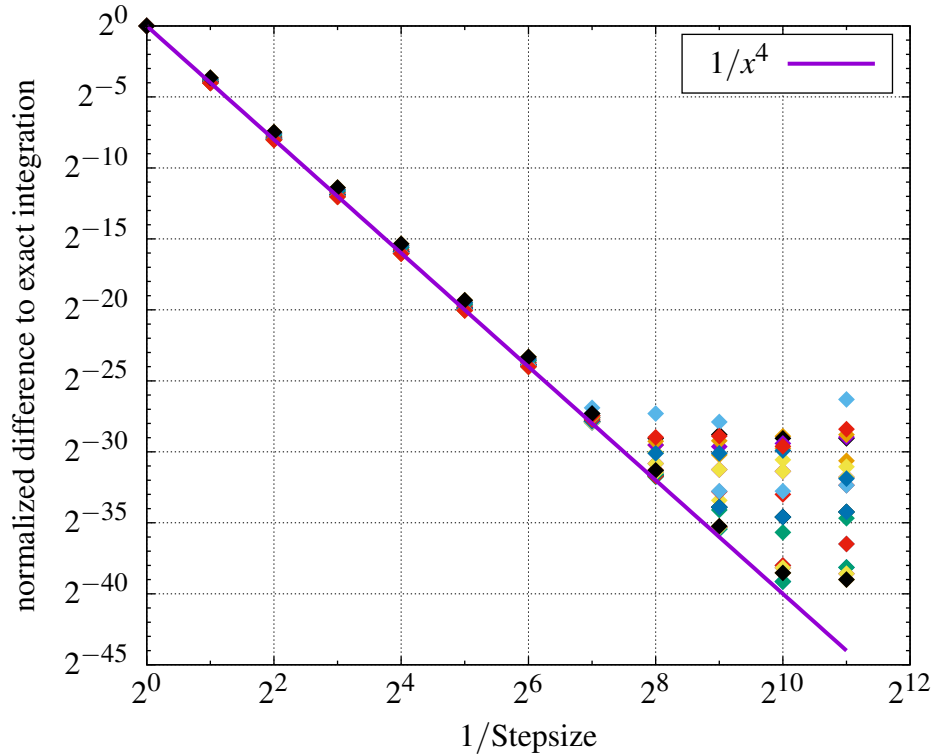


Figure 2.1 The graph illustrates how the total error of a DA based RK4-integration drops $\sim h^4$ until a certain critical step size is reached. From this step-size onwards, more steps do not result in more precise results since the maximum precision, determined by the floating point calculation errors, is reached. For this example, the critical step-size is approximately $2^{-10}h_0 \approx 10^{-4}h_0$. The error is estimated by calculating the difference of the result from the step-size $2^{-k}h_0$ to the result from the step-size $2^{-12}h_0$, which is considered the 'exact' solution. The difference is then normalized to the respective result of the 2^0h_0 -step-size-calculation. The different plots/colors represent the coefficients of different terms of the $t = 2h_0$ map of the Pendulum ODE (eq. 5.4) after the integration from the $t = h_0$ map using a different number of steps according to the step-size.

For comparison the 'exact' result is calculated by 256, 128, 64, ..., 2 steps of $h_0/512$, respectively. The difference of one-step-result to the 'exact' result is plotted against the number of steps. The 5^{th} -order dependence becomes apparent in the linear correlation of the log-log scaled graph, which is shown in figure 2.2. It should go without saying that the DA variable h_0 in the integration was only introduced for the purpose of illustrating the error behavior of the DA based RK4-integrator. In the general application, the variable h_0 is replaced by the specific step-size value. Therefore,

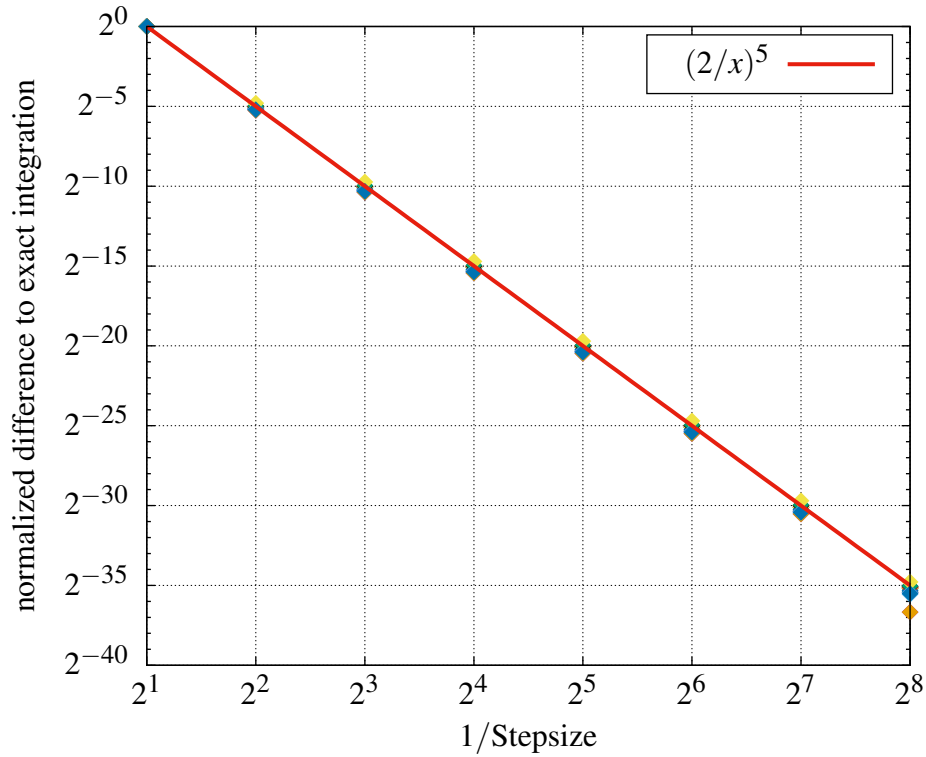


Figure 2.2 The graph illustrates how the single-step error of a DA based RK4-integration step drops $\sim h^5$ with h being the step-size. The error is estimated by calculating the difference of the result from the step-size $2^{-k}h_0$ to the result from the step-size $2^{-9}h_0$, which is considered the exact solution in this case. The difference is then normalized to the respective result of the $2^{-1}h_0$ -step-size-calculation. The different plots represent the coefficients of different terms of the $t = h_0 + h$ map of the Pendulum ODE (eq. 5.4) after the integration from the $t = h_0$ map using one step of step-size h . The additional factor of 2^5 in the error to 1/step-size ratio originates from normalization with respect to the $2^{-1}h_0$ -step-size-calculation.

the generated transfer maps do not represent the state after an arbitrary time h_0 , but a specific time such as $t = 1$. The generalization of adding a step-size variable is not needed in most cases and would therefore only increase the total order of the single terms. Since the calculation is order truncated, the general result would be significantly less precise than the direct calculations with a specific value. Considering an order truncation of 5, terms like $q^2\alpha^2t^2$ would not be represented in the general solution, due to the total order of 6 of the term. But for a specific step-size like 1, the term is represented together with the other $q^2\alpha^2$ -terms.

2.5 Integrator comparison

To investigate how the various DA based integrators compare, the integration of the Pendulum oscillation ODE (eq. 5.26) is investigated. All integrators kept the step-size $t = h$ a variable. The ODE was integrated in one step from $t = 0$ to t . The resulting transfer maps for the q and p -component are given in table 2.1 and 2.2, respectively. The order truncation was set to 11. Both the fixed point Integrator as well as the Flow Integrator yield the same result up to the set order truncation. This is not very surprising since both of them approximate the exact solution order by order, which results in both yielding the same result, namely, the exact solution (with floating point accuracy) up to order 11. The RK4 on the other hand simulates the Taylor expansion up to 4th-order, therefore all terms with t of order 4 or lower coincide with the Flow/fixed point integration. From the theory above it is known, that the error of a single RK4-step is of order $\mathcal{O}(h^5)$. This can be observed in the tables (2.1 and 2.2) as well. Terms of t with order 5 or higher are either zero or different to the fixed point/Flow integration, just as expected.

Table 2.1 The table represents the q-component of the transfer map of the initial state from $t = 0$ to t in the Pendulum vector field from equation 5.26 up to the 11th order. The transfer map was calculated with one step via the three different DA base integrators. The columns with bold order numbers indicate terms of $\mathcal{O}(t^5)$, which are the first error affected terms of the RK4 integrator, which supports the theory discussed in section 2.4. Furthermore, the results of fixed point integration and Flow integration are identical, which also agrees with the theory.

Order	Factor	RK4(t)	Fixed-P(t)	Flow(t)
1	q	1,00000E+00	1,00000E+00	1,00000E+00
2	pt	1,00000E+00	1,00000E+00	1,00000E+00
3	qt^2	-5,00000E-01	-5,00000E-01	-5,00000E-01
4	pt^3	-1,66667E-01	-1,66667E-01	-1,66667E-01
5	qt^4	4,16667E-02	4,16667E-02	4,16667E-02
6	$q^3t^2\alpha$	8,33333E-02	8,33333E-02	8,33333E-02
6	pt^5		8,33333E-03	8,33333E-03
7	$q^2pt^3\alpha$	8,33333E-02	8,33333E-02	8,33333E-02
7	qt^6		-1,38889E-03	-1,38889E-03
8	$q^3t^4\alpha$	-2,77778E-02	-2,77778E-02	-2,77778E-02
8	$qp^2t^4\alpha$	4,16667E-02	4,16667E-02	4,16667E-02
8	pt^7		-1,98413E-04	-1,98413E-04
9	$q^5t^2\alpha^2$	-4,16667E-03	-4,16667E-03	-4,16667E-03
9	$q^2pt^5\alpha$	-2,08333E-02	-3,33333E-02	-3,33333E-02
9	$p^3t^5\alpha$	6,94444E-03	8,33333E-03	8,33333E-03
9	qt^8		2,48016E-05	2,48016E-05
10	$q^4pt^3\alpha^2$	-6,94444E-03	-6,94444E-03	-6,94444E-03
10	$q^3t^6\alpha$	5,20833E-03	5,78704E-03	5,78704E-03
10	$qp^2t^6\alpha$	-5,20833E-03	-1,52778E-02	-1,52778E-02
10	pt^9		2,75573E-06	2,75573E-06
11	$q^5t^4\alpha^2$	5,55556E-03	5,55556E-03	5,55556E-03
11	$q^3p^2t^4\alpha^2$	-6,94444E-03	-6,94444E-03	-6,94444E-03
11	$q^2pt^7\alpha$	2,60417E-03	6,84524E-03	6,84524E-03
11	$p^3t^7\alpha$		-2,18254E-03	-2,18254E-03
11	qt^{10}		-2,75573E-07	-2,75573E-07

Table 2.2 The table shows the p-component equivalent to Table 2.1.

Order	Factor	RK4(t)	Fixed-P(t)	Flow(t)
1	p	1,00000E+00	1,00000E+00	1,00000E+00
2	qt	-1,00000E+00	-1,00000E+00	-1,00000E+00
3	pt^2	-5,00000E-01	-5,00000E-01	-5,00000E-01
4	qt^3	1,66667E-01	1,66667E-01	1,66667E-01
5	$q^3t\alpha$	1,66667E-01	1,66667E-01	1,66667E-01
5	pt^4	4,16667E-02	4,16667E-02	4,16667E-02
6	$q^2pt^2\alpha$	2,50000E-01	2,50000E-01	2,50000E-01
6	qt^5		-8,33333E-03	-8,33333E-03
7	$q^3t^3\alpha$	-1,11111E-01	-1,11111E-01	-1,11111E-01
7	$qp^2t^3\alpha$	1,66667E-01	1,66667E-01	1,66667E-01
7	pt^6		-1,38889E-03	-1,38889E-03
8	$q^5t\alpha^2$	-8,33333E-03	-8,33333E-03	-8,33333E-03
8	$q^2pt^4\alpha$	-1,66667E-01	-1,66667E-01	-1,66667E-01
8	$p^3t^4\alpha$	4,16667E-02	4,16667E-02	4,16667E-02
8	qt^7		1,98413E-04	1,98413E-04
9	$q^4pt^2\alpha^2$	-2,08333E-02	-2,08333E-02	-2,08333E-02
9	$q^3t^5\alpha$	3,12500E-02	3,47222E-02	3,47222E-02
9	$qp^2t^5\alpha$	-1,04167E-01	-9,16667E-02	-9,16667E-02
9	pt^8		2,48016E-05	2,48016E-05
10	$q^5t^3\alpha^2$	2,22222E-02	2,22222E-02	2,22222E-02
10	$q^3p^2t^3\alpha^2$	-2,77778E-02	-2,77778E-02	-2,77778E-02
10	$q^2pt^6\alpha$	4,68750E-02	4,79167E-02	4,79167E-02
10	$p^3t^6\alpha$	-2,25694E-02	-1,52778E-02	-1,52778E-02
10	qt^9		-2,75573E-06	-2,75573E-06
11	$q^7t\alpha^3$	1,98413E-04	1,98413E-04	1,98413E-04
11	$q^4pt^4\alpha^2$	5,55556E-02	5,55556E-02	5,55556E-02
11	$q^2p^3t^4\alpha^2$	-2,08333E-02	-2,08333E-02	-2,08333E-02
11	$q^3t^7\alpha$	-4,34028E-03	-6,87831E-03	-6,87831E-03
11	$qp^2t^7\alpha$	2,60417E-02	2,02381E-02	2,02381E-02
11	pt^{10}		-2,75573E-07	-2,75573E-07

CHAPTER 3

THE NORMAL FORM ALGORITHM

In the previous chapter, the different DA based integrators were discussed, which yield a transfer map, that algebraically connects the initial state to the state at time t : $\vec{z}_f = \mathcal{M}(\vec{z}_i, \vec{\delta})$, where $\vec{\delta}$ represents possible parameter dependencies. Considering a repetitive Hamiltonian system, where the components of the resulting map are in phase-space coordinates, the Normal Form Algorithm provides a nonlinear change of variables for the given map \mathcal{M} , which significantly simplifies all terms up to an arbitrary order m_{max} . In the transformed variables, the transfer map will represent circular motion with only amplitude dependent frequencies [6]. Those frequencies are the key quantity of every periodic system and in most cases make the explicit trajectory superfluous. This simplified form of the map is called the 'Normal Form of \mathcal{M} ' or \mathcal{M}_{NF} , in the shorthand notation. The following introduction to the DA Normal Form Algorithm largely draws from [6] and is complemented with an explicit calculation for a symplectic system with $\nu = 1$ up to 3rd order. The specification is chosen, since only Hamiltonian systems are discussed in this thesis. Symplectic maps are canonical [6] and therefore preserve the Hamiltonian form (see 1.2.5).

3.1 The DA Normal Form Algorithm

The DA Normal Form Algorithm uses the DA framework implemented in COSY INFINITY to express the Normal Form of the map \mathcal{M} in algebraic relation to the initial state using a sequence of order-by-order coordinate transformations \mathcal{A}_m applied to the map \mathcal{M} in the following way:

$$\mathcal{A}_m \circ \mathcal{M} \circ \mathcal{A}_m^{-1} \tag{3.1}$$

In the general form, the map $\mathcal{M} = \mathcal{C}_0 + \mathcal{L} + \sum_m \mathcal{U}_m$ consists of a constant part \mathcal{C}_0 , a linear part \mathcal{L} and the nonlinear parts \mathcal{U}_m of order m . \mathcal{M} is 2ν -dimensional, with ν position/momentum entry

pairs \mathcal{M}_j^\pm . For $\nu = 1$ the map can be explicitly written as

$$\begin{aligned}
\mathcal{M}(x, p) = \begin{pmatrix} \mathcal{M}^+ \\ \mathcal{M}^- \end{pmatrix} &= \underbrace{\begin{pmatrix} x_0 \\ p_0 \end{pmatrix}}_{\mathcal{C}_0} + \underbrace{\begin{pmatrix} (x|x) & (x|p) \\ (p|x) & (p|p) \end{pmatrix}}_{\mathcal{L}} \begin{pmatrix} x \\ p \end{pmatrix} \\
&+ \underbrace{\begin{pmatrix} \mathcal{U}_{2(2,0)}^+ \\ \mathcal{U}_{2(2,0)}^- \end{pmatrix}}_{\mathcal{U}_2} x^2 + \underbrace{\begin{pmatrix} \mathcal{U}_{2(1,1)}^+ \\ \mathcal{U}_{2(1,1)}^- \end{pmatrix}}_{\mathcal{U}_2} xp + \underbrace{\begin{pmatrix} \mathcal{U}_{2(0,2)}^+ \\ \mathcal{U}_{2(0,2)}^- \end{pmatrix}}_{\mathcal{U}_2} p^2 \\
&+ \underbrace{\begin{pmatrix} \mathcal{U}_{3(3,0)}^+ \\ \mathcal{U}_{3(3,0)}^- \end{pmatrix}}_{\mathcal{U}_3} x^3 + \underbrace{\begin{pmatrix} \mathcal{U}_{3(2,1)}^+ \\ \mathcal{U}_{3(2,1)}^- \end{pmatrix}}_{\mathcal{U}_3} x^2 p + \dots
\end{aligned} \tag{3.2}$$

In the first step of the Normal Form Algorithm, the parameter-dependent fixed point $(\vec{z}_{Fix}, \vec{\delta})$ is translated to the origin, so $\mathcal{M}(\vec{0}, \vec{\delta}) = 0$ to make the map origin preserving. This fixed point represents the reference orbit in phase space, which can often be obtained by solving the unperturbed ODE of the problem. In most cases the constant part \mathcal{C}_0 points to the reference orbit. Therefore, it can be removed, which yields $\mathcal{M}_0 = \mathcal{L} + \sum_m \mathcal{U}_m$. Following [6], the fixed point problem

$$\mathcal{M}(\vec{z}_{Fix}, \vec{\delta}) = (\vec{z}_{Fix}, \vec{\delta}) \tag{3.3}$$

has to be solved for the nontrivial case, which is done by the following equation:

$$(\vec{z}_{Fix}, \vec{\delta}) = (\mathcal{M} - \mathcal{I})^{-1}(\vec{0}, \vec{\delta}). \tag{3.4}$$

From 1.2.3 it is known that polynomials with non-zero constant terms, like the identity, have an inverse which can be calculated up to order m_{max} using equation 3.30.

3.1.1 Diagonalization

The diagonalization is important for the computation, since it decouples the 2ν phase space into ν subspaces, which can then be treated independently. The matrix $\hat{\mathcal{L}}$ is associated with the linear part of \mathcal{M} . It is transformed into a diagonal-block-matrix, which has 2×2 -submatrices on its diagonal:

$$\begin{pmatrix} \hat{\mathcal{L}}_1 & & & & \\ & \ddots & & & \\ & & \hat{\mathcal{L}}_j & & \\ & & & \ddots & \\ & & & & \hat{\mathcal{L}}_\nu \end{pmatrix} \quad \text{with} \quad \hat{\mathcal{L}}_j = \begin{pmatrix} a_j & b_j \\ c_j & d_j \end{pmatrix} \quad (3.5)$$

Consequently, the map can now be treated in the two-component subspace. More information on the block matrix creation can be found in [6].

3.1.1.1 Diagonalization transformation of the linear part

In the first order correction, the linear part of the map \mathcal{L} must be diagonalized. Thus, it is assumed that $\hat{\mathcal{L}}$ is diagonalizable and has ν distinct complex conjugate eigenvalue pairs λ_j^\pm . Furthermore, it is required that no eigenvalue is unity and the product of all eigenvalues is positive, which is generally true for a repetitive system under normal conditions [6]. The first order transformation matrix $\hat{\mathcal{A}}_1^{-1} = (\vec{v}_1, \vec{v}_1, \dots, \vec{v}_j, \vec{v}_j, \dots, \vec{v}_\nu, \vec{v}_\nu)$ consists of the ν complex conjugate eigenvector pairs (\vec{v}_j, \vec{v}_j) of $\hat{\mathcal{L}}$ resulting in the diagonalized linear matrix $\hat{\mathcal{R}}$ with components:

$$\hat{\mathcal{R}}_j = \mathcal{A}_{1,j} \circ \hat{\mathcal{L}}_j \circ \mathcal{A}_{1,j}^{-1} = \begin{pmatrix} \lambda_j^+ & 0 \\ 0 & \lambda_j^- \end{pmatrix} = \begin{pmatrix} e^{i\mu_j} & 0 \\ 0 & e^{-i\mu_j} \end{pmatrix} \quad (3.6)$$

It is essential for the transformation of the higher order terms that $|\text{Det}(\hat{\mathcal{A}})| = 1$ to keep the transformation scaling-neutral.

For the $\nu = 1$ the eigenvalues can be derived from the eigenvalue equation 1.28 which yields the following results for the eigenvalues and their phase:

$$\lambda^{\pm} = \frac{(x|x) + (p|p)}{2} \pm \sqrt{\frac{((x|x) + (p|p))^2}{4} - (x|x)(p|p) + (p|x)(x|p)} = re^{\pm i\mu} \quad (3.7)$$

$$\mu = \text{sign}((x|p)) \arccos\left(\frac{(x|x) + (p|p)}{2\sqrt{(x|x)(p|p) - (p|x)(x|p)}}\right) \quad (3.8)$$

where $(r = 1) \wedge (\mu \in \mathbb{R})$, since in the example a symplectic system is considered. The eigenvectors of $\hat{\mathcal{L}}$ can then be expressed in the Twiss parameters as follows:

$$\vec{v}^{\pm} = \begin{pmatrix} \beta \\ \alpha \pm i \end{pmatrix} \quad (3.9)$$

$$\alpha = \frac{(x|x) - (p|p)}{2r \sin \mu} \quad \beta = \frac{(x|p)}{r \sin \mu} \quad \gamma = \frac{-(p|x)}{r \sin \mu} \quad (3.10)$$

To follow the example in the case of $\beta = 0$, one can either use the eigenvectors described in equation 1.47, which are in terms of γ and α and follow the diagonalization steps with those or one can transform the current map to a different form, where the new $\beta' = \gamma$, $\gamma' = 1/\gamma$ and $\alpha' = 0$. This map can be generated by using the transformation \mathcal{A}_0 with:

$$\hat{\mathcal{A}}_0^{-1} = \begin{pmatrix} 1/\gamma & -\alpha \\ 0 & \gamma \end{pmatrix} \quad \hat{\mathcal{A}}_0 = \begin{pmatrix} \gamma & \alpha \\ 0 & 1/\gamma \end{pmatrix} \quad (3.11)$$

$$\mathcal{A}_0 \circ \mathcal{L} \circ \mathcal{A}_0^{-1} = \begin{pmatrix} \cos \mu & \gamma \sin \mu \\ -\frac{\sin \mu}{\gamma} & \cos \mu \end{pmatrix} \quad (3.12)$$

The higher order terms have to be transformed accordingly (see 3.1.1.2).

Whether with the original map or the transformed map, the eigenvectors of the linear part have a magnitude and phase-freedom to them. In this calculation the phase-freedom is used to make sure that the transformation matrix consist of a complex conjugate eigenvector pair. This assures certain complex conjugate properties of the transformed map. Since the transformation of nonlinear terms

is also relevant in this process, it is necessary for the transformation matrix to satisfy $|Det(\mathcal{A})| = 1$. The 1^{st} -order transformation matrix $\hat{\mathcal{A}}_1^{-1} = (\vec{v}^+, \vec{v}^-)$ and its inverse $\hat{\mathcal{A}}_1$ (see 1.2.4) are given as follows:

$$\hat{\mathcal{A}}_1^{-1} = \begin{pmatrix} (x|s_1^+) & (x|s_1^-) \\ (x|s_1^+) & (p|s_1^-) \end{pmatrix} = \frac{1}{\sqrt{2\beta}} \begin{pmatrix} -\beta & -\beta \\ \alpha + i & \alpha - i \end{pmatrix} \quad (3.13)$$

Note the scaling factor of $1/|\det(\hat{\mathcal{A}}_1^{-1})|$, that assures a scaling neutral transformation.

$$\hat{\mathcal{A}}_1 = \frac{-1}{\sqrt{2\beta}} \begin{pmatrix} 1 + i\alpha & i\beta \\ 1 - i\alpha & -i\beta \end{pmatrix} = \begin{pmatrix} (s_1^+|x) & (s_1^+|p) \\ (s_1^-|x) & (s_1^-|p) \end{pmatrix} \quad (3.14)$$

For the linear part the transformation yields:

$$\hat{\mathcal{R}} = \hat{\mathcal{A}}_1 \circ \hat{\mathcal{L}} \circ \hat{\mathcal{A}}_1^{-1} = \begin{pmatrix} \lambda^+ & 0 \\ 0 & \lambda^- \end{pmatrix} = \begin{pmatrix} e^{i\mu} & 0 \\ 0 & e^{-i\mu} \end{pmatrix} \quad (3.15)$$

3.1.1.2 Diagonalization transformation of the non-linear parts

The linear transformation for the diagonalization of the linear part also transforms the nonlinear parts \mathcal{U}_m from position/momentum basis $(x_1 \vec{e}_{x_1}, p_1 \vec{e}_{p_1}, \dots, x_j \vec{e}_{x_j}, p_j \vec{e}_{p_j}, \dots)$ to the complex eigenvector basis of $\hat{\mathcal{L}}$: $(s_1^+ \vec{v}_1, s_1^- \vec{v}_1, \dots, s_j^+ \vec{v}_j, s_j^- \vec{v}_j, \dots)$, as follows:

$$\begin{pmatrix} x_j \\ p_j \end{pmatrix} = \mathcal{A}_{1.j} \circ \begin{pmatrix} s_j^+ \\ s_j^- \end{pmatrix} = \begin{pmatrix} (x_j|s_j^+)s_j^+ + (x_j|s_j^-)s_j^- \\ (p_j|s_j^+)s_j^+ + (p_j|s_j^-)s_j^- \end{pmatrix} \quad (3.16)$$

The map after the first order transformation into the eigenvector basis can therefore be written as follows: $\mathcal{M}_1 = \mathcal{R} + \sum_m \mathcal{S}_m$, where \mathcal{S}_m are the transformed nonlinear parts, which now depend on \vec{s}^+ and \vec{s}^- , the eigenvector coefficients, instead of \vec{x} and \vec{p} . A more explicit form of the j^{th} -

component with a similar notation as introduced in [6, 7.63] looks like this:

$$\mathcal{S}_{m,j} = \sum_{\|\vec{k}^+ + \vec{k}^-\|_1 = m} \left(\mathcal{S}_{m,j}^{\pm} | \vec{k}^+, \vec{k}^- \right) \prod_{l=1}^{\nu} (s_l^+)^{k_l^+} (s_l^-)^{k_l^-} \quad (3.17)$$

where k_j^{\pm} represents the positive integer exponent of s_j^{\pm} summarized in \vec{k}^{\pm} and $\|\vec{k}\|_1 := \sum |k_l|$ is the L^1 -Norm (also known as Manhattan Norm), which assures that only polynomial-terms of order m are considered. $\left(\mathcal{S}_{m,j}^{\pm} | \vec{k}^+, \vec{k}^- \right)$ is the Taylor expansion coefficient with respect to $\prod_{l=1}^{\nu} (s_l^+)^{k_l^+} (s_l^-)^{k_l^-}$. So,

$$\mathcal{M}_j^{\pm} (\vec{s}^+, \vec{s}^-) = r_j e^{\pm i \mu_j} s_j^{\pm} + \sum_{m=2}^{m_{\max}} \mathcal{S}_{m,j} \quad (3.18)$$

$$= r_j e^{\pm i \mu_j} s_j^{\pm} + \sum_{m=2}^{m_{\max}} \sum_{\|\vec{k}^+ + \vec{k}^-\|_1 = m} \left(\mathcal{S}_{m,j}^{\pm} | \vec{k}^+, \vec{k}^- \right) \prod_{l=1}^{\nu} (s_l^+)^{k_l^+} (s_l^-)^{k_l^-} \quad (3.19)$$

Also note, since s_l^+ and s_l^- are complex conjugate pairs, that $\overline{s_l^+} = s_l^-$ and therefore:

$$\begin{aligned} \overline{\mathcal{M}_j^{\pm} (\vec{s}^+, \vec{s}^-)} &= r_j e^{\mp i \mu_j} s_j^{\mp} + \sum_{m=2}^{m_{\max}} \sum_{\|\vec{k}^+ + \vec{k}^-\|_1 = m} \overline{\left(\mathcal{S}_{m,j}^{\pm} | \vec{k}^+, \vec{k}^- \right) \prod_{l=1}^{\nu} (s_l^+)^{k_l^+} (s_l^-)^{k_l^-}} \\ &= \mathcal{M}_j^{\mp} (\vec{s}^+, \vec{s}^-) \text{ with } \overline{\left(\mathcal{S}_{m,j}^{\pm} | \vec{k}^+, \vec{k}^- \right)} = \left(\mathcal{S}_{m,j}^{\mp} | \vec{k}^-, \vec{k}^+ \right) \end{aligned} \quad (3.20)$$

For $\nu = 1$ the explicit transformation of the nonlinear parts is done as follows: The individual transformation of single parts of the map is only possible in the case of a linear transformation, which is given for the diagonalization. Therefore, the transformation of the term $\mathcal{U}_{m(k^+, k^-)} x^{k^+} p^{k^-}$ with $k^+ + k^- = m$ can be shown in general: First \mathcal{A}_1^{-1} transforms the new complex conjugate variables (s^+, s^-) into the old variables (x, p) to make them suitable for $\mathcal{U}_{m(k^+, k^-)} x^{k^+} p^{k^-}$, which is a function of x and p .

$$\frac{1}{\sqrt{2\beta}} \begin{pmatrix} -\beta & -\beta \\ \alpha + i & \alpha - i \end{pmatrix} \begin{pmatrix} s^+ \\ s^- \end{pmatrix} = \sqrt{\frac{2}{\beta}} \begin{pmatrix} \operatorname{Re}(-\beta s^+) \\ \operatorname{Re}((\alpha - i)s^-) \end{pmatrix} \quad (3.21)$$

The result in (x, p) -coordinates, which is real since (x, p) are real, can now be inserted into the nonlinear part $\mathcal{U}_{m(k^+, k^-)} x^{k^+} p^{k^-}$:

$$\left(\mathcal{U}_{m(k^+, k^-)} x^{k^+} p^{k^-} \right) \circ \mathcal{A}_1^{-1} = \left(\frac{2}{\beta} \right)^{\frac{m}{2}} \mathcal{U}_{m(k^+, k^-)} \operatorname{Re}(-\beta s^+)^{k^+} \operatorname{Re}((\alpha - i)s^-)^{k^-} \quad (3.22)$$

In the last part of the transformation, the current result in (x, p) -coordinates is transformed back to (s^+, s^-) -coordinates with $\mathcal{A}_1 \circ (\mathcal{U}_{m(k^+, k^-)} x^{k^+} p^{k^-}) \circ \mathcal{A}_1^{-1}$

$$= \frac{1}{2} \left(\frac{2}{\beta} \right)^{\frac{m+1}{2}} \mathbb{R}e(-\beta s^+)^{k^+} \mathbb{R}e((\alpha - i)s^-)^{k^-} \begin{pmatrix} i\alpha - 1 & -\beta i \\ -i\alpha - 1 & \beta i \end{pmatrix} \mathcal{U}_{m(k^+, k^-)} \quad (3.23)$$

$$= \frac{1}{2} \left(\frac{2}{\beta} \right)^{\frac{m+1}{2}} \mathbb{R}e(-\beta s^+)^{k^+} \mathbb{R}e((\alpha - i)s^-)^{k^-} \quad (3.24)$$

$$\cdot \left(\begin{pmatrix} i\alpha - 1 \\ -i\alpha - i \end{pmatrix} \mathcal{U}_{m(k^+, k^-)}^+ + \begin{pmatrix} -\beta i \\ \beta i \end{pmatrix} \mathcal{U}_{m(k^+, k^-)}^- \right) \quad (3.25)$$

The result of the transformation is a vector with complex conjugate entries. Since all transformed terms can just be added due to the linearity of the transformation, the result \mathcal{M}_1 will have complex conjugate entries

$$\mathcal{M} = \begin{pmatrix} \mathcal{M}^+ \\ \mathcal{M}^- \end{pmatrix} = \begin{pmatrix} \overline{\mathcal{M}^-} \\ \overline{\mathcal{M}^+} \end{pmatrix} \quad (3.26)$$

as already suggested in equation 3.20. After the transformation, all terms will be expanded and summarized with respect to the new coordinates $(s^+)^{k^+} (s^-)^{k^-}$ giving the new Taylor expansion coefficient $\mathcal{S}_{m(k^+, k^-)}$ where $m = k^+ + k^-$.

The two components (\pm) of the new map \mathcal{M}_1^\pm look like this:

$$\mathcal{M}_1^\pm = e^{\pm i\mu} s^\pm + \sum_{m=2}^{m_{max}} \sum_{k^++k^-=m} \mathcal{S}_{m(k^+, k^-)}^\pm (s^+)^{k^+} (s^-)^{k^-} \quad (3.27)$$

$$\text{with } \mathcal{S}_2 = \mathcal{S}_{2(2,0)}(s^+)^2 + \mathcal{S}_{2(1,1)}s^+s^- + \mathcal{S}_{2(0,2)}(s^-)^2 \quad (3.28)$$

$$= \begin{pmatrix} (s^+ | s^+ s^+) \\ (s^- | s^+ s^+) \end{pmatrix} (s^+)^2 + \begin{pmatrix} (s^+ | s^+ s^-) \\ (s^- | s^+ s^-) \end{pmatrix} s^+ s^- + \begin{pmatrix} (s^+ | s^- s^-) \\ (s^- | s^- s^-) \end{pmatrix} (s^-)^2 \quad (3.29)$$

3.1.2 The non-linear transformation

The diagonalization is followed by the nonlinear transformations, which are the key transformations of the algorithm. The transformations are conducted order by order starting with the 2^{nd} . The process is equivalent for each order and is therefore described in general for the m^{th} -order transformation drawing largely from [6]. The map \mathcal{M}_{m-1} , which is already simplified up to order $m-1$, is transformed as follows: $\mathcal{A}_m \circ \mathcal{M}_{m-1} \circ \mathcal{A}_m^{-1}$, where $\mathcal{A}_m = \mathcal{I} + \mathcal{T}_m$ and \mathcal{A}_m^{-1} [6, 7.60+61]:

$$\mathcal{A}_m^{-1} = \mathcal{I} - \mathcal{T}_m + \mathcal{T}_m^2 - \mathcal{T}_m^3 + \dots \quad (3.30)$$

Since only the m^{th} -order of \mathcal{M}_{m-1} is relevant for the determination of the m^{th} -order transformation, all higher order terms can be ignored. The transformation yields the following terms of m^{th} order [6, cf 7.62]:

$$\mathcal{A}_m \circ \mathcal{M}_{m-1} \circ \mathcal{A}_m^{-1} =_m (\mathcal{I} + \mathcal{T}_m) \circ (\mathcal{R} + \mathcal{S}) \circ (\mathcal{I} - \mathcal{T}_m + \cancel{\mathcal{T}_m^2} - \cancel{\mathcal{T}_m^3} + \dots) \quad (3.31)$$

$$=_m (\mathcal{I} + \mathcal{T}_m) \circ (\mathcal{R} \circ (\mathcal{I} - \mathcal{T}_m) + \mathcal{S} \circ (\mathcal{I} - \mathcal{T}_m)) \quad (3.32)$$

$$=_m (\mathcal{I} + \mathcal{T}_m) \circ (\mathcal{R} - \mathcal{R} \circ \mathcal{T}_m + \mathcal{S}) \quad (3.33)$$

$$=_m \mathcal{R} - \mathcal{R} \circ \mathcal{T}_m + \mathcal{S} + \mathcal{T}_m \circ (\mathcal{R} - \cancel{\mathcal{R} \circ \mathcal{T}_m} + \mathcal{S}) \quad (3.34)$$

$$=_m \mathcal{R} + \mathcal{S}_{<m} + \mathcal{S}_m + \cancel{\mathcal{S}_{>m}} + [\mathcal{T}_m, \mathcal{R}] \quad (3.35)$$

In equation 3.31, all terms of \mathcal{T}_m^n with $n > 1$ are irrelevant, since they are at least of order m^2 . In equation 3.32, the term $\mathcal{S} \circ \mathcal{T}_m$ was canceled for the same reason - the resulting expression is at least of order $m+1$, just like the term $\mathcal{T}_m \circ \mathcal{S}$ in equation 3.34. In that same equation, the term $\mathcal{T}_m \circ \mathcal{R} \circ \mathcal{T}_m$ is irrelevant, because it is at least of order m^2 . The term $\mathcal{S}_{>m}$ in equation 3.35 denotes only terms of order $> m$ and therefore is also canceled. The goal is to find \mathcal{T}_m , such that the commutator $\mathcal{C}_m = [\mathcal{T}_m, \mathcal{R}] = -\mathcal{S}_m$, to eliminate all terms of order m . This is in general not always possible and in the next steps, it will become more apparent which terms of \mathcal{S}_m cannot be eliminated. Similar to \mathcal{S}_m , the j^{th} -component of \mathcal{T}_m can be written as:

$$\mathcal{T}_{m,j} = \sum_{\|\vec{k}^+ + \vec{k}^-\|_1 = m} \left(\mathcal{T}_{m,j}^{\pm} | \vec{k}^+, \vec{k}^- \right) \prod_{l=1}^v (s_l^+)^{k_l^+} (s_l^-)^{k_l^-} \quad (3.36)$$

Hence, the j^{th} -component of the two parts of the commutator can be written as follows:

$$(\mathcal{T}_m \circ \mathcal{R})_j = \sum_{\|\vec{k}^+ + \vec{k}^-\|_1 = m} \left(\mathcal{T}_{m,j}^\pm | \vec{k}^+, \vec{k}^- \right) \prod_{l=1}^{\nu} \left(r_l e^{+i\mu_l s_l^+} \right)^{k_l^+} \left(r_l e^{-i\mu_l s_l^-} \right)^{k_l^-} \quad (3.37)$$

$$= \sum_{\|\vec{k}^+ + \vec{k}^-\|_1 = m} \left(\mathcal{T}_{m,j}^\pm | \vec{k}^+, \vec{k}^- \right) e^{i\vec{\mu}(\vec{k}^+ - \vec{k}^-)} \prod_{l=1}^{\nu} r_l^{(k_l^+ + k_l^-)} (s_l^+)^{k_l^+} (s_l^-)^{k_l^-} \quad (3.38)$$

$$(\mathcal{R} \circ \mathcal{T}_m)_j = r_j e^{\pm i\mu_j} \mathcal{T}_{m,j} \quad (3.39)$$

Combining both to $(\mathcal{T}_m \circ \mathcal{R} - \mathcal{R} \circ \mathcal{T}_m)_j = C_{m,j}$ results in [6, cf 7.64]:

$$C_{m,j} = \sum_{\|\vec{k}^+ + \vec{k}^-\|_1 = m} \left(\mathcal{C}_{m,j}^\pm | \vec{k}^+, \vec{k}^- \right) \prod_{l=1}^{\nu} (s_l^+)^{k_l^+} (s_l^-)^{k_l^-} \quad (3.40)$$

$$\left(\mathcal{C}_{m,j}^\pm | \vec{k}^+, \vec{k}^- \right) = \left(\mathcal{T}_{m,j}^\pm | \vec{k}^+, \vec{k}^- \right) \left(e^{i\vec{\mu}(\vec{k}^+ - \vec{k}^-)} \left(\prod_{l=1}^{\nu} r_l^{(k_l^+ + k_l^-)} \right) - r_j e^{\pm i\mu_j} \right) \quad (3.41)$$

It follows immediately, that the term associated with $\left(\mathcal{S}_{m,j}^\pm | \vec{k}^+, \vec{k}^- \right)$ can only be eliminated, if the factor $\left(\mathcal{C}_{m,j}^\pm | \vec{k}^+, \vec{k}^- \right)$ is nonzero, in which case $\left(\mathcal{T}_{m,j}^\pm | \vec{k}^+, \vec{k}^- \right)$ is given by [6, cf 7.72]:

$$\left(\mathcal{T}_{m,j}^\pm | \vec{k}^+, \vec{k}^- \right) = \frac{- \left(\mathcal{S}_{m,j}^\pm | \vec{k}^+, \vec{k}^- \right)}{\left(e^{i\vec{\mu}(\vec{k}^+ - \vec{k}^-)} \left(\prod_{l=1}^{\nu} r_l^{(k_l^+ + k_l^-)} \right) - r_j e^{\pm i\mu_j} \right)} \quad (3.42)$$

$\left(\mathcal{C}_{m,j}^\pm | \vec{k}^+, \vec{k}^- \right)$ given in equation 3.41 is zero under the following condition [6]:

$$e^{i\vec{\mu}(\vec{k}^+ - \vec{k}^-)} \left(\prod_{l=1}^{\nu} r_l^{(k_l^+ + k_l^-)} \right) = r_j e^{\pm i\mu_j} \quad (3.43)$$

For non-symplectic systems, the further approach can be found in [6]. For symplectic systems, where $(r_j = 1) \wedge (\mu_j \in \mathbb{R}) \forall j$, the condition in equation 3.43 simplifies to

$$e^{i\vec{\mu}(\vec{k}^+ - \vec{k}^-)} = e^{\pm i\mu_j} \quad (3.44)$$

and even further to [6, cf 7.65]:

$$\mu_j (k_j^+ - k_j^- \mp 1) + \sum_{l \neq j} \mu_l (\vec{k}^+ - \vec{k}^-) = 0 \pmod{2\pi} \quad (3.45)$$

$$\langle \vec{\mu}, \vec{k}^+ - \vec{k}^- \mp \vec{e}_j \rangle = 0 \pmod{2\pi} \quad (3.46)$$

In the trivial case, the condition is met for:

$$k_j^+ - k_j^- = \pm 1 \text{ and } k_l^+ = k_l^- \forall l \neq j \quad (3.47)$$

which yields terms that are responsible for the amplitude-dependent tune shifts and is therefore the heart of the Normal Form Algorithm. This condition is purely mathematical. All other non-trivial solutions to equation 3.46 are of a physical nature, which means that, purely mathematically it is quite impossible to find a linear combination of integer multiples of the eigenvalues μ_l so that the result is exactly $\pm\mu_j(\text{mod } 2\pi)$ even for orders $m \gg 10$. From a computational/physical point of view it is sufficient, for the linear combination to be close enough to $\pm\mu_j(\text{mod } 2\pi)$ for $(\mathcal{T}_{m,j}^\pm | \vec{k}^+, \vec{k}^-)$ to 'blow up'. This case represents higher order resonances, which are of a physical nature.

Considering the first condition it becomes apparent, that the only terms that are mathematically impossible to remove are:

$$\begin{aligned} & \left(\mathcal{S}_{m,j}^+ | \vec{k} + \vec{e}_j, \vec{k} \right) (s_j^+) \prod_{l=1}^{\nu} (s_l^+ s_l^-)^{k_l} \\ & \left(\mathcal{S}_{m,j}^- | \vec{k}, \vec{k} + \vec{e}_j \right) (s_j^-) \prod_{l=1}^{\nu} (s_l^+ s_l^-)^{k_l} \end{aligned} \quad \text{for } m = \|\vec{2k} + \vec{e}_j\|_1 \quad (3.48)$$

which only occur for odd orders.

It is important to recognize that the nonlinear terms $\mathcal{S}_{>m}$ with a higher order than the order of the current coordinate transformation m are very likely to change due to the m^{th} -order coordinate transformation.

The following example of the non-linear 2^{nd} order transformation for $\nu = 1$ will illustrate how higher orders like the 3^{rd} order are affected. In order to eliminate all \mathcal{S}_2 -terms with the 2^{nd} order transformation, \mathcal{T}_2 in the transformation $\mathcal{A}_2 = \mathcal{I} + \mathcal{T}_2$ has to be

$$(\mathcal{T}_2^\pm | k^+, k^-) = \frac{-(\mathcal{S}_2^\pm | k^+, k^-)}{(e^{i\mu(k^+ - k^-)} - e^{\pm i\mu})} \quad (3.49)$$

according to equation 3.42. To study how the transformation affects the higher orders, the

second order transformation is considered up to 3rd-order.

$$\mathcal{M}_2 =_3 \mathcal{A}_2 \circ \mathcal{M}_1 \circ \mathcal{A}_2^{-1} \quad (3.50)$$

$$=_3 (\mathcal{I} + \mathcal{T}_2) \circ (\mathcal{R} + \mathcal{S}_2 + \mathcal{S}_3) \circ (\mathcal{I} - \mathcal{T}_2 + \cancel{\mathcal{T}_2^2} \dots) \quad (3.51)$$

$$=_3 (\mathcal{I} + \mathcal{T}_2) \circ (\mathcal{R} \circ (\mathcal{I} - \mathcal{T}_2) + \mathcal{S}_2 \circ (\mathcal{I} - \mathcal{T}_2) + \mathcal{S}_3) \quad (3.52)$$

$$=_3 (\mathcal{I} + \mathcal{T}_2) \circ (\mathcal{R} - \mathcal{R} \circ \mathcal{T}_2 + \mathcal{S}_2 + \mathcal{S}_{2 \rightarrow 3} + \mathcal{S}_3) \quad (3.53)$$

$$=_3 \mathcal{R} - \mathcal{R} \circ \mathcal{T}_2 + \mathcal{S}_2 + \mathcal{S}_{2 \rightarrow 3} + \mathcal{S}_3 \quad (3.54)$$

$$+ \mathcal{T}_2 \circ (\mathcal{R} - \mathcal{R} \circ \mathcal{T}_2 + \cancel{\mathcal{S}_2 + \mathcal{S}_{2 \rightarrow 3}} + \mathcal{S}_3) \quad (3.55)$$

$$=_3 \mathcal{R} - \mathcal{R} \circ \mathcal{T}_2 + \mathcal{S}_2 + \mathcal{S}_{2 \rightarrow 3} + \mathcal{S}_3 + \mathcal{T}_2 \circ \mathcal{R} \quad (3.56)$$

$$=_3 \mathcal{R} + \underbrace{\mathcal{S}_2 + [\mathcal{T}_2 \circ \mathcal{R}]}_{=0} + \underbrace{\mathcal{S}_3 + \mathcal{S}_{2 \rightarrow 3}}_{\mathcal{S}_{3,new}} \quad (3.57)$$

All the crossed-out terms in equation 3.51 and 3.55 represent parts that won't contribute to the result up to order 3, each of them is at least of order $m + 1$. As a result, there is a new 3rd-order part, which consists of the unchanged old \mathcal{S}_3 and a new $\mathcal{S}_{2 \rightarrow 3}$ -term. In the following calculation, the new term is examined further.

$$\begin{aligned} \mathcal{S}_{2 \rightarrow 3} &= \mathcal{S}_2 \circ (\mathcal{I} - \mathcal{T}_2) - \mathcal{S}_2 \\ &= \mathcal{S}_{2(2,0)} (s^+ - \mathcal{T}_2^+)^2 + \mathcal{S}_{2(0,2)} (s^- - \mathcal{T}_2^-)^2 \\ &\quad + \left(\mathcal{S}_{2(1,1)} (s^+ - \mathcal{T}_2^+) (s^- - \mathcal{T}_2^-) \right)_3 - \mathcal{S}_2 \\ &= \mathcal{S}_{2(2,0)} (s^+)^2 + \mathcal{S}_{2(1,1)} s^+ s^- + \mathcal{S}_{2(0,2)} (s^-)^2 - \mathcal{S}_2 \\ &\quad + \mathcal{S}_{2(2,0)} (\mathcal{T}_2^+)^2 + \mathcal{S}_{2(1,1)} \mathcal{T}_2^+ \mathcal{T}_2^- + \mathcal{S}_{2(0,2)} (\mathcal{T}_2^-)^2 \\ &\quad - 2\mathcal{S}_{2(2,0)} \mathcal{T}_2^+ s^+ - \mathcal{S}_{2(1,1)} (\mathcal{T}_2^+ s^- + \mathcal{T}_2^- s^+) - 2\mathcal{S}_{2(0,2)} \mathcal{T}_2^- s^- \\ &= -2\mathcal{S}_{2(2,0)} \mathcal{T}_2^+ s^+ - \mathcal{S}_{2(1,1)} (\mathcal{T}_2^+ s^- + \mathcal{T}_2^- s^+) - 2\mathcal{S}_{2(0,2)} \mathcal{T}_2^- s^- \end{aligned} \quad (3.58)$$

where the \mathcal{T}_2^2 terms can be neglected because they are of order 4. Note that the \mathcal{T}_2 -terms also depend on \mathcal{S}_2 as equation 3.49 shows. It becomes apparent that the transformation has a significant

effect on the higher order terms and therefore it is necessary to determine an upper bound for the order to which the normal form is calculated beforehand.

For the next step, the 3^{rd} -order correction, the same calculations are done. Assuming that the truncation order $m_{max} = 3$, it will not be necessary to calculate the transformation explicitly, because it is known from equation 3.48, which terms will cancel out and the changes to the higher orders are irrelevant. Only the terms $\mathcal{S}_{3,new(2,1)}^+$ and $\mathcal{S}_{3,new(1,2)}^-$ cannot be canceled, due to the condition in equation 3.47. Therefore the remaining parts of equation 3.58 are given as follows:

$$\begin{aligned}\mathcal{S}_{2 \rightarrow 3(2,1)}^+ &= -2\mathcal{S}_{2(2,0)}^+ \mathcal{T}_{2(1,1)}^+ - \mathcal{S}_{2(1,1)}^+ \left(\mathcal{T}_{2(2,0)}^+ + \mathcal{T}_{2(1,1)}^- \right) - 2\mathcal{S}_{2(0,2)}^+ \mathcal{T}_{2(2,0)}^- \\ &= \frac{2\mathcal{S}_{2(2,0)}^+ \mathcal{S}_{2(1,1)}^+}{1 - e^{i\mu}} + \frac{\mathcal{S}_{2(1,1)}^+ \mathcal{S}_{2(2,0)}^+}{e^{2i\mu} - e^{i\mu}} + \frac{\mathcal{S}_{2(1,1)}^+ \mathcal{S}_{2(1,1)}^-}{1 - e^{-i\mu}} + \frac{2\mathcal{S}_{2(0,2)}^+ \mathcal{S}_{2(2,0)}^-}{e^{2i\mu} - e^{-i\mu}}\end{aligned}\quad (3.59)$$

$$\begin{aligned}\mathcal{S}_{2 \rightarrow 3(1,2)}^- &= -2\mathcal{S}_{2(2,0)}^- \mathcal{T}_{2(0,2)}^+ - \mathcal{S}_{2(1,1)}^- \left(\mathcal{T}_{2(1,1)}^+ + \mathcal{T}_{2(0,2)}^- \right) - 2\mathcal{S}_{2(0,2)}^- \mathcal{T}_{2(1,1)}^- \\ &= \frac{2\mathcal{S}_{2(2,0)}^- \mathcal{S}_{2(0,2)}^+}{e^{-2i\mu} - e^{i\mu}} + \frac{\mathcal{S}_{2(1,1)}^- \mathcal{S}_{2(1,1)}^+}{1 - e^{i\mu}} + \frac{\mathcal{S}_{2(1,1)}^- \mathcal{S}_{2(0,2)}^-}{e^{-2i\mu} - e^{-i\mu}} + \frac{2\mathcal{S}_{2(0,2)}^- \mathcal{S}_{2(1,1)}^-}{1 - e^{-i\mu}}\end{aligned}\quad (3.60)$$

Note that complex conjugate relation still holds with: $\mathcal{S}_{2 \rightarrow 3(2,1)}^+ = \overline{\mathcal{S}_{2 \rightarrow 3(1,2)}^-}$. Unfortunately, the expression of $\mathcal{S}_{2 \rightarrow 3(2,1)}^+$ in terms of \mathcal{U}_2 is already very long and therefore not given. This shows how the computer-based calculation using the DA framework in COSY INFINITY is essential. The original \mathcal{S}_3 -term, which is the entire $\mathcal{S}_{3,new}$ -term for $\mathcal{U}_2 = 0$, can be derived in a short formula in terms of \mathcal{U}_3 :

$$\begin{aligned}\mathcal{S}_{3(2,1)}^+ &= \frac{1}{4} \left(\gamma(3\mathcal{U}_{3(0,3)}^- + \mathcal{U}_{3(1,2)}^+) + \beta(3\mathcal{U}_{3(3,0)}^+ + \mathcal{U}_{3(2,1)}^-) - 2\alpha(\mathcal{U}_{3(2,1)}^+ + \mathcal{U}_{3(1,2)}^-) \right) \\ &\quad - \frac{3i}{4} \left(\mathcal{U}_{3(0,3)}^+ \gamma^2 - \mathcal{U}_{3(3,0)}^- \beta^2 + \alpha(\gamma(\mathcal{U}_{3(0,3)}^- - \mathcal{U}_{3(1,2)}^+) + \beta(\mathcal{U}_{3(2,1)}^- - \mathcal{U}_{3(3,0)}^+)) \right) \\ &\quad - \frac{i}{4} (\mathcal{U}_{3(2,1)}^+ + \mathcal{U}_{3(1,2)}^-) (\beta\gamma + \alpha^2) = \overline{\mathcal{S}_{3(1,2)}^-}\end{aligned}\quad (3.61)$$

As previously noted, all terms surviving after the 3^{rd} -order transformation are the following:

$$\mathcal{M}_3 = \begin{pmatrix} \mathcal{M}^+ \\ \mathcal{M}^- \end{pmatrix} =_3 \begin{pmatrix} s^+ \left(e^{+i\mu} + \mathcal{S}_{3,new(2,1)}^+ s^+ s^- \right) \\ s^- \left(e^{-i\mu} + \mathcal{S}_{3,new(1,2)}^- s^+ s^- \right) \end{pmatrix}\quad (3.62)$$

3.1.3 Transformation to Normal Form coordinates

In the last step, the simplified map is finally transformed into Normal Form. After the m_{max} -order transformation, the j^{th} -component of \mathcal{M} has the following form [6, 7.66].

$$\begin{pmatrix} \mathcal{M}_j^+ \\ \mathcal{M}_j^- \end{pmatrix} = \begin{pmatrix} s_j^+ \left(e^{+i\mu} + \sum_{m=\|2\vec{k}+\vec{e}_j\|_1}^{m_{max}} \left(\mathcal{S}_{m,j}^+ | \vec{k} + \vec{e}_j, \vec{k} \right) \prod_{l=1}^v (s_l^+ s_l^-)^{k_l} \right) \\ s_j^- \left(e^{-i\mu} + \sum_{m=\|2\vec{k}+\vec{e}_j\|_1}^{m_{max}} \left(\mathcal{S}_{m,j}^- | \vec{k}, \vec{k} + \vec{e}_j \right) \prod_{l=1}^v (s_l^+ s_l^-)^{k_l} \right) \end{pmatrix} \quad (3.63)$$

$$= \begin{pmatrix} s_j^+ f_j (s_1^+ s_1^-, \dots, s_l^+ s_l^-, \dots, s_v^+ s_v^-) \\ s_j^- \bar{f}_j (s_1^+ s_1^-, \dots, s_l^+ s_l^-, \dots, s_v^+ s_v^-) \end{pmatrix} \quad (3.64)$$

The simplification to f_j and its complex conjugate \bar{f}_j above is possible due to the complex conjugate relationship between \mathcal{M}_j^+ and \mathcal{M}_j^- shown in equation 3.20. Rewriting $f_j = a_j e^{i\phi_j}$ yields

$$\mathcal{M}_j^\pm = s_j^\pm a_j e^{\pm i\phi_j} (s_1^+ s_1^-, \dots, s_l^+ s_l^-, \dots, s_v^+ s_v^-) \quad (3.65)$$

Since the original map only operates in real space, but the current basis consists of complex conjugate pairs, a real basis t_j^\pm from the real and imaginary part of the current complex basis s_j^\pm is introduced as follows [6, cf 7.58]:

$$t_j^+ = (s_j^+ + s_j^-) / 2 \quad (3.66)$$

$$t_j^- = (s_j^+ - s_j^-) / 2i \quad (3.67)$$

The associated transfer matrix to the real basis is

$$\mathcal{A}_j = \frac{1}{\sqrt{2}} \begin{pmatrix} 1 & 1 \\ -i & i \end{pmatrix} = \begin{pmatrix} (t_j^+ | s_j^+) & (t_j^+ | s_j^-) \\ (t_j^- | s_j^+) & (t_j^- | s_j^-) \end{pmatrix} \quad (3.68)$$

and the inverse relation accordingly [6, cf 7.59]:

$$s_j^\pm = t_j^+ \pm i t_j^- \quad (3.69)$$

$$\mathcal{A}_j^{-1} = \frac{1}{\sqrt{2}} \begin{pmatrix} 1 & i \\ 1 & -i \end{pmatrix} = \begin{pmatrix} (s_j^+ | t_j^+) & (s_j^+ | t_j^-) \\ (s_j^- | t_j^+) & (s_j^- | t_j^-) \end{pmatrix} \quad (3.70)$$

The amplitude ϕ_j consists of $s_j^+ s_j^-$ terms, which are summarized to r_j^2 [6, 7.67] using equation 3.69:

$$s_j^+ s_j^- = (t_j^+ + it_j^-) (t_j^+ - it_j^-) = (t_j^+)^2 + (t_j^-)^2 = r_j^2 \quad (3.71)$$

The transformation from the simplified map to the real basis coordinates t_j^\pm in Normal Form is conducted as follows [6, cf 7.68]:

$$\begin{aligned} \mathcal{M}_{j,NF}^\pm &= \mathcal{A}_j \circ \mathcal{M}_j^\pm \circ \mathcal{A}_j^{-1} = \begin{pmatrix} 1/2 & 1/2 \\ 1/2i & -1/2i \end{pmatrix} \\ &\cdot (t_j^\pm \pm it_j^\mp) a_j e^{\pm i\phi_j} \left((t_1^+)^2 + (t_1^-)^2, \dots, (t_j^+)^2 + (t_j^-)^2, \dots, (t_v^+)^2 + (t_v^-)^2 \right) \\ &= \frac{a_j}{2} \begin{pmatrix} t_j^+ (e^{+i\phi_j} + e^{-i\phi_j}) + t_j^- i (e^{+i\phi_j} - e^{-i\phi_j}) \\ -t_j^+ i (e^{+i\phi_j} - e^{-i\phi_j}) + t_j^- (e^{+i\phi_j} + e^{-i\phi_j}) \end{pmatrix} \\ &= a_j \begin{pmatrix} \cos(\phi_j) & -\sin(\phi_j) \\ \sin(\phi_j) & \cos(\phi_j) \end{pmatrix} \cdot \begin{pmatrix} t_j^+ \\ t_j^- \end{pmatrix} \end{aligned} \quad (3.72)$$

Equation 3.72 illustrates the properties of the Normal Form best, which consists of circular curves in phase space with only with amplitude depended tune shifts. This form was already referred to as Normal Form in examples in section 1.2.6, where the solutions were already circles in phase space. The constant radius of the curve can be shown by:

$$\left(\mathcal{M}_j^+ \right)^2 + \left(\mathcal{M}_j^- \right)^2 = a_j^2 r_j^2 = \text{const.} \quad (3.73)$$

Furthermore, the only amplitude-dependent tune shifts are constant along one curve, which makes the Normal Form rotationally invariant:

$$\mathcal{M}_{NF} = \mathcal{R} \circ \mathcal{M}_{NF} \circ \mathcal{R}^{-1} \quad (3.74)$$

The Normal Form output of the COSY INFINITY calculation will be in the form of a Taylor expansion

$$\mathcal{M}_{j,NF}^{\pm} = a_j \begin{pmatrix} t_j^+ \left(\cos \mu_j + \mathcal{N}_{2c} r_j^2 + \mathcal{N}_{4c} r_j^4 \dots \right) - t_j^- \left(\sin \mu_j + \mathcal{N}_{2s} r_j^2 + \mathcal{N}_{4s} r_j^4 \dots \right) \\ t_j^+ \left(\sin \mu_j + \mathcal{N}_{2s} r_j^2 + \mathcal{N}_{4s} r_j^4 \dots \right) + t_j^- \left(\cos \mu_j + \mathcal{N}_{2c} r_j^2 + \mathcal{N}_{4c} r_j^4 \dots \right) \end{pmatrix} \quad (3.75)$$

where $r^2 = (t_j^+)^2 + (t_j^-)^2$.

From this form the tunes and tune shifts can be calculated with

$$\phi = \arccos \left(\cos \mu + \mathcal{N}_{2c} r^2 + \mathcal{N}_{4c} r^4 \dots \right) = \arcsin \left(\sin \mu + \mathcal{N}_{2s} r^2 + \mathcal{N}_{4s} r^4 \dots \right) \quad (3.76)$$

which takes the following form in the COSY INFINITY representation:

$$\arccos \left(\cos \mu + r^2 f(r^2) \right) = \mu - \frac{f(r^2)}{\sin \mu} r^2 - \frac{\cos \mu f^2(r^2)}{2 \sin^3 \mu} r^4 - \frac{(2 \cos^2 \mu + 1) f^3(r^2)}{6 \sin^5 \mu} r^6 \dots \quad (3.77)$$

Transforming the map \mathcal{M}_3 to Normal Form coordinates yields:

$$\mathcal{NF}_3 = \mathcal{A} \circ \mathcal{M}_3 \circ \mathcal{A}^{-1} \quad (3.78)$$

$$= \frac{1}{2} \begin{pmatrix} 1 & 1 \\ -i & i \end{pmatrix} \begin{pmatrix} (t^+ + it^-) \left(e^{+i\mu} + \frac{1}{2} \mathcal{S}_{3,new(2,1)}^+ \left((t^+)^2 + (t^-)^2 \right) \right) \\ (t^+ - it^-) \left(e^{-i\mu} + \frac{1}{2} \mathcal{S}_{3,new(1,2)}^- \left((t^+)^2 + (t^-)^2 \right) \right) \end{pmatrix} \quad (3.79)$$

$$= \frac{1}{2} \begin{pmatrix} \left(e^{+i\mu} + e^{-i\mu} + \frac{1}{2} \left(\mathcal{S}_{3,new(2,1)}^+ + \mathcal{S}_{3,new(1,2)}^- \right) r^2 \right) t^+ \\ -i \left(e^{+i\mu} - e^{-i\mu} + \frac{1}{2} \left(\mathcal{S}_{3,new(2,1)}^+ - \mathcal{S}_{3,new(1,2)}^- \right) r^2 \right) t^+ \end{pmatrix} \quad (3.80)$$

$$- \frac{1}{2i} \begin{pmatrix} \left(e^{+i\mu} - e^{-i\mu} + \frac{1}{2} \left(\mathcal{S}_{3,new(2,1)}^+ - \mathcal{S}_{3,new(1,2)}^- \right) r^2 \right) t^- \\ -i \left(e^{+i\mu} + e^{-i\mu} + \frac{1}{2} \left(\mathcal{S}_{3,new(2,1)}^+ + \mathcal{S}_{3,new(1,2)}^- \right) r^2 \right) t^- \end{pmatrix} \quad (3.81)$$

$$= \begin{pmatrix} \left(\cos \mu + \frac{1}{2} \Re \left(\mathcal{S}_{3,new(2,1)}^+ \right) r^2 \right) t^+ - \left(\sin \mu + \frac{1}{2} \Im \left(\mathcal{S}_{3,new(2,1)}^+ \right) r^2 \right) t^- \\ \left(\sin \mu + \frac{1}{2} \Im \left(\mathcal{S}_{3,new(2,1)}^+ \right) r^2 \right) t^+ + \left(\cos \mu + \frac{1}{2} \Re \left(\mathcal{S}_{3,new(2,1)}^+ \right) r^2 \right) t^- \end{pmatrix} \quad (3.82)$$

Comparing equation 3.82 to the Normal Form representation in equation 3.72 yields:

$$\cos \phi = \cos \mu + \frac{1}{2} \operatorname{Re} \left(\mathcal{S}_{3,new(2,1)}^+ \right) r^2 \quad (3.83)$$

$$\sin \phi = \sin \mu + \frac{1}{2} \operatorname{Im} \left(\mathcal{S}_{3,new(2,1)}^+ \right) r^2 \quad (3.84)$$

using the arccos or arcsin, respectively in a Taylor expansion at $r = 0$ up to the 3^{rd} -order yields:

$$\phi = \mu - \frac{\operatorname{Re} \left(\mathcal{S}_{3,new(2,1)}^+ \right)}{2 \sin \mu} r^2 = \mu + \frac{\operatorname{Im} \left(\mathcal{S}_{3,new(2,1)}^+ \right)}{2 \cos \mu} r^2 \quad (3.85)$$

Assuming that all second order terms of the original map are zero ($\mathcal{U}_2 = 0$), the tunes

$$\phi = \mu - \frac{r^2}{8 \sin \mu} \left(\gamma(3\mathcal{U}_{3(0,3)}^- + \mathcal{U}_{3(1,2)}^+) + \beta(3\mathcal{U}_{3(3,0)}^+ + \mathcal{U}_{3(2,1)}^-) - 2\alpha(\mathcal{U}_{3(2,1)}^+ + \mathcal{U}_{3(1,2)}^-) \right) \quad (3.86)$$

can be simply calculated using equation 3.61.

In most applications it is useful to know r_j^2 in terms of the original coordinates. The transformation \mathcal{A} transforms $(\vec{q}, \vec{p}) \rightarrow (\vec{t}^+(\vec{q}, \vec{p}), \vec{t}^-(\vec{q}, \vec{p}))$ and consists of the composition of all the single transformations for the Normal Form, namely:

$$\mathcal{A} = \mathcal{A}_{mmax} \circ \mathcal{A}_{mmax-1} \circ \dots \circ \mathcal{A}_2 \circ \mathcal{A}_1 \circ \mathcal{A}_0 \quad (3.87)$$

For the symplectic example case up to 3^{rd} order with $\beta \neq 0$ and $\mathcal{U}_2 = 0$ the transformation is already represents a very extensive formula with $(t^+, t^-) = \mathcal{A}_3 \circ \mathcal{A}_1(q, p) =$

$$\frac{-1}{\sqrt{2\beta}} \left(\mathcal{I} - \sum_{k^++k^-=3} \frac{(\mathcal{S}_2^\pm | k^+, k^-)}{(e^{i\mu(k^+-k^-)} - e^{\pm i\mu})} (s^+)^{k^+} (s^-)^{k^-} \right) \circ \begin{pmatrix} 1+i\alpha & i\beta \\ 1-i\alpha & -i\beta \end{pmatrix} \begin{pmatrix} q \\ p \end{pmatrix} \quad (3.88)$$

Luckily, all these procedures can be conducted fully automatically in COSY INFINITY. The Normal Form Algorithm is a very intense analytic process that is only practically usable due to the DA based implementation in COSY INFINITY.

CHAPTER 4

PROTRACTING CALCULATIONS IN PERTURBATION THEORY

To show how painful an analytic approach to solving a perturbed harmonic oscillator system can be, the following section will present such an example. In the course of the calculation the tediousness and the increase in complexity should become apparent, even though both examples are on the rather non-complex side of the difficulty spectrum. One main process of the approach is the method called 'variation of parameters', which is introduced in the following subsection.

4.1 Variation of parameters

The variation of parameters is a well-known technique to obtain solutions of an inhomogeneous ODE given the solution to the homogeneous case. Therefore, the following inhomogeneous differential equation with a linear homogeneous part is considered:

$$\dot{\vec{z}}(t) = \hat{L}\vec{z}(t) + \vec{f}(t) \quad (4.1)$$

where \hat{L} is the linear coupling matrix and \vec{f} is the nonlinear inhomogeneity. The solution to the linear homogeneous problem $\dot{\vec{z}}(t) = \hat{L}\vec{z}(t)$ is assumed to be known:

$$\vec{z}_{hom}(t) = \hat{Z}(t)\vec{c} \quad (4.2)$$

where \vec{c} is just a parameter, that can potentially represent the initial conditions and $\hat{Z}(t)$ is the time dependent solution matrix. Substituting this solution back in the homogeneous ODE yields the connection of solution matrix \hat{Z} and the ODE-coupling matrix \hat{L} :

$$\dot{\vec{z}}_{hom}(t) = \dot{\hat{Z}}(t)\vec{c} \stackrel{!}{=} \hat{L}\vec{z}_{hom}(t) = \hat{L}\hat{Z}(t)\vec{c} \quad \Rightarrow \dot{\hat{Z}}(t) = \hat{L}\hat{Z}(t) \quad (4.3)$$

To solve equation 4.1, the solution in equation 4.2 is modified by the method of variation of the parameter. In this case, the constant parameter \vec{c} is given a variation, which means it is changed from a constant to a time dependent variable $\vec{v}(t)$, so that

$$\vec{z}_{par}(t) = \hat{Z}(t)\vec{v}(t) \quad (4.4)$$

where $\vec{z}_{par}(t)$ represents a particular solution to the inhomogeneous case. Using this ansatz for equation 4.1 yields:

$$\dot{\vec{z}}_{par}(t) = \dot{\hat{Z}}(t)\vec{v}(t) + \hat{Z}(t)\dot{\vec{v}}(t) \stackrel{4.3}{=} \hat{L}\hat{Z}(t)\vec{v}(t) + \hat{Z}(t)\dot{\vec{v}}(t) = \hat{L}\vec{z}_{par}(t) + \vec{f}(t) \quad (4.5)$$

Therefore,

$$\hat{Z}(t)\dot{\vec{v}}(t) = \vec{f}(t) \quad \Rightarrow \quad \vec{v}(t) = \int_0^t \hat{Z}^{-1}(t')\vec{f}(t')dt' + \vec{v}(0) \quad (4.6)$$

Solving the integral means solving for \vec{z}_{par} , whereas the complexity of this integral may vary from trivial to unsolvable, depending on the integrand $\hat{Z}^{-1}(t)\vec{f}(t)$. The solution for equation 4.1 is hence:

$$\vec{z} = \vec{z}_{hom} + \vec{z}_{par} = \hat{Z}(\vec{c} + \vec{v}(t)) \quad (4.7)$$

4.2 Example of an analytical perturbation theory approach

To illustrate the method of variation of parameters, two problems shall be discussed in the following section. The solutions will be approximated order by order. The first problem is almost trivial but makes the process clearer. The actual solution has a very simple form and makes the comparison to the order by order approximation of the method possible. The second example is only a slight variation of the first one, which removes the symmetry in the problem. This causes a dramatic increase in the analytic complexity concerning the solving of the integral from equation 4.1.

4.2.1 Symmetric perturbed harmonic oscillator example

First, the symmetrically perturbed harmonic oscillator, that is already known from the example in the Flow Operator section 1.2.6.1, is considered. The solution to this problem is given by

$$\underbrace{\begin{pmatrix} x(t) \\ p(t) \end{pmatrix}}_{\vec{z}(t)} = \underbrace{\begin{pmatrix} \cos((1 + \alpha r^2)t) & \sin((1 + \alpha r^2)t) \\ -\sin((1 + \alpha r^2)t) & \cos((1 + \alpha r^2)t) \end{pmatrix}}_{\hat{Z}(t)} \underbrace{\begin{pmatrix} x_0 \\ p_0 \end{pmatrix}}_{\vec{c}_0} \quad (4.8)$$

where $r^2 = x^2 + p^2 = x_0^2 + p_0^2$. Using the sum angular formula and the Taylor expansion at $\alpha r^2 = 0$ the solution can be rewritten as follows:

$$\begin{aligned} \begin{pmatrix} x(t) \\ p(t) \end{pmatrix} &= \begin{pmatrix} \cos(t) \cos(\alpha r^2 t) - \sin(t) \sin(\alpha r^2 t) & \sin(t) \cos(\alpha r^2 t) + \cos(t) \sin(\alpha r^2 t) \\ -\sin(t) \cos(\alpha r^2 t) - \cos(t) \sin(\alpha r^2 t) & \cos(t) \cos(\alpha r^2 t) - \sin(t) \sin(\alpha r^2 t) \end{pmatrix} \begin{pmatrix} x_0 \\ p_0 \end{pmatrix} \\ &= \begin{pmatrix} \cos(t) & \sin(t) \\ -\sin(t) & \cos(t) \end{pmatrix} \begin{pmatrix} x_0 \cos(\alpha r^2 t) + p_0 \sin(\alpha r^2 t) \\ p_0 \cos(\alpha r^2 t) - x_0 \sin(\alpha r^2 t) \end{pmatrix} \\ &= \hat{Z}(t) \begin{pmatrix} x_0 + p_0 \alpha r^2 t - \frac{x_0}{2} (\alpha r^2 t)^2 - \frac{p_0}{6} (\alpha r^2 t)^3 + \frac{x_0}{24} (\alpha r^2 t)^4 + \mathcal{O}(t^5) \\ p_0 - x_0 \alpha r^2 t - \frac{p_0}{2} (\alpha r^2 t)^2 + \frac{x_0}{6} (\alpha r^2 t)^3 + \frac{p_0}{24} (\alpha r^2 t)^4 - \mathcal{O}(t^5) \end{pmatrix} \\ &= \hat{Z}(t) \left(\vec{c}_0 + (\alpha r^2 t) \vec{d}_0 - (\alpha r^2 t)^2 \frac{\vec{c}_0}{2} - (\alpha r^2 t)^3 \frac{\vec{d}_0}{6} + (\alpha r^2 t)^4 \frac{\vec{c}_0}{24} + \mathcal{O}(t^5) \right) \end{aligned} \quad (4.9)$$

The goal of the following calculation is, to step by step calculate the terms of the equation above to show how the perturbation method approaches the solution. The approach starts off with the equations of motions which are given by the Hamiltonian and its Hamilton equations: as follows:

$$H_\alpha = \frac{p^2}{2} + \frac{x^2}{2} + \frac{\alpha}{4} (p^2 + x^2)^2 \quad (4.10)$$

$$\underbrace{\begin{pmatrix} \dot{q} \\ \dot{p} \end{pmatrix}}_{\dot{\vec{z}}(t)} = \begin{pmatrix} \frac{\partial H_\alpha}{\partial p} \\ -\frac{\partial H_\alpha}{\partial q} \end{pmatrix} = \underbrace{\begin{pmatrix} 0 & 1 \\ -1 & 0 \end{pmatrix}}_{\hat{L}} \underbrace{\begin{pmatrix} q \\ p \end{pmatrix}}_{\vec{z}(t)} + \alpha \begin{pmatrix} p^3 + x^2 p \\ -x^3 - p^2 x \end{pmatrix} \quad (4.11)$$

First, the solution to the homogeneous part of the differential equation $\dot{\vec{z}}(t) = \hat{L}\vec{z}(t)$:

$$\underbrace{\begin{pmatrix} x_{hom}(t) \\ p_{hom}(t) \end{pmatrix}}_{\vec{z}_{hom}(t)} = \underbrace{\begin{pmatrix} \cos(t) & \sin(t) \\ -\sin(t) & \cos(t) \end{pmatrix}}_{\hat{Z}(t)} \underbrace{\begin{pmatrix} x_0 \\ p_0 \end{pmatrix}}_{\vec{c}_0} \quad (4.12)$$

is required. Afterwards, the well-known ansatz

$$x_1(t) = x_{hom}(t) + \Delta x_1(t) \quad (4.13)$$

$$p_1(t) = p_{hom}(t) + \Delta p_1(t) \quad (4.14)$$

is substituted in the inhomogeneous ODE from equation 4.11 which yields:

$$\dot{\vec{z}}_{hom} + \Delta \dot{\vec{z}}_1 = \dot{\vec{z}}_1 = \hat{L}\vec{z}_1 + \alpha \begin{pmatrix} p_1^3 + x_1^2 p_1 \\ -x_1^3 - p_1^2 x_1 \end{pmatrix} \quad (4.15)$$

$$= \hat{L}(\vec{z}_{hom} + \Delta \vec{z}_1) + \alpha \begin{pmatrix} p_{hom}^3 + x_{hom}^2 p_{hom} \\ -x_{hom}^3 - p_{hom}^2 x_{hom} \end{pmatrix} + \alpha \mathcal{O}(\Delta x_1, \Delta p_1) \quad (4.16)$$

For the first order calculation, only terms linear to $\Delta x_1, \Delta p_1$ or α are considered, therefore:

$$\underbrace{\begin{pmatrix} \Delta x_1(t) \\ \Delta p_1(t) \end{pmatrix}}_{\Delta \dot{\vec{z}}_1(t)} = \underbrace{\begin{pmatrix} 0 & 1 \\ -1 & 0 \end{pmatrix}}_{\hat{L}} \underbrace{\begin{pmatrix} \Delta x_1(t) \\ \Delta p_1(t) \end{pmatrix}}_{\Delta \vec{z}_1(t)} + \alpha \underbrace{\begin{pmatrix} p_{hom}^3 + x_{hom}^2 p_{hom} \\ -x_{hom}^3 - p_{hom}^2 x_{hom} \end{pmatrix}}_{\vec{f}_0(t)} \quad (4.17)$$

To make the integration from the variation-of-the-parameter method as easy as possible it is useful

to simplify \vec{f}_0 :

$$\vec{f}_0(t) = \begin{pmatrix} (p_0 \cos t - x_0 \sin t)^3 + (x_0 \cos t + p_0 \sin t)^2 (p_0 \cos t - x_0 \sin t) \\ -(x_0 \cos t + p_0 \sin t)^3 - (p_0 \cos t - x_0 \sin t)^2 (x_0 \cos t + p_0 \sin t) \end{pmatrix} \quad (4.18)$$

$$= \alpha \begin{pmatrix} p_0 \cos t - x_0 \sin t \\ -x_0 \cos t - p_0 \sin t \end{pmatrix} \left((x_0 \cos t + p_0 \sin t)^2 + (p_0 \cos t - x_0 \sin t)^2 \right) \quad (4.19)$$

$$= \alpha \hat{Z}(t) \begin{pmatrix} p_0 \\ -x_0 \end{pmatrix} (p_0^2 + x_0^2) = \alpha r^2 \hat{Z}(t) \vec{d}_0 \quad (4.20)$$

From equation 4.6 it is known, that $\Delta \vec{z}_1$ can be calculated with the variation of the parameter as follows:

$$\Delta \vec{z}_1(t) = \hat{Z} \vec{v}(t) = \hat{Z} \int_0^t \hat{Z}^{-1} \vec{f}_0(t') dt' = \hat{Z} \alpha r^2 \vec{d}_0 \int_0^t \hat{Z}^{-1} \hat{Z}(t) dt' = \hat{Z} \alpha r^2 \vec{d}_0 t \quad (4.21)$$

Therefore, the combined solution for \vec{z}_1 is:

$$\vec{z}_1 = \vec{z}_0 + \Delta \vec{z}_1 = \hat{Z} \left(\vec{c}_0 + \alpha r^2 \vec{d}_0 t \right) \quad (4.22)$$

which is the first part of the solution in equation 4.9 up to 1st-order in α .

For the 2nd-order perturbation an equivalent ansatz to the first one is used:

$$x_2(t) = x_1(t) + \Delta x_2(t) \quad (4.23)$$

$$p_2(t) = p_1(t) + \Delta p_2(t) \quad (4.24)$$

By substituting this ansatz in the Hamilton equations the following differential equations are obtained:

$$\dot{z}_{hom} + \Delta\dot{z}_1 + \Delta\dot{z}_2 = \dot{z}_2 = \hat{L}z_2 + \alpha \begin{pmatrix} p_2^3 + x_2^2 p_2 \\ -x_2^3 - p_2^2 x_2 \end{pmatrix} \quad (4.25)$$

$$\Delta\dot{z}_1 + \Delta\dot{z}_2 = \hat{L}\Delta z_1 + \vec{f}_1 + \Delta\dot{z}_2 \quad (4.26)$$

$$= \hat{L}(\Delta z_1 + \Delta z_2) + \alpha \begin{pmatrix} p_1^3 + x_1^2 p_1 \\ -x_1^3 - p_1^2 x_1 \end{pmatrix} + \alpha \mathcal{O}(\Delta x_1, \Delta p_1) \quad (4.27)$$

which can be summarized to

$$\underbrace{\begin{pmatrix} \Delta x_2(t) \\ \Delta p_2(t) \end{pmatrix}}_{\Delta \vec{z}_2(t)} = \underbrace{\begin{pmatrix} 0 & 1 \\ -1 & 0 \end{pmatrix}}_{\hat{L}} \underbrace{\begin{pmatrix} \Delta x_2(t) \\ \Delta p_2(t) \end{pmatrix}}_{\Delta \vec{z}_2(t)} + \alpha \underbrace{\begin{pmatrix} p_1^3 + x_1^2 p_1 \\ -x_1^3 - p_1^2 x_1 \end{pmatrix}}_{\vec{f}_1(t)} - \alpha \underbrace{\begin{pmatrix} p_{hom}^3 + x_{hom}^2 p_{hom} \\ -x_{hom}^3 - p_{hom}^2 x_{hom} \end{pmatrix}}_{\vec{f}_0(t)} \quad (4.28)$$

From this, the general pattern becomes apparent:

$$\dot{z}_n + \Delta\dot{z}_{n+1} = \hat{L}(\vec{z}_n + \Delta\vec{z}_{n+1}) + \vec{f}_{n+1} \quad (4.29)$$

$$\Delta\dot{z}_{n+1} = \hat{L}\Delta\vec{z}_{n+1} + \alpha \mathcal{O}(\Delta x_{n+1}, \Delta p_{n+1}) + \sum_{i=0}^n (-1)^{n+i} \vec{f}_i(t) \quad (4.30)$$

$$\text{with } \vec{f}_i = \alpha \begin{pmatrix} p_i^3 + x_i^2 p_i \\ -x_i^3 - p_i^2 x_i \end{pmatrix} \stackrel{i=0}{=} \alpha \begin{pmatrix} p_{hom}^3 + x_{hom}^2 p_{hom} \\ -x_{hom}^3 - p_{hom}^2 x_{hom} \end{pmatrix} \quad (4.31)$$

Therefore:

$$\Delta\dot{z}_n(t) = \hat{L}\Delta\vec{z}_n(t) + (-1)^n \sum_{i=1}^n (-1)^i \vec{f}_i(t) \quad (4.32)$$

Once again all terms involving an α together with a Δx_{n+1} or Δp_{n+1} are neglected for the specific perturbation order and marked as $\mathcal{O}(\Delta x_{n+1}, \Delta p_{n+1})$. To finish the second order approximation, the inhomogeneity \vec{f}_1 from equation 4.28 can be simplified by using the solution for \vec{f}_0 from equation 4.20 and replacing the components (x_0, p_0) in \vec{c}_0 by the components (x'_0, p'_0) of $\vec{c}'_0 = \vec{c}_0 + \alpha r^2 \vec{d}_0 t$ from equation 4.22:

$$\vec{f}_1(t) = \alpha \begin{pmatrix} p_1^3 + x_1^2 p_1 \\ -x_1^3 - p_1^2 x_1 \end{pmatrix} = \alpha \hat{Z} \begin{pmatrix} p'_0 \\ -x'_0 \end{pmatrix} (p_0'^2 + x_0'^2) \quad (4.33)$$

$$= \alpha \hat{Z} r^2 (\alpha^2 r^4 t^2 + 1) \begin{pmatrix} p_0 - \alpha r^2 t x_0 \\ -(x_0 + \alpha r^2 t p_0) \end{pmatrix} \quad (4.34)$$

$$= \alpha \hat{Z} r^2 (\alpha^2 r^4 t^2 + 1) (\vec{d}_0 - \alpha r^2 t \vec{c}_0) \quad (4.35)$$

the total inhomogeneous part is therefore:

$$\vec{f}_1 - \vec{f}_0 = \hat{Z} \left(\alpha^3 r^6 t^2 (\vec{d}_0 - \alpha r^2 t \vec{c}_0) - \alpha^2 r^4 t \vec{c}_0 \right) \quad (4.36)$$

Integrating according to equation 4.6 yields:

$$\vec{v}_2(t) = -(\alpha r^2 t)^2 \frac{\vec{c}_0}{2} + (\alpha r^2 t)^3 \frac{\vec{d}_0}{3} - (\alpha r^2 t)^4 \frac{\vec{c}_0}{4} \quad (4.37)$$

$$\vec{z}_2(t) = \hat{Z}(t) (\vec{c}_0 + \vec{v}_1(t) + \vec{v}_2(t)) \quad (4.38)$$

$$= \hat{Z}(t) \left(\vec{c}_0 + (\alpha r^2 t) \vec{d}_0 - (\alpha r^2 t)^2 \frac{\vec{c}_0}{2} + (\alpha r^2 t)^3 \frac{\vec{d}_0}{3} - (\alpha r^2 t)^4 \frac{\vec{c}_0}{4} \right) \quad (4.39)$$

which agrees with the exact solution in equation 4.9 now up to 4th-order in α .

For the n^2 -order in α , the process is equivalent. Beginning with the ansatz

$$x_n(t) = x_{n-1}(t) + \Delta x_n(t) \quad (4.40)$$

$$p_n(t) = p_{n-1}(t) + \Delta p_n(t) \quad (4.41)$$

and solving the inhomogeneous ODE

$$\Delta \dot{\vec{z}}_n(t) = \hat{L} \Delta \vec{z}_n(t) + (-1)^n \sum_{i=1}^n (-1)^i \vec{f}_i(t) \quad (4.42)$$

by solving the integral given in equation 4.6.

4.2.2 Asymmetric perturbation

In this next example, the process becomes a lot more tedious, due to the symmetry break in the Hamiltonian. The new system is given by the following Hamiltonian and its Hamilton equations:

$$H = \frac{p^2}{2} + \frac{x^2}{2} + \alpha \frac{x^4}{4} \quad (4.43)$$

$$\text{with } \begin{pmatrix} \dot{x} \\ \dot{p} \end{pmatrix} = \begin{pmatrix} \frac{\partial H_\alpha}{\partial p} \\ -\frac{\partial H_\alpha}{\partial x} \end{pmatrix} = \underbrace{\begin{pmatrix} 0 & 1 \\ -1 & 0 \end{pmatrix}}_{\hat{L}} \underbrace{\begin{pmatrix} x \\ p \end{pmatrix}}_{\vec{z}(t)} - \begin{pmatrix} 0 \\ \alpha x^3 \end{pmatrix} \quad (4.44)$$

using the same ansatz

$$\begin{aligned} x_1(t) &= x_{hom}(t) + \Delta x_1(t) \\ p_1(t) &= p_{hom}(t) + \Delta p_1(t) \end{aligned}$$

as above, the Hamilton equations in first order perturbation can be derived as follows:

$$\begin{pmatrix} \dot{x}_1 \\ \dot{p}_1 \end{pmatrix} = \begin{pmatrix} -p_1 \\ x_1 \end{pmatrix} - \begin{pmatrix} 0 \\ \alpha x_1^3 \end{pmatrix} = \begin{pmatrix} 0 & 1 \\ -1 & 0 \end{pmatrix} \begin{pmatrix} x_1 \\ p_1 \end{pmatrix} - \begin{pmatrix} 0 \\ \alpha x_{hom}^3 \end{pmatrix} + \alpha \mathcal{O}(\Delta x_1) \quad (4.45)$$

$$\begin{pmatrix} \Delta \dot{x}_1 \\ \Delta \dot{p}_1 \end{pmatrix} = \begin{pmatrix} 0 & 1 \\ -1 & 0 \end{pmatrix} \begin{pmatrix} \Delta x_1 \\ \Delta p_1 \end{pmatrix} - \begin{pmatrix} 0 \\ \alpha x_{hom}^3 \end{pmatrix} \quad (4.46)$$

Following the method of variation of the parameter, the following integral of the inhomogeneity has to be solved:

$$\vec{v}_1(t) = -\alpha \int_0^t \hat{Z}^{-1}(t) \vec{e}_p (x_0 \cos t + p_0 \sin t)^3 dt \quad (4.47)$$

$$= -\alpha \int_0^t \begin{pmatrix} \sin t \\ \cos t \end{pmatrix} (x_0 \cos t + p_0 \sin t)^3 dt \quad (4.48)$$

Even though the calculation by hand is possible, a computer algebra program as it is implemented in *WolframAlpha*®[®], was used to calculate the following solution:

$$\vec{v}_1(t) = \frac{\alpha}{32} \begin{pmatrix} p_0 (12r^2t + (p_0^2 - 3x_0^2) \sin 4t - 8p_0^2 \sin 2t) \\ x_0 (12r^2t + (x_0^2 - 3p_0^2) \sin 4t + 8x_0^2 \sin 2t) \end{pmatrix} \quad (4.49)$$

$$- \frac{\alpha}{32} \begin{pmatrix} 4x_0(3p_0^2 + x_0^2) \cos 2t - x_0(x_0^2 - 3p_0^2) \cos 4t \\ 4p_0(p_0^2 + 3x_0^2) \cos 2t + p_0(p_0^2 - 3x_0^2) \cos 4t \end{pmatrix} \quad (4.50)$$

The first order solution is then $\vec{z}_1 = \hat{Z}(\vec{c}_0 + \vec{v}_1(t))$. This method produces already quite extensive calculations in the first step. For every following step even more extensive integrals of the form

$$\vec{v}_n(t) = \alpha \int_0^t \begin{pmatrix} \sin t \\ \cos t \end{pmatrix} \sum_{i=0}^{n-1} (-1)^{n+i} x_i^3 dt$$

where $x_i = x_{hom}$ for $i = 0$, have to be solved. Considering that the problems are still rather basic, but the calculations are already very extensive, the need for a different approach becomes apparent. The following chapter, therefore, introduces a computer-based approach that is generally applicable for time independent perturbation to the harmonic oscillator. The DA framework, which is implemented in the COSY INFINITY program used for the calculation makes an automatic calculation of the solution up to arbitrary order possible.

CHAPTER 5

PERTURBED HARMONIC OSCILLATOR

The Harmonic Oscillator is one of the basic models that is used in many fields of physics and therefore is of great importance. In most cases, the periodic model considers a Harmonic oscillator with parameter-dependent perturbations. A perturbed harmonic oscillator can be represented by the sum of the Hamiltonian of the unperturbed case H_0 and the perturbation term: $H = H_0 + H_{per}$. The perturbation term can generally consist of multiple parameter-dependent terms.

5.1 The Pendulum

In this section, the Pendulum oscillation is considered as a perturbation to the small angle approximation, which represents the unperturbed classic harmonic oscillator. The example shall illustrate how the DA framework in COSY INFINITY together with implemented the Normal Form Algorithm can be used to approximate the amplitude and possibly parameter-dependent tune shifts of a perturbed Hamiltonian, numerically as an algebraic expression the in form of a polynomial.

5.1.1 Introduction to the Problem

Considering a mathematical Pendulum of with point mass m at a length l from the pivot point in a constant gravitational field with gravitation constant g . The Pendulum encloses an angle θ with the vertical axis as illustrated in figure 5.1. Therefore, the Lagrangian in the given coordinates is:

$$L = \frac{ml^2}{2}\dot{\theta}^2 - ml^2\omega_0^2(1 - \cos(\theta)) \quad (5.1)$$

where $\omega_0^2 = \frac{g}{l}$. The Hamiltonian can be derived as follows in the generalized canonical coordinate and momentum (q, p) :

$$H = \dot{\theta}p_{\theta} - L = \dot{\theta} \left(\frac{\partial L}{\partial \dot{\theta}} \right) - L = \frac{ml^2}{2}\dot{\theta}^2 + ml^2\omega_0^2(1 - \cos(\theta)) \quad (5.2)$$

$$H = \frac{p_{\theta}^2}{2ml^2} + ml^2\omega_0^2(1 - \cos(q)) \quad (5.3)$$

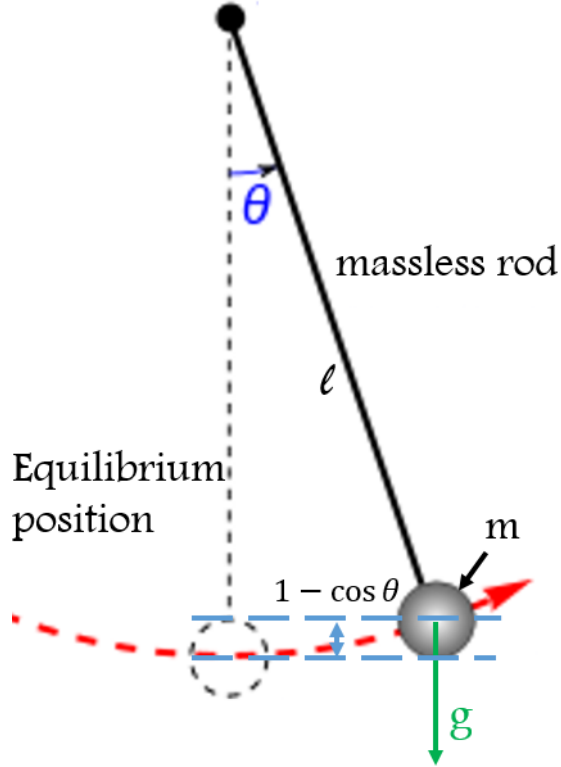


Figure 5.1 Illustration shows mathematical Pendulum of length l with point mass m in a gravitational field of strength g [10].

Using the Hamilton equations, the first order ODE can be derived:

$$\begin{pmatrix} \dot{q} \\ \dot{p} \end{pmatrix} = \begin{pmatrix} \frac{\partial H}{\partial p} \\ -\frac{\partial H}{\partial q} \end{pmatrix} = \begin{pmatrix} 0 & \frac{1}{ml^2} \\ -ml^2\omega_0^2 & 0 \end{pmatrix} \begin{pmatrix} \sin(q) \\ p \end{pmatrix} \quad (5.4)$$

$$= \begin{pmatrix} 0 & \frac{1}{ml^2} \\ -ml^2\omega_0^2 & 0 \end{pmatrix} \begin{pmatrix} q \\ p \end{pmatrix} - ml^2\omega_0^2 \begin{pmatrix} 0 \\ -\frac{q^3}{3!} + \frac{q^5}{5!} - \frac{q^7}{7!} + \dots \end{pmatrix} \quad (5.5)$$

The DA Normal Form Algorithm requires a non-zero constant linear term of the map to be able to generate certain inverse functions within the process. As already mentioned in section 1.2.3, the DA framework only works within a ring, since the inverse element is only defined for elements with a non-zero constant part. Hence, a transformation to coordinates in which the system has a linear part that is not purely parameter-dependent. For the investigation of this transformation it is

helpful to consider the unperturbed harmonic oscillator, where no nonlinear terms appear and the solution is known.

5.1.2 Unperturbed case

To solve the problem or approximate a solution, it is often helpful to consider the unperturbed case first. For the Pendulum, this case is known as the small angle approximation, where either the $1 - \cos \theta \approx \theta^2/2$ expression in the Hamiltonian or $\sin \theta \approx \theta$ in the Hamilton equations are substituted. With respect to further references the following general unperturbed classic harmonic oscillator with its Hamiltonian and its Hamilton equations are defined:

$$H = \frac{p^2}{2m} + m\omega_0^2 \frac{q^2}{2} \quad (5.6)$$

$$\begin{pmatrix} \dot{q} \\ \dot{p} \end{pmatrix} = \begin{pmatrix} \frac{\partial H}{\partial p} \\ -\frac{\partial H}{\partial q} \end{pmatrix} = \begin{pmatrix} 0 & \frac{1}{m} \\ -m\omega_0^2 & 0 \end{pmatrix} \begin{pmatrix} q \\ p \end{pmatrix} \quad (5.7)$$

A suitable transformation of the (q, p) -coordinates to make the linear part of the ODE parameter independent consists of the real and imaginary part of the two complex conjugate eigenvectors of the coupling matrix:

$$\vec{v}^{\pm} = \begin{pmatrix} \frac{\mp i}{m\omega_0} \\ 1 \end{pmatrix} \quad (5.8)$$

The transformation \hat{T} and its inverse are scaled as already discussed in the diagonalization section 1.2.4, so that the determinate of the transformation is of magnitude 1.

$$\hat{T}^{-1} = \sqrt{m\omega_0} \begin{pmatrix} 0 & \frac{-1}{m\omega_0} \\ 1 & 0 \end{pmatrix} \quad \hat{T} = \frac{1}{\sqrt{m\omega_0}} \begin{pmatrix} 0 & 1 \\ -m\omega_0 & 0 \end{pmatrix} \quad (5.9)$$

The transformation is applied to the ODE in equation 5.7:

$$\hat{T} \begin{pmatrix} \dot{q} \\ \dot{p} \end{pmatrix} = \hat{T} \begin{pmatrix} 0 & \frac{1}{m} \\ -m\omega_0^2 & 0 \end{pmatrix} \hat{T}^{-1} \hat{T} \begin{pmatrix} q \\ p \end{pmatrix} \quad (5.10)$$

$$\begin{pmatrix} \frac{\dot{p}}{\sqrt{m\omega_0}} \\ -\sqrt{m\omega_0}\dot{q} \end{pmatrix} = \begin{pmatrix} 0 & \omega_0 \\ -\omega_0 & 0 \end{pmatrix} \begin{pmatrix} \frac{p}{\sqrt{m\omega_0}} \\ -\sqrt{m\omega_0}q \end{pmatrix} \quad (5.11)$$

$$\begin{pmatrix} \frac{\dot{p}}{\sqrt{m\omega_0}} \\ \sqrt{m\omega_0}\dot{q} \end{pmatrix} = \begin{pmatrix} 0 & -\omega_0 \\ \omega_0 & 0 \end{pmatrix} \begin{pmatrix} \frac{p}{\sqrt{m\omega_0}} \\ \sqrt{m\omega_0}q \end{pmatrix} \quad (5.12)$$

$$\begin{pmatrix} \dot{p}_1 \\ \dot{q}_1 \end{pmatrix} = \omega_0 \begin{pmatrix} 0 & -1 \\ 1 & 0 \end{pmatrix} \begin{pmatrix} p_1 \\ q_1 \end{pmatrix} \quad (5.13)$$

where the transformed variables are $(q_1, p_1) = \left(\sqrt{m\omega_0}q, \frac{p}{\sqrt{m\omega_0}}\right)$. This transformation preserves the symplectic structure of the Hamiltonian since the new coordinates also satisfy the Poisson bracket condition:

$$\{q_1, p_1\} = 1 \quad (5.14)$$

Hence, the transformation is a canonical transformation which preserving the form of the Hamilton equations. This is especially essential for the transformation of the perturbed Hamiltonians later on. In addition to the coordinate transformation, a scaling of the time t to $t' = \omega_0 t$ is necessary to accomplish a parameter independent linear part. Therefore, $d_{t'} = \frac{1}{\omega_0} d_t$ and the transformed Hamilton equations yield:

$$\begin{pmatrix} \dot{p}_1 \\ \dot{q}_1 \end{pmatrix} = \begin{pmatrix} 0 & -1 \\ 1 & 0 \end{pmatrix} \begin{pmatrix} p_1 \\ q_1 \end{pmatrix} \quad (5.15)$$

This form of the ODE is suitable for the DA based Normal Form Algorithm implemented in COSY INFINITY. The solution to this ODE is already known from various textbooks:

$$\begin{pmatrix} p_1 \\ q_1 \end{pmatrix} = \begin{pmatrix} \cos(t') & -\sin(t') \\ \sin(t') & \cos(t') \end{pmatrix} \begin{pmatrix} \bar{p}_1 \\ \bar{q}_1 \end{pmatrix} \quad (5.16)$$

where $(\bar{q}_1, \bar{p}_1) = \left(\sqrt{m\omega_0}\bar{q}, \frac{\bar{p}}{\sqrt{m\omega_0}} \right)$ is the initial state at $t' = 0$. The example in section 1.2.6 also solves the ODE 1.64, which is equivalent to equation 5.15 for $(1 + \alpha r^2) = 1$ using the Flow Operator. Note that equation 5.16 is already in Normal Form coordinates and therefore does not require any further DA manipulation. After transforming back to the (q, p) -system and rescaling the time $t' = \omega_0 t$, the result is given in its well-known form:

$$\hat{T}^{-1} \begin{pmatrix} p_1 \\ q_1 \end{pmatrix} = \hat{T}^{-1} \begin{pmatrix} \cos(t') & -\sin(t') \\ \sin(t') & \cos(t') \end{pmatrix} \hat{T} \hat{T}^{-1} \begin{pmatrix} \bar{p}_1 \\ \bar{q}_1 \end{pmatrix} \quad (5.17)$$

$$\begin{pmatrix} q \\ p \end{pmatrix} = \begin{pmatrix} \cos(\omega_0 t) & \frac{\sin(\omega_0 t)}{m\omega_0} \\ -m\omega_0 \sin(\omega_0 t) & \cos(\omega_0 t) \end{pmatrix} \begin{pmatrix} \bar{q} \\ \bar{p} \end{pmatrix} \quad (5.18)$$

The tune (unperturbed frequency of oscillation) in this example is simply ω_0 . Note that

$$E_0 = \frac{p^2}{2m} + m\omega_0^2 \frac{q^2}{2} = \frac{\bar{p}^2}{2m} + m\omega_0^2 \frac{\bar{q}^2}{2} = \text{const.} \quad (5.19)$$

is also satisfied for $\bar{p} = -r \sin(\varphi_0)$, $\bar{q} = \frac{r}{m\omega_0} \cos(\varphi_0)$ with $r = \sqrt{2E_0 m}$. Therefore the solution in

equation 5.18 can be rewritten to:

$$\begin{pmatrix} q \\ p \end{pmatrix} = \begin{pmatrix} \bar{q} \cos(\omega_0 t) + \bar{p} \frac{\sin(\omega_0 t)}{m\omega_0} \\ -\bar{q} m \omega_0 \sin(\omega_0 t) + \bar{p} \cos(\omega_0 t) \end{pmatrix} \quad (5.20)$$

$$= \begin{pmatrix} \frac{r}{m\omega_0} \cos(\omega_0 t) \cos(\varphi) - r \frac{\sin(\omega_0 t)}{m\omega_0} \sin(\varphi) \\ -m\omega_0 \frac{r}{m\omega_0} \sin(\omega_0 t) \cos(\varphi) - r \cos(\omega_0 t) \sin(\varphi) \end{pmatrix} \quad (5.21)$$

$$= \begin{pmatrix} \frac{r}{m\omega_0} \cos(\omega_0 t + \varphi) \\ -r \sin(\omega_0 t + \varphi) \end{pmatrix} \quad (5.22)$$

This derivation will be helpful later on in section 5.3. After this extensive revisit of the unperturbed classic harmonic oscillator, a collection of various forms of the unperturbed solutions and the canonical transformation needed to make the linear part of the Pendulum equation 5.4 parameter-independent have been derived.

5.1.3 Pendulum transformation

From the unperturbed case above, the transformation \hat{T} and its inverse are known and given in equation 5.9. The same transformation can be applied to the Pendulum equation 5.4 with $m' = ml^2$, which yields the following differential equation:

$$\begin{pmatrix} \frac{\dot{p}}{\sqrt{ml^2 \omega_0}} \\ -\sqrt{ml^2 \omega_0} \dot{q} \end{pmatrix} = \begin{pmatrix} -\frac{ml^2 \omega_0^2}{\sqrt{ml^2 \omega_0}} \sin(q) \\ -\sqrt{ml^2 \omega_0} \frac{p}{ml^2} \end{pmatrix} = \begin{pmatrix} -\frac{ml^2 \omega_0^2}{\sqrt{ml^2 \omega_0}} \sin\left(\frac{q_1}{\sqrt{ml^2 \omega_0}}\right) \\ -\omega_0 p_1 \end{pmatrix} \quad (5.23)$$

$$\begin{pmatrix} \dot{p}_1 \\ \dot{q}_1 \end{pmatrix} = \omega_0 \begin{pmatrix} -q_1 - \sqrt{ml^2 \omega_0} \left(\sin\left(\frac{q_1}{\sqrt{ml^2 \omega_0}}\right) - \frac{q_1}{\sqrt{ml^2 \omega_0}} \right) \\ p_1 \end{pmatrix} \quad (5.24)$$

with the transformation $(q, p) = \left(\frac{q_1}{\sqrt{ml^2\omega_0}}, \sqrt{ml^2\omega_0}p_1 \right)$ and the appropriate scaling of the time to $t' = \omega_0 t$, the following form with linear parameter-independence is given:

$$\begin{pmatrix} \dot{p}_1 \\ \dot{q}_1 \end{pmatrix} = \begin{pmatrix} 0 & -1 \\ 1 & 0 \end{pmatrix} \begin{pmatrix} p_1 \\ q_1 \end{pmatrix} + \begin{pmatrix} \frac{q_1^3}{3!ml^2\omega_0} - \frac{q_1^5}{5!(ml^2\omega_0)^2} + \frac{q_1^7}{7!(ml^2\omega_0)^3} - \dots \\ 0 \end{pmatrix} \quad (5.25)$$

$$= \begin{pmatrix} 0 & -1 \\ 1 & 0 \end{pmatrix} \begin{pmatrix} p_1 \\ q_1 \end{pmatrix} + \begin{pmatrix} \frac{aq_1^3}{3!} - \frac{a^2q_1^5}{5!} + \frac{a^3q_1^7}{7!} - \frac{a^4q_1^9}{9!} + \dots \\ 0 \end{pmatrix} \quad (5.26)$$

for the implantation in COSY INFINITY the parameter $a = 1/ml^2\omega_0$ is introduced. The first step of the in COSY INFINITY implemented procedure is the calculation of a transfer map \mathcal{M} from $t' = 0$ to $t' = 1$ regarding the Pendulum ODE 5.26, with one of the DA based integrators mentioned above. An illustration of the transfer map using RK4 with $h = 0.001$ is in figure 5.2.

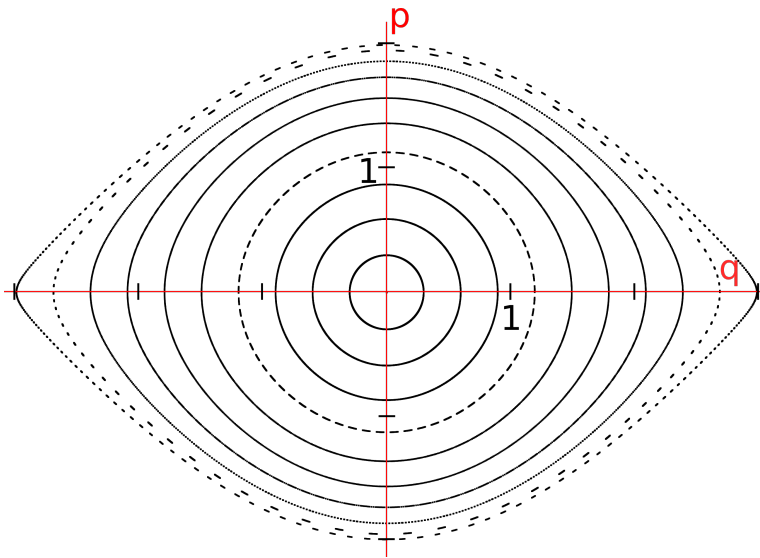


Figure 5.2 The figure shows the phase space curves of the Pendulum oscillation according to the transfer map at $t' = 1$, which was generated by integrating equation 5.4 with the DA based RK4 in 1000 steps of step-size $h = 0.001$. For the illustration, all parameters were set to 1. The transfer map was tracked for 1000 iterations. The different curves represent the following initial conditions, listed from inner to outer curve: $q = .3, .6, .9, 1.2, \dots, 3.0$; $p = 0$. Details regarding the seemingly closed and fragmented curves can be found in section 5.2.

In the next step of the procedure, the transfer map is transformed by \mathcal{A} into the Normal Form coordinates (t^+, t^-) using the DA Normal Form Algorithm introduced in the chapter above. \mathcal{M}_{NF} .

$$\mathcal{M}_{NF} = \mathcal{A} \circ \mathcal{M} \circ \mathcal{A}^{-1} \quad (5.27)$$

The transfer map in Normal Form coordinates is illustrated in figure 5.3. The Normal Form coor-

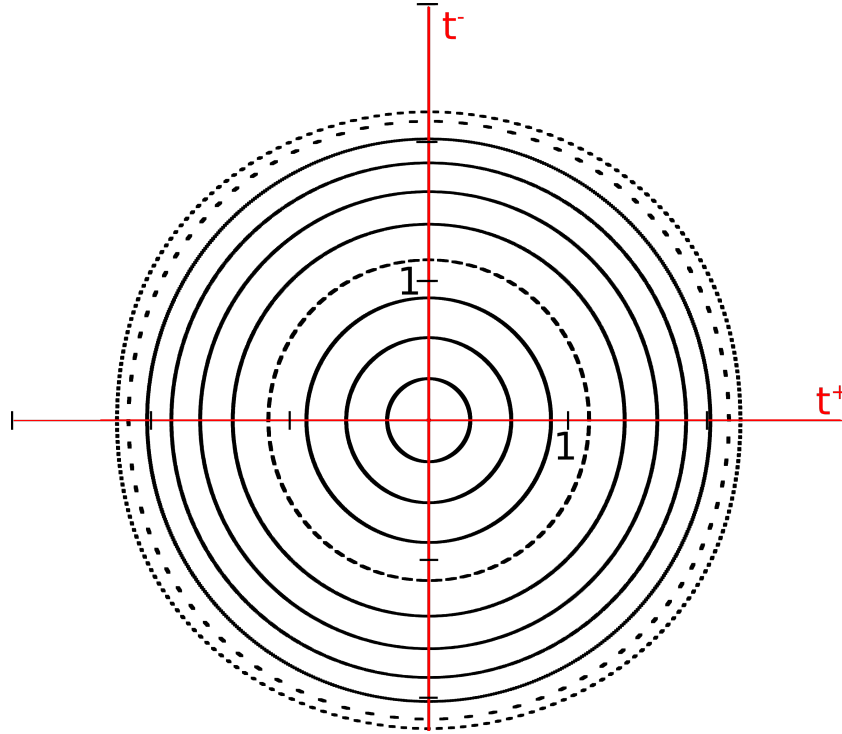


Figure 5.3 The figure shows the phase space curves of the Pendulum oscillation according to the transfer map at $t = 1$, which was generated by integrating equation 5.4 with the DA based RK4 in 1000 steps of step-size $h = 0.001$ with order truncation 20. For the illustration, all parameters are set to 1. The transfer map at $t = 1$ was transformed to Normal form coordinates and tracked for 1000 iterations. The different curves represent the following initial conditions, listed from inner to outer curve: $q = .3, .6, .9, 1.2, \dots, 3.0$; $p = 0$. The curves show circular motion and the separation in the fragmented curves has a constant distance in contrast to figure 5.2. Details regarding this are in section 5.2.

dinates reveal the desired tune shifts using equation 3.76. Scaled to the original time $t = \omega_0 t'$ the tune shifts are given as follows:

$$\omega = \omega_0 \left(1 - \frac{ar^2}{16} - \frac{3a^2r^4}{1024} - \frac{5a^3r^6}{16384} - \frac{165a^4r^8}{2^{22}} - \frac{189a^5r^{10}}{2^{25}} - \mathcal{O}(a^6r^{12}) \right) \quad (5.28)$$

Note that the actual COSY INFINITY coefficients are given in the scaled time of t' , which means without the ω_0 . Additionally, the coefficients are given in floating point number representation in base₁₀ as shown in table 5.1. The fractions in equation 5.28 were only used for illustrative purposes, but agree with the COSY result with an error $< 10^{-14}$, which is the magnitude of floating point accuracy.

Table 5.1 Coefficients of the COSY result up to order 10 in r for the Pendulum tunes $\omega_{t'}(r)$ shown in equation 5.28 with corresponding fraction representation and maximal error in the representation.

Factor	Coefficient	Fraction	Difference in representation
1	0.9999999999999908	1	$< 9.2 \cdot 10^{-15}$
ar^2	-.6249999999999629E-01	$\frac{-1}{16} = -2^{-4}$	$< 3.8 \cdot 10^{-15}$
a^2r^4	-.2929687500000584E-02	$\frac{-3}{1024} = -3 \cdot 2^{-10}$	$< 5.9 \cdot 10^{-16}$
a^3r^6	-.3051757812506449E-03	$\frac{-5}{16384} = -5 \cdot 2^{-14}$	$< 6.5 \cdot 10^{-16}$
a^4r^8	-.3933906555075291E-04	$\frac{-165}{4194304} = -165 \cdot 2^{-22}$	$< 1.1 \cdot 10^{-15}$
a^5r^{10}	-.5632638932827286E-05	$\frac{-189}{33554432} = -189 \cdot 2^{-25}$	$< 1.6 \cdot 10^{-15}$

For applications the quantity ω in terms of r^2 is not very useful as presented in equation 5.28. The given Normal Form transformation: $\mathcal{A} : (q_1, p_1) \rightarrow (t^+, t^-)$ from equation 5.27 and equation 3.71, make it possible to represent r^2 in terms of the known quantities (q_1, p_1) . The corresponding COSY INFINITY terms and coefficients for $r^2(q_1, p_1)$ can be found in APPENDIX table A.1 as well as $\omega_{t'}(q_1, p_1)$, which is in table A.2. In general, $\omega_{t'}(q_1, p_1)$ is the final COSY INFINITY approximation to the problem, but in this special case the transformation (q_1, p_1) back into the (q, p) -system can be easily preformed by COSY INFINITY. The difficulty lies within the relation $(q_1, p_1) = \left(\sqrt{m\omega_0}q, \frac{p}{\sqrt{m\omega_0}} \right) = \left(\frac{q}{\sqrt{a}}, \sqrt{ap} \right)$, where neither $1/x$ nor \sqrt{x} are possible operations in the DA arithmetic. Hence, a second variable $b = 1/a$ with the property that $ab = 1$ is introduced. The square-root issue is in this specific case not relevant, since q_1 and p_1 only occur with even exponents and therefore:

$$q_1^2 = bq^2 \quad p_1^2 = ap^2 \quad \text{with } b = \frac{1}{a} = ml^2 \omega_0 \quad (5.29)$$

Note that the order is raised due to the substitution in equation 5.29. For each two orders of q_1 or p_1 respectively, come two orders of q or p and one order of a or b , respectively, which will automatically result in order loss for higher orders due to the order truncation of the process. The following substitution solves this problem, by simply introducing $q' = q^2$ and $p' = p^2$ to keep the order of the respective terms constant. Possible additional procedures, that have not yet been implemented, could cancel all terms with

$$a^m b^n \longrightarrow a^{m-\min(m,n)} b^{n-\min(m,n)} \quad (5.30)$$

resulting in at least one of the exponents of a or b to be zero for each term. A table with the COSY INFINITY output, for $\omega_{t'}$ (q, p) in the t' time frame, can be found in table A.3 in the appendix and the first terms in the fractional approximation are

$$\omega_{t'}(q, p) = \left(1 - \frac{q^2 + a^2 p^2}{16} + \frac{q^4}{3072} - \frac{5p^4}{1024} - \frac{5a^2 p^2}{512} + \dots \right) \quad (5.31)$$

The period T can be calculated by taking the inverse of the equation above according to equation 3.30. The Inversion is possible in the DA framework, due to the nonzero constant part of $\omega_{t'} = 1 + f(q, p)$. Hence, T is

$$T = \frac{2\pi}{\omega} = \frac{2\pi}{\omega_0} \frac{1}{\omega_{t'}} = \frac{2\pi}{\omega_0} \frac{1}{1 + f(q, p)} \quad (5.32)$$

The result for T disregarding the prefactor of $\frac{2\pi}{\omega_0}$ is given in table 5.2. The first terms in the fraction representation are written in equation 5.33.

$$T = \frac{2\pi}{\omega_0} \left(1 + \frac{q^2 + a^2 p^2}{2^4} + \frac{11q^4}{3 \cdot 2^{10}} + \frac{9q^2 a^2 p^2}{2^9} + \frac{9a^4 p^4}{2^{10}} + \dots \right) \quad (5.33)$$

Since the pair (q, p) represents any point on the phase space curve of the motion, a specific set of initial conditions $(q_0, p_0) = (\theta_0, 0)$ can be chosen to simplify the equation for T . The amplitude θ_0 of the oscillation can be derived from any set of initial conditions as follows:

$$\theta_0 = \arccos \left(\cos(q_0) - \frac{p_0^2}{2m^2 l^4 \omega_0^2} \right) \quad (5.34)$$

For $(q, p) = (\theta_0, 0)$, T yields the following result:

$$T =_{10} \frac{2\pi}{\omega_0} \left(1 + \frac{\theta_0^2}{16} + \frac{11\theta_0^4}{3072} + \frac{173\theta_0^6}{737280} + \frac{22931\theta_0^8}{1321205760} + \frac{1319183\theta_0^{10}}{951268147200} \right) \quad (5.35)$$

Table 5.2 Coefficients of the COSY result for the Pendulum Period $T_p(q, p)$ shown in equation 5.33 with corresponding fraction representation and maximal error in the representation.

Factor	Coefficient	Fraction	Difference in representation
1	0.9999999999999996	1	$< 4.0 \cdot 10^{-16}$
q^2	0.6250000000000076E-01	$\frac{1}{2^4}$	$< 7.6 \cdot 10^{-16}$
$a^2 p^2$	0.6250000000000079E-01	$\frac{1}{2^4}$	$< 7.9 \cdot 10^{-16}$
q^4	0.3580729166662193E-02	$\frac{11}{2^{10} 3}$	$< 4.5 \cdot 10^{-15}$
$q^2 a^2 p^2$	0.1757812499999105E-01	$\frac{3^3}{2^9}$	$< 9.0 \cdot 10^{-15}$
$a^4 p^4$	0.8789062499995597E-02	$\frac{3^3}{2^{10}}$	$< 4.5 \cdot 10^{-15}$
q^6	0.2346462673688346E-03	$\frac{173}{2^{14} \cdot 3^2 \cdot 5}$	$< 7.8 \cdot 10^{-15}$
$q^4 a^2 p^2$	0.3112792968767812E-02	$\frac{3 \cdot 17}{2^{14}}$	$< 1.8 \cdot 10^{-14}$
$q^2 a^4 p^4$	0.4577636718776126E-02	$\frac{3 \cdot 5^2}{2^{14}}$	$< 2.7 \cdot 10^{-14}$
$a^6 p^6$	0.1525878906257389E-02	$\frac{5^2}{2^{14}}$	$< 7.4 \cdot 10^{-15}$
q^8	0.1735611567867274E-04	$\frac{23 \cdot 997}{2^{22} \cdot 3^2 \cdot 5 \cdot 7}$	$< 4.5 \cdot 10^{-15}$
$q^6 a^2 p^2$	0.4541397095222981E-03	$\frac{2381}{2^{20} \cdot 5}$	$< 5.0 \cdot 10^{-14}$
$q^4 a^4 p^4$	0.1370906829873207E-02	$\frac{5^3 \cdot 23}{2^{21}}$	$< 4.0 \cdot 10^{-14}$
$q^2 a^6 p^6$	0.1168251037599050E-02	$\frac{5^2 \cdot 7^2}{2^{20}}$	$< 1.4 \cdot 10^{-15}$
$a^8 p^8$	0.2920627594054748E-03	$\frac{5^2 \cdot 7^2}{2^{22}}$	$< 6.1 \cdot 10^{-15}$
q^{10}	0.1386762528983589E-05	$\frac{17 \cdot 73 \cdot 1063}{2^{26} \cdot 3^4 \cdot 5^2 \cdot 7}$	$< 2.3 \cdot 10^{-14}$
$q^8 a^2 p^2$	0.5999931270428728E-04	$\frac{53 \cdot 2659}{2^{26} \cdot 5 \cdot 7}$	$< 3.1 \cdot 10^{-14}$
$q^6 a^4 p^4$	0.3120799860718536E-03	$\frac{5 \cdot 61 \cdot 103}{2^{25} \cdot 3}$	$< 1.4 \cdot 10^{-13}$
$q^4 a^6 p^6$	0.4940728349303492E-03	$\frac{5 \cdot 7^3 \cdot 29}{2^{25} \cdot 3}$	$< 2.8 \cdot 10^{-13}$
$q^2 a^8 p^8$	0.2957135440714151E-03	$\frac{3^4 \cdot 7^2 \cdot 5}{2^{26}}$	$< 1.8 \cdot 10^{-13}$
$a^{10} p^{10}$	0.5914270880263635E-04	$\frac{3^4 \cdot 7^2}{2^{26}}$	$< 2.3 \cdot 10^{-14}$

Note that the exact same coefficients from table 5.2 were used for $(q, p) = (\theta_0, 0)$. This result coincides with the general analytic formula for the Pendulum:

$$\frac{\Delta T}{T_0} = \sum_{n=1}^{\infty} \left(\frac{(2n)!}{2^{2n} (n!)^2} \right)^2 \sin^{2n} \left(\frac{\theta_0^2}{2} \right) = \frac{\theta_0^2}{16} + \frac{11\theta_0^4}{3072} + \frac{173\theta_0^6}{737280} + \dots \quad (5.36)$$

which is given in equation (8) of [20], with $T_0 = \frac{2\pi}{\omega_0}$ and $\Delta T = T - T_0$. The COSY results were

therefore accurate up to the tiny floating point errors $< 2.3 \cdot 10^{-14}$. The approximation to fraction seems reasonable for those small errors.

Considering grandpas Pendulum clock, which oscillates with a certain period T_1 and amplitude θ_0 , how does the period change, with small variations to the amplitude? The relative error in the period is defined as follows:

$$\frac{\Delta T}{T_1} = \frac{T(\theta_0 + \Delta\theta) - T(\theta_0)}{T(\theta_0)} \quad (5.37)$$

Figure 5.4 illustrates the dependence of the relative error in the period on θ_0 and $\Delta\theta$. Assuming that the Pendulum is supposed to oscillate with an amplitude of $\theta_0 = \frac{\pi}{6} = 30$ deg and is offset by $\sigma_\theta = \frac{\pi}{36} = 5$ deg, the relative error is approximately 0.63%, which is already 9 min/day . Even worse is to calculate the period $T_0 = 2\pi\sqrt{\frac{l}{g}}$ of the Pendulum from the small angle approximation, compared to the actual period at an amplitude of $\theta_0 = \frac{\pi}{6} = 30$ deg, which yields a relative error of 1.74%, which is approximately 25 min/day .

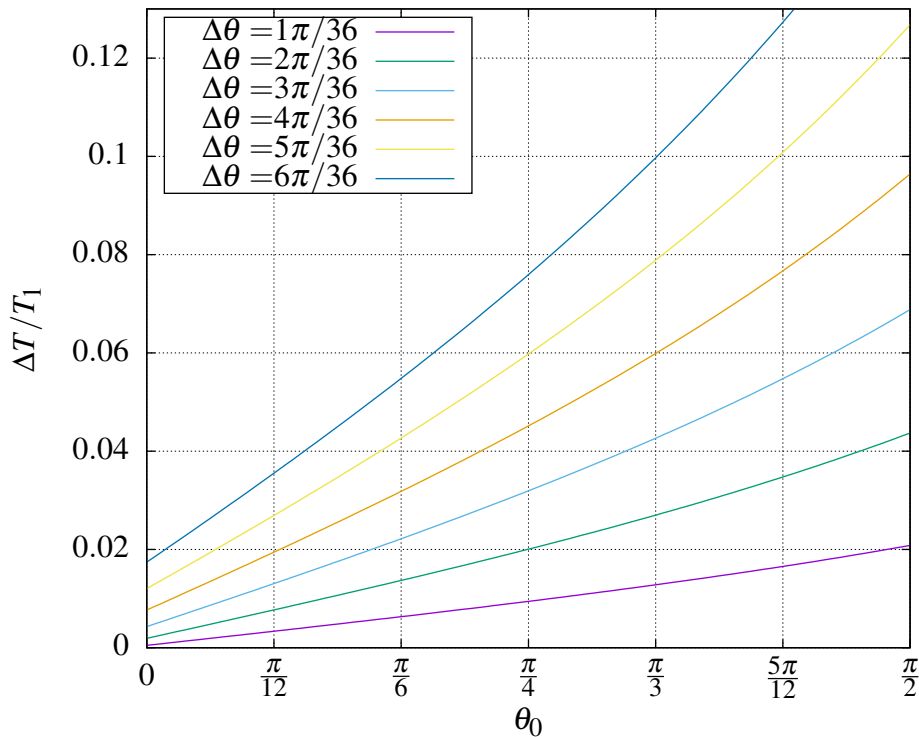


Figure 5.4 The graph illustrates the amplitude θ_0 dependence of the relative period-error for different amplitude shifts $\Delta\theta$.

5.2 Normal Form Uniqueness

The following section largely draws from [2]. Looking at the illustrations of the transfer map in the Pendulum calculation (figure 5.2 and 5.3), it becomes apparent that both show 'fragmented' and seemingly continuous curves. The reason for this bares some unique properties. With every iteration of the transfer map \mathcal{M}_{t_0} , the state is mapped one time step of t_0 further. Since it is a periodic system, the number of iterations it takes for the iteration to reach the original starting point can be calculated. If the period of the curve $T(r)$ divided by the time step-size of the transfer map t_0 can be expressed as a fraction of integer values (a rational number), then the numerator determines the required number of iterations and the denominator determines the number of revolutions required before ending up at the starting point again.

$$\frac{T(r)}{t_0} = \frac{\text{Iterations}}{\text{Revolutions}} = \frac{n}{k} \quad (5.38)$$

In this case, the iteration resonates, which means that only certain points on the curve are reached and form a closed system. These points are period n fixed points, which can be related to the associated amplitude dependent frequency, which is specific for the particular curve. If the ratio of the amplitude dependent Period and step-size is not a rational number, the iterations will never resonate with earlier iterations and therefore not create any fixed points, which generates the seemingly continuous curves. The period n fixed points do not change under bijective transformations.

Also, they form a fixed point structure, which is a dense subset of the completeness of all curves just like the rational numbers form a dense subset of the real numbers. The invariance of the fixed points conserves the associated resonances and makes them an invariant as well. The Normal Form coordinates are special coordinates, in which the frequency along the phase space curve is constant and therefore rotationally invariant. This makes these coordinates uniquely 'natural' for the resonance extraction. Figure 5.6 illustrates this by presenting some 'low' period fixed points, which have the same distance between each fixed point of the curve. The original representation in 5.5 does not have that property, which can be seen especially further away from the origin. This special property makes the Normal Form unique.

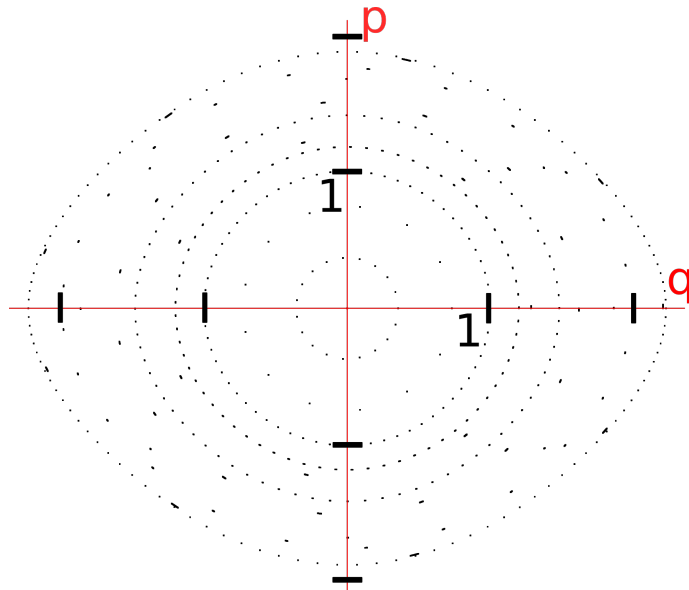


Figure 5.5 The phase space curves originate from the same map used in figure 5.2. The different curves consist of 'low' period fixed points, which represent the specific resonances of the curve. The distance between the single resonance points illustrates how the frequency changes along the curve.

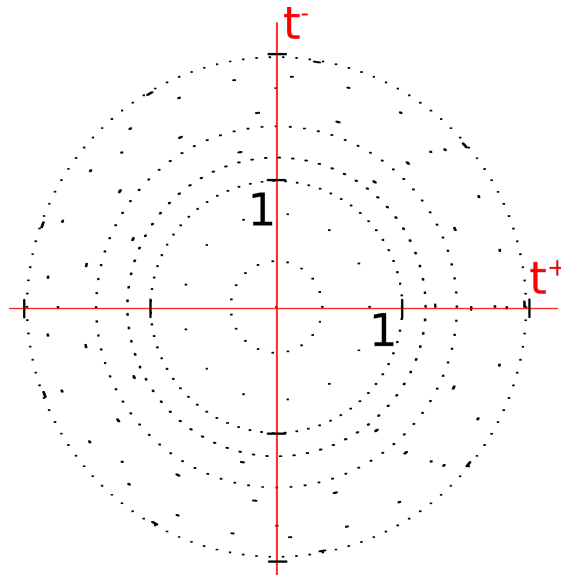


Figure 5.6 The phase space curves originate from the same map used in figure 5.3. The different curves consist of 'low' period fixed points, which represent the specific resonances of the curve. In the Normal Form, the distance between the single resonance points is constant along one curve, which means that the frequency does not change along the curve. The Normal Form coordinates are unique in this property.

5.3 Comparison to Lie Transform perturbation Theory

John Cary discussed Lie Transform perturbation Theory for Hamiltonian systems [9] on an example of an anharmonic oscillator. The Hamiltonian of this example system is given in [9, 4.18] as follows:

$$H(p, q) = \frac{p^2}{2} + \frac{\omega_0^2 q^2}{2} + \frac{\varepsilon \omega_0^2 q^4}{4} + \frac{\varepsilon^2 a \omega_0^3 q^6}{8} \quad (5.39)$$

In this section, the results of the paper [9] and the DA Normal Form Algorithm approach shall be compared. The COSY INFINITY solution of ω is given in terms of (q, p) , while the paper uses Action-Angle coordinates of the perturbed Hamiltonian (J, ϕ) . To make the results comparable, the steps in the paper [9] shall be followed to the minimum extent required to understand the transformation from the Action-Angle variables back to (q, p) .

In the paper, the Hamiltonian is first rewritten in terms of the Action-Angle variables of the unperturbed case ($\varepsilon = 0$). The unperturbed Hamiltonian shall be called H_0 and is equal to E_0 the energy, as a constant of the system. From equation 5.22 the solution of the unperturbed harmonic oscillator with $m = 1$ is known to be the following:

$$p = -r \sin(\omega_0 t + \varphi_0) \quad q = \frac{r}{\omega_0} \cos(\omega_0 t + \varphi_0) \quad (5.40)$$

$$r = \sqrt{p^2 + \omega_0^2 q^2} = \sqrt{2E_0} \quad (5.41)$$

The section on Action-Angle variables and equation 1.53 show how the action j of the ($\varepsilon = 0$)-case can be derived as follows:

$$j = \frac{1}{2\pi} \oint p(E_0, q) dq = \frac{1}{2\pi} \oint \sqrt{2E_0 - \omega_0^2 q^2} dq \quad (5.42)$$

$$= \frac{\sqrt{2E_0}}{2\pi} \oint \sqrt{1 - \frac{\omega_0^2 q^2}{2E_0}} dq = \frac{\sqrt{2E_0}}{2\pi} \oint \sqrt{1 - \sin^2 Q} dq \quad (5.43)$$

where $\sin Q = \frac{\omega_0 q}{\sqrt{2E_0}}$ and $\cos Q \frac{dQ}{dq} = \frac{\omega_0}{\sqrt{2E_0}}$. Therefore, $dq = \frac{\sqrt{2E_0}}{\omega_0} \cos Q$ and it follows for j :

$$j = \frac{\sqrt{2E_0}}{2\pi} \oint \cos Q \frac{\sqrt{2E_0} \cos Q}{\omega_0} dQ \quad (5.44)$$

$$= \frac{2E_0}{2\pi \omega_0} \oint \cos^2 Q dQ = \frac{E_0}{\omega_0} \quad (5.45)$$

comparing the result for j in terms of E_0 with the relation in equation 5.41 yields:

$$j = \frac{E_0}{\omega_0} = \frac{r^2}{2\omega_0} \quad (5.46)$$

with this result the Action-Angle φ can be derived from equation 1.52:

$$H_0 = E_0 = \omega_0 j \quad \frac{\partial H_0}{\partial j} = \omega_0 = \dot{\varphi} \quad (5.47)$$

$$\varphi(t) = \omega_0 t + \varphi_0 \quad (5.48)$$

Therefore, the original Hamiltonian can be rewritten in terms of the unperturbed Action-Angle variables with $p = -\sqrt{2j\omega_0} \sin \varphi$ $q = \sqrt{\frac{2j}{\omega_0}} \cos \varphi$ is given as [9, 4.19]

$$h(j, \varphi) = \omega_0 j + \varepsilon j^2 \cos^4 \varphi + \varepsilon^2 a j^3 \cos^6 \varphi. \quad (5.49)$$

The following derivation leading to equation 5.53 is shown using [9, 4.30-31+35-37]. The unperturbed Action-Angle variables are then transformed into the new Action-Angle variables to first order of the perturbed system. The relationship between old (j, φ) and new variables (J, ϕ) is given as follows:

$$\begin{pmatrix} \varphi \\ j \end{pmatrix} = \begin{pmatrix} \phi \\ J \end{pmatrix} + \frac{\varepsilon J}{\omega_0} \begin{pmatrix} \frac{1}{16} \sin(4\phi) + \frac{1}{2} \sin(2\phi) \\ -\frac{J}{8} \cos(4\phi) - \frac{J}{2} \cos(2\phi) \end{pmatrix} \quad (5.50)$$

The solution for ω up to 2^{nd} order in J is then given with

$$\omega(J) =_2 \omega_0 + \frac{3}{4} \varepsilon J + \varepsilon^2 \left(\frac{15a}{16} - \frac{51}{64\omega_0} \right) J^2 \quad (5.51)$$

Using the energy of the system in the transformed variables

$$K =_3 \omega_0 J + \frac{3}{8} \varepsilon J^2 + \varepsilon^2 J^3 \left(\frac{5a}{16} - \frac{17}{64\omega_0} \right) \quad (5.52)$$

the solution for ω is given up to 2^{nd} order in E :

$$\omega(E) =_2 \omega_0 + \frac{3}{4} \varepsilon \frac{E}{\omega_0} + \varepsilon^2 \left(\frac{E}{\omega_0} \right)^2 \left(\frac{15a}{16} - \frac{51}{64\omega_0} \right) \quad (5.53)$$

The result from equation 5.53 is written in terms of (q, p) up to 4th order to make it comparable to the result from the COSY based method later on:

$$\begin{aligned} \omega =_4 \omega_0 & \left(1 + \frac{3\varepsilon}{8} \left(q^2 + \frac{p^2}{\omega_0^2} \right) + \varepsilon^2 \left(q^2 + \frac{p^2}{\omega_0^2} \right)^2 \left(\frac{15a\omega_0}{64} - \frac{21}{256} \right) \right) \\ & - \omega_0 \frac{3\varepsilon^2}{8\omega_0^2} \left(\frac{\omega_0^2 p^4}{2} + p^2 q^2 \right) \end{aligned} \quad (5.54)$$

The goal of this section is to show, that the result from equation 5.54 can be reproduced with a much simpler approach using COSY, which would even include the correct terms for p^4 and furthermore, allow a calculation of terms up to arbitrary order.

From the Hamiltonian in equation 5.39 the Hamilton equations are given as follows:

$$\vec{f} = \begin{pmatrix} \dot{q} \\ \dot{p} \end{pmatrix} = \begin{pmatrix} p \\ -\omega_0^2 q - \varepsilon \omega_0^2 q^3 - \frac{3}{4} \varepsilon^2 a \omega_0^3 q^5 \end{pmatrix} \quad (5.55)$$

From the section above it is known that implementing this formula in COSY would result in an error in the DA Normal Form Algorithm, since the linear part is only parameter-dependent. Therefore, the ODE has to be transformed. From the Pendulum section (5.1) it is known that the form of the Hamiltonian and its Hamilton equations is only conserved for canonical transformations like in equation 5.9. Thus, the ODE can be transformed to:

$$\vec{f} = \begin{pmatrix} \dot{p}_1 \\ \dot{q}_1 \end{pmatrix} = \begin{pmatrix} -\omega_0 q_1 - \varepsilon q_1^3 - \frac{3}{4} \varepsilon^2 a q_1^5 \\ \omega_0 p_1 \end{pmatrix} \quad (5.56)$$

with the known time scaling of $t' = \omega_0 t$ the ODE can be written as:

$$\begin{pmatrix} \dot{p}_1 \\ \dot{q}_1 \end{pmatrix} = \begin{pmatrix} -q_1 - \frac{\varepsilon}{\omega_0} q_1^3 - \frac{3}{4} \frac{\varepsilon^2 a}{\omega_0} q_1^5 \\ p_1 \end{pmatrix} \quad (5.57)$$

$$= \begin{pmatrix} -q_1 - a_1 q_1^3 - \frac{3}{4} a_2 q_1^5 \\ p_1 \end{pmatrix} \quad (5.58)$$

where $a_1 = \frac{\varepsilon}{\omega_0}$ and $a_2 = \frac{\varepsilon^2 a}{\omega_0^2}$ resulting in the following tunes in the fraction representation:

$$\begin{aligned}
\omega_{I'} &= 1 + \frac{3a_1 (q_1^2 + p_1^2)}{8} + \frac{15a_2 (q_1^2 + p_1^2)^2}{64} - a_1^2 \left(\frac{21q_1^4 + 138q_1^2 p_1^2 + 69p_1^4}{256} \right) \\
&= 1 + \frac{3\varepsilon}{8\omega_0} (q_1^2 + p_1^2) + \frac{\varepsilon^2}{\omega_0^2} (q_1^2 + p_1^2)^2 \left(\frac{15a\omega_0}{64} - \frac{21}{256} \right) - \frac{3\varepsilon^2}{8\omega_0^2} \left(q_1^2 p_1^2 + \frac{p_1^4}{2} \right) \\
&= 1 + \frac{3\varepsilon}{8} \left(q^2 + \frac{p^2}{\omega_0^2} \right) + \varepsilon^2 \left(q^2 + \frac{p^2}{\omega_0^2} \right)^2 \left(\frac{15a\omega_0}{64} - \frac{21}{256} \right) \\
&\quad - \frac{3\varepsilon^2}{8\omega_0^2} \left(\frac{\omega_0^2 p^4}{2} + p^2 q^2 \right) \tag{5.59}
\end{aligned}$$

the COSY coefficients are listed in table 5.3 with the difference of the results to the fraction representations. Again, the accuracy is in the margin of the floating point calculation error.

Table 5.3 Coefficients of the COSY result for the tunes $\omega_{I'}(q_1, p_1)$ shown in equation 5.59 with corresponding fraction representation and maximal error in the representation. A table with coefficients to equation 5.59 up to order 10 in (q_1, p_1) are listed in the appendix in table 5.4.

Factor	Coefficient	Fraction	Difference in representation
1	0.9999999999999908	1	$< 9.2 \cdot 10^{-15}$
$a_1 q_1^2$	0.37499999999999779	$\frac{3}{8}$	$< 2.3 \cdot 10^{-14}$
$a_1 p_1^2$	0.37499999999999780	$\frac{3}{8}$	$< 2.2 \cdot 10^{-14}$
$a_2 q_1^4$	0.23437499999999911	$\frac{15}{64}$	$< 9 \cdot 10^{-15}$
$a_2 q_1^2 p_1^2$	0.46874999999999823	$\frac{15}{32}$	$< 1.8 \cdot 10^{-14}$
$a_2 p_1^4$	0.23437499999999913	$\frac{15}{64}$	$< 9 \cdot 10^{-15}$
$a_1^2 q_1^4$	-8.203125000003507E-01	$-\frac{21}{256}$	$< 3.5 \cdot 10^{-14}$
$a_1^2 q_1^2 p_1^2$	-.5390625000000708	$-\frac{69}{128}$	$< 7.1 \cdot 10^{-14}$
$a_1^2 p_1^4$	-.2695312500000204	$-\frac{69}{256}$	$< 2.1 \cdot 10^{-14}$

The COSY result from equation 5.59 agrees with the transformed solution from the paper [9] in equation 5.54, up to 4th order in (q, p) and floating point accuracy. While the Cary approach requires a great investment in calculation which becomes more and more complex with higher orders, COSY offers the result with floating point accuracy up to arbitrary order as table 5.4 illustrates with minimal trade-offs in computation time.

Table 5.4 COSY coefficients of $\omega_r(q_1, p_1)$ up to order 14 for the calculation in equation 5.59.

Order	Factor	Coefficient	Order	Factor	Coefficient
0	1	0.9999999999999990	12	$q_1^8 a_1^4$	-0.024982452392576
3	$q_1^2 a_1$	0.3749999999999977	12	$q_1^6 p_1^2 a_1^4$	-0.757644653320320
3	$p_1^2 a_1$	0.3749999999999978	12	$q_1^4 p_1^4 a_1^4$	-2.063713073730610
5	$q_1^4 a_2$	0.2343749999999991	12	$q_1^2 p_1^6 a_1^4$	-1.684890747070440
5	$q_1^2 p_1^2 a_2$	0.4687499999999982	12	$p_1^8 a_1^4$	-0.421222686767588
5	$p_1^4 a_2$	0.2343749999999991	13	$q_1^{10} a_1 a_2^2$	0.061683654785137
6	$q_1^4 a_1^2$	-0.0820312500000035	13	$q_1^8 p_1^2 a_1 a_2^2$	1.630439758300960
6	$q_1^2 p_1^2 a_1^2$	-0.5390625000000070	13	$q_1^7 p_1^3 a_1 a_2^2$	0.0000000000000006
6	$p_1^4 a_1^2$	-0.2695312500000020	13	$q_1^6 p_1^4 a_1 a_2^2$	5.188980102540040
8	$q_1^6 a_1 a_2$	-0.1113281250000058	13	$q_1^5 p_1^5 a_1 a_2^2$	0.0000000000000022
8	$q_1^4 p_1^2 a_1 a_2$	-1.083984375000230	13	$q_1^4 p_1^6 a_1 a_2^2$	6.144790649415080
8	$q_1^2 p_1^4 a_1 a_2$	-1.318359375000150	13	$q_1^3 p_1^7 a_1 a_2^2$	0.0000000000000006
8	$p_1^6 a_1 a_2$	-0.439453125000043	13	$q_1^2 p_1^8 a_1 a_2^2$	3.228950500488710
9	$q_1^6 a_1^3$	0.039550781249991	13	$p_1^{10} a_1 a_2^2$	0.645790100097742
9	$q_1^4 p_1^2 a_1^3$	0.657714843750032	14	$q_1^{10} a_1^3 a_2$	-0.072978973388661
9	$q_1^2 p_1^4 a_1^3$	0.927246093750080	14	$q_1^9 p_1 a_1^3 a_2$	0.0000000000000015
9	$p_1^6 a_1^3$	0.309082031250014	14	$q_1^8 p_1^2 a_1^3 a_2$	-2.684474945068560
10	$q_1^8 a_2^2$	-0.039367675781281	14	$q_1^7 p_1^3 a_1^3 a_2$	-0.0000000000000034
10	$q_1^6 p_1^2 a_2^2$	-0.509033203125187	14	$q_1^6 p_1^4 a_1^3 a_2$	-10.324333190919100
10	$q_1^4 p_1^4 a_2^2$	-0.939331054687730	14	$q_1^5 p_1^5 a_1^3 a_2$	-0.0000000000000081
10	$q_1^2 p_1^6 a_2^2$	-0.626220703125106	14	$q_1^4 p_1^6 a_1^3 a_2$	-13.835563659669400
10	$p_1^8 a_2^2$	-0.156555175781281	14	$q_1^3 p_1^7 a_1^3 a_2$	-0.0000000000000035
11	$q_1^8 a_1^2 a_2$	0.084503173828104	14	$q_1^2 p_1^8 a_1^3 a_2$	-7.737636566162740
11	$q_1^6 p_1^2 a_1^2 a_2$	1.826293945312620	14	$q_1 p_1^9 a_1^3 a_2$	0.0000000000000015
11	$q_1^4 p_1^4 a_1^2 a_2$	4.259948730469280	14	$p_1^{10} a_1^3 a_2$	-1.547527313232520

The COSY result shall be compared to the earlier result from the Pendulum by inserting $\varepsilon = -1/6$ and $a = 2/5\omega_0$. This substitution converts the Hamiltonian from equation 5.39 into the

Pendulum Hamiltonian from the section before (5.1) up to 6th order:

$$H = \frac{p^2}{2} + \omega_0^2 \left(\frac{q^2}{2} - \frac{q^4}{24} + \frac{q^6}{720} \right) \stackrel{6}{=} \frac{p^2}{2} + \omega_0^2 (1 - \cos(q)) \quad (5.60)$$

substituting the given values for ε and a in equation 5.59 yields:

$$\omega_{1l} = 1 - \frac{q^2 + a^2 p^2}{16} + \frac{q^4}{3072} - \frac{5p^4}{1024} - \frac{5a^2 p^2}{512} + \dots \quad (5.61)$$

This equation coincides in all terms of order $m \leq 6$ with the Pendulum solution in equation 5.31, which supports the consistency within the COSY calculations.

To investigate the COSY result a bit further, the transfer map is tracked for the following parameters $(\omega_0, \varepsilon, a) = (1, 2, 2/9)$ which correspond to a potential V in the Hamiltonian of the form shown in figure 5.7. The potential has three stable stationary points and two unstable stationary points in between. The tracking of the transfer map of the system from $t = 0$ to $t = 0.1$ with the

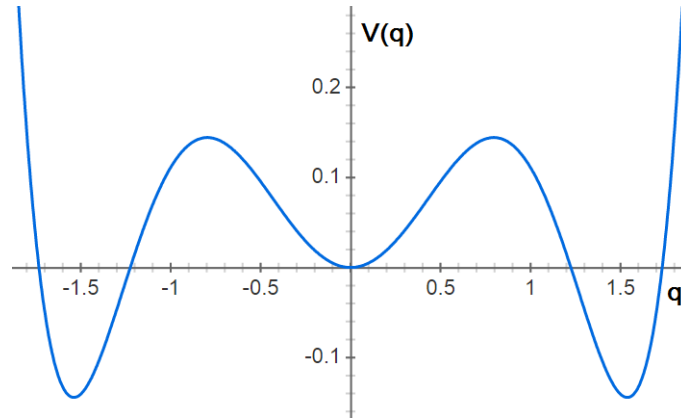


Figure 5.7 The graph shows the potential $V = \frac{q^2}{2} - \frac{q^4}{24} + \frac{q^6}{720}$ of the Hamiltonian in equation 5.39 for the parameters $(\omega_0, \varepsilon, a) = (1, 2, 2/9)$. There are three stable stationary points at the origin and $q = \pm\sqrt{\frac{3}{2} + \frac{\sqrt{3}}{2}}$. The two unstable stationary points are at $q = \pm\sqrt{\frac{3}{2} - \frac{\sqrt{3}}{2}}$. The potential allows oscillation in each of the three valleys as well as a global oscillation over large p .

parameters mentioned above is shown in figure 5.8. It shows phase space curves around the the fixed points (stable stationary points of the potential) as well as a global curve for larger p . The considered perturbation in the calculation above was with respect to the origin. Perturbation theory in general is only able to solve for the direct surrounding of the considered fixed point, which is the unperturbed harmonic oscillator around the origin in this case. Therefore, neither the solution of

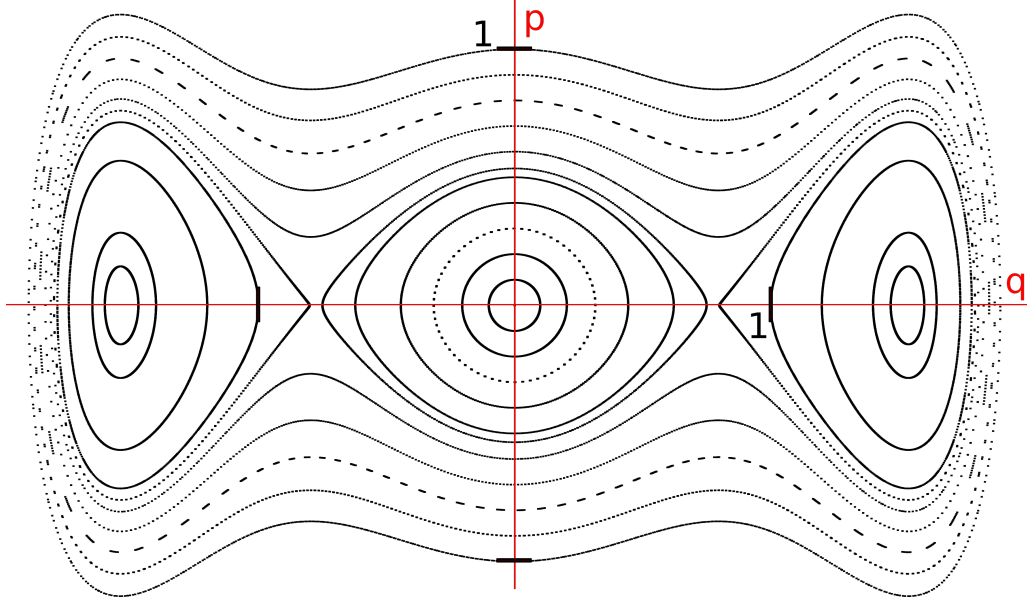


Figure 5.8 The transfer map of the ODE in equation 5.57 was calculated using the RK4 with 100 steps of step-size $h = 0.001$ until $t = 0.1$. The illustration shows the phase space tracking of 1000 iterations using the parameters $(\omega_0, \varepsilon, a) = (1, 2, 2/9)$. The curves around the origin are similar to the one in the Pendulum example in figure 5.2. For larger $|q|$ and small p the phase space curve oscillates around a different fixed point at approximately $(\pm 1.5, 0)$. For large q and p the phase space curve oscillates around all three fixed points. Figure 5.7 makes this behavior apparent.

the Lie Perturbation approach nor the COSY result, yield the frequencies for any other oscillations that around the origin fixed point. The tracking of the Normal Form of the transfer map illustrates this property in figure 5.9.

In contrast to the Lie Perturbation theory, the tracking pictures identified the surrounding fixed points. The COSY approach can easily be varied in its initial conditions to consider a perturbation around the fixed point at $(q_0, p_0) = \left(\sqrt{\frac{3}{2}} + \frac{\sqrt{3}}{2}, 0\right)$. The tracking picture of the shifted system with the same parameters is shown in figure 5.10.

It is apparent, that the fixed point at $(q_0, p_0) = \left(-\sqrt{\frac{3}{2}} + \frac{\sqrt{3}}{2}, 0\right)$ is not depicted. It seems like the transfer map can only determine fixed points in the direct surrounding of the considered fixed point. The Normal Form to this fixed point perturbation reveals the tune shifts with respect to the unperturbed case. Table 5.5 lists the coefficients for the tunes $\omega_{l'}(q', p)$.

Directly at the fixed point, the frequency of the oscillation is at least double the frequency of the

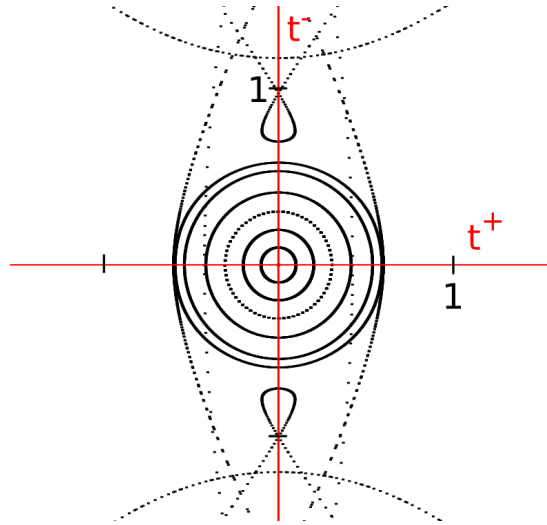


Figure 5.9 Tracking of 1000 iterations using the parameters $(\omega_0, \epsilon, a) = (1, 2, 2/9)$ of the transfer map used in figure 5.8 in Normal Form. In comparison to figure 5.8 only the curves around the origin are preserved, which illustrates how perturbation theory only works in the direct surrounding of the considered fixed point.

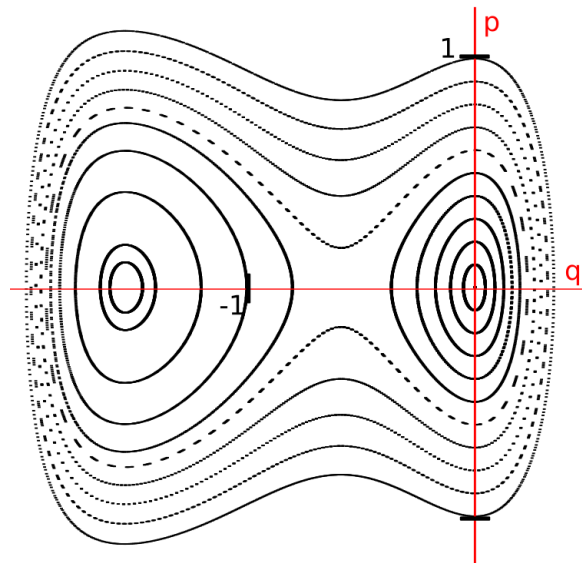


Figure 5.10 Tracking picture of the same transfer map used in figure 5.8 only with a shifted reference point for the perturbation.

unperturbed case at the origin, which can be determined by the constant term of the frequencies. Already small variations to q' make the frequency drop a lot faster than in the origin-related case, which can be determined by the large negative coefficients for terms in q' . In general, the example shows how adaptable and effective the COSY approach is.

Table 5.5 The table reveals the terms and related coefficients of $\omega_r(q', p)$ for the oscillation around the fixed point $(q'_0, p_0) = \left(\sqrt{\frac{3}{2} + \frac{\sqrt{3}}{2}}, 0\right)$ of the Hamiltonian in equation 5.39 with the parameters $(\omega_0, \varepsilon, a) = (1, 2, 2/9)$ and $q' = q - q_0$.

Coefficients	Order	Factor	Coefficients	Order	Factor
2.33754178896010E+00	0	1	1.21382387121546E-12	6	$q'^5 p$
-5.16315324537914E+00	2	q'^2	-5.45104992215302E+01	6	$q'^4 p^2$
-9.44922625720420E-01	2	p^2	-1.45822595527180E-13	6	$q'^3 p^3$
-9.47032596684882E+00	3	q'^3	-8.60580684709545E+00	6	$q'^2 p^4$
3.23158337141804E-12	3	$q' p^2$	-1.90397253907876E-14	6	$q' p^5$
-2.27378667458620E+01	4	q'^4	-5.24990654350866E-01	6	p^6
-5.94074588085554E+00	4	$q'^2 p^2$	-5.58506174494210E+02	7	q'^7
-5.43615977456575E-01	4	p^4	4.99636191467564E-12	7	$q'^6 p$
-6.14780725235178E+01	5	q'^5	-1.74730289073416E+02	7	$q'^5 p^2$
3.15815384599474E-13	5	$q'^4 p$	1.69335451054548E-12	7	$q'^4 p^3$
-1.08965969639085E+01	5	$q'^3 p^2$	-1.57848880666779E+01	7	$q'^3 p^4$
7.53952744185456E-14	5	$q'^2 p^3$	-1.20261466986781E-13	7	$q'^2 p^5$
3.69557903192260E-12	5	$q' p^4$	5.32068881682924E-12	7	$q' p^6$
-1.81373221158553E+02	6	q'^6			

5.4 Solving perturbed Harmonic oscillator with perharmosc.fox

After those two specific examples of using the DA Framework in COSY INFINITY, the general algorithm in perharmosc.fox for an arbitrary time-independent perturbed Harmonic oscillator of the following form shall be explained:

$$H = a_0 \frac{q^2}{2} + a_k q^k + b_0 \frac{p^2}{2} + b_l p^l + c_i q^j p^n \quad (5.62)$$

where the terms of $a_k q^k$, $b_l p^l$ and $c_i q^j p^n$ can occur for various k 's, l 's and combinations of (j, n) as long as $k > 2$, $l > 2$ and $j + n > 2$ for all terms. To use the already established framework, the following variables are defined: $a_0 = m\omega_0^2$ and $b_0 = \frac{1}{m}$. Rewriting the equations yields: $m = \frac{1}{b_0}$

and $\omega_0^2 = a_0 b_0$. Hence, $m\omega_0 = \sqrt{\frac{a_0}{b_0}}$. The Hamilton equations are therefore given as follows:

$$\begin{pmatrix} \dot{q} \\ \dot{p} \end{pmatrix} = \begin{pmatrix} \frac{\partial H}{\partial p} \\ -\frac{\partial H}{\partial q} \end{pmatrix} = \begin{pmatrix} b_0 p + lb_l p^{l-1} + nc_i q^j p^{n-1} \\ -a_0 q - ka_k q^{k-1} + jc_i q^{j-1} p^n \end{pmatrix} \quad (5.63)$$

$$= \begin{pmatrix} 0 & \frac{1}{m} \\ -m\omega_0^2 & 0 \end{pmatrix} \begin{pmatrix} q \\ p \end{pmatrix} + \begin{pmatrix} lb_l p^{l-1} + nc_i q^j p^{n-1} \\ -ka_k q^{k-1} + jc_i q^{j-1} p^n \end{pmatrix} \quad (5.64)$$

The known transformation \hat{T} from equation 5.9 and the time scaling to $t' = \omega_0 t$, to unparameterise the linear part of the differential equation then yield:

$$\begin{pmatrix} \frac{\dot{p}}{\sqrt{m\omega_0}} \\ -\sqrt{m\omega_0}\dot{q} \end{pmatrix} = \begin{pmatrix} -\frac{a_0 q + ka_k q^{k-1} + jc_i q^{j-1} p^n}{\sqrt{m\omega_0}} \\ -\sqrt{m\omega_0} (b_0 p + lb_l p^{l-1} + nc_i q^j p^{n-1}) \end{pmatrix} \quad (5.65)$$

$$\begin{pmatrix} \dot{p}_1 \\ -\dot{q}_1 \end{pmatrix} = \begin{pmatrix} -\frac{a_0 q_1}{m\omega_0} - \frac{ka_k q_1^{k-1}}{(m\omega_0)^{\frac{k}{2}}} - j(m\omega_0)^{\frac{n-j}{2}} c_i q_1^{j-1} p_1^n \\ -m\omega_0 b_0 p_1 - (m\omega_0)^{\frac{l}{2}} lb_l p_1^{l-1} + n(m\omega_0)^{\frac{n-j}{2}} c_i q_1^j p_1^{n-1} \end{pmatrix} \quad (5.66)$$

$$\begin{pmatrix} \dot{p}_1 \\ \dot{q}_1 \end{pmatrix} = \omega_0 \begin{pmatrix} 0 & -1 \\ 1 & 0 \end{pmatrix} \begin{pmatrix} p_1 \\ q_1 \end{pmatrix} + \begin{pmatrix} -\frac{ka_k q_1^{k-1}}{\omega_0 (m\omega_0)^{\frac{k}{2}}} - \frac{jc_i q_1^{j-1} p_1^n}{\omega_0 (m\omega_0)^{\frac{j-n}{2}}} \\ \frac{(m\omega_0)^{\frac{l}{2}} lb_l p_1^{l-1}}{\omega_0} + \frac{nc_i q_1^j p_1^{n-1}}{\omega_0 (m\omega_0)^{\frac{j-n}{2}}} \end{pmatrix} \quad (5.67)$$

$$\begin{pmatrix} \dot{p}_1 \\ \dot{q}_1 \end{pmatrix} = \begin{pmatrix} 0 & -1 \\ 1 & 0 \end{pmatrix} \begin{pmatrix} p_1 \\ q_1 \end{pmatrix} + \begin{pmatrix} -kd_k q_1^{k-1} - jg_i q_1^{j-1} p_1^n \\ le_l p_1^{l-1} + ng_i q_1^j p_1^{n-1} \end{pmatrix} \quad (5.68)$$

The final ODE in equation 5.68 is integrated into COSY and the resulting transfer map from the initial state at $t' = 0$ to $t' = 1$ is transformed to Normal Form coordinates, yielding the tunes in the following form $\omega_{t'}(q_1, p_1, d_k, e_l, g_i)$ and the period $T_{t'}(q_1, p_1, d_k, e_l, g_i)$. With the following

substitutions, the result can be rewritten in terms of the original coordinates. One step is to bring the respective quantity to the original time scaling:

$$T(q_1, p_1, d_k, e_l, g_i) = \frac{2\pi}{\omega_0} T_{t'}(q_1, p_1, d_k, e_l, g_i) \quad (5.69)$$

$$\omega(q_1, p_1, d_k, e_l, g_i) = \omega_0 \omega_{t'}(q_1, p_1, d_k, e_l, g_i) \quad (5.70)$$

The coordinates (q_1, p_1) can be transformed back to the original coordinates q, p , with

$$(q_1, p_1) = \left(\sqrt{m\omega_0} q, \frac{p}{\sqrt{m\omega_0}} \right) = \left(\sqrt[4]{\frac{a_0}{b_0}} q, \sqrt[4]{\frac{b_0}{a_0}} p \right) \quad (5.71)$$

Finally, the parameters used in the Algorithm can be scaled back to the original:

$$d_k = \frac{a_k}{\omega_0} (m\omega_0)^{-\frac{k}{4}} \quad e_l = \frac{b_l}{\omega_0} (m\omega_0)^{\frac{l}{4}} \quad g_i = \frac{c_i}{\omega_0} (m\omega_0)^{\frac{n-j}{4}} \quad (5.72)$$

$$d_k = \frac{a_k}{\sqrt{a_0 b_0}} \left(\frac{b_0}{a_0} \right)^{\frac{k}{4}} \quad e_l = \frac{b_l}{\sqrt{a_0 b_0}} \left(\frac{a_0}{b_0} \right)^{\frac{l}{4}} \quad g_i = \frac{c_i}{\sqrt{a_0 b_0}} \left(\frac{b_0}{a_0} \right)^{\frac{j-n}{4}} \quad (5.73)$$

The COSY result will be given in $(q_1, p_1, d_k, e_l, g_i)$ and appears as it is illustrated in table 5.6.

This method of substituting the original parameters and variables at the end makes the algorithm most efficient, because it operates with the minimal amount of orders and therefore yields maximum precision. There are ways to implement problematic parameters, like \sqrt{a} or $1/\sqrt{a}$, by introducing additional variables $c = \sqrt{a}$ and $d = 1/\sqrt{a}$, but that reduces the precision. Additionally, procedures would have to be implemented that assure, that parameters are canceled according to $cd = 1$, $c^2 = a$ and $d^2 = b$. Those procedures would only simplify the result at the cost of a lower precision and and increase in computing time.

Table 5.6 The table illustrates an example output of COSY for the period T in the (q_1, p_1) -coordinates up to 5^{th} order in (q_1, p_1) . The column 'I' denotes the row-counter. The columns under 'EXPONENTS' each represent one variable. The first two are the (q_1, p_1) -coordinates. Each additional column denotes a parameter d_k, e_l or g_i starting with the parameter associated with the first perturbation term entered to the program. The number in the respective column denotes the exponent of the variable/parameter. The column 'ORDER' sums up all the exponents and presents the total order of the term. The second column 'COEFFICIENT' yields the COSY Taylor expansion coefficient regarding the associated term.

I	COEFFICIENT	ORDER	EXPONENTS			
1	-0.84147098	1	1	0	0	0
2	0.54030231	1	0	1	0	0
3	-0.50509902	4	3	0	1	0
4	-0.74594703	4	2	1	1	0
5	-0.55736289	4	1	2	1	0
6	-0.17208648	4	0	3	1	0
7	-0.30059578	6	5	0	0	1
8	-0.61324672	6	4	1	0	1
9	-0.78228485	6	3	2	0	1
10	-0.63837415	6	2	3	0	1
11	-0.30556118	6	1	4	0	1
12	-6.52E-02	6	0	5	0	1

CHAPTER 6

CONCLUSION

This thesis introduced a very efficient approach to solving periodic, time independent, Hamiltonian systems with parameter-dependent perturbations up to arbitrary order. The foundation of the method proved to be the DA framework implemented within COSY INFINITY, which allows for the computer-based numerical calculation of algebraic structures. Well known methods like the fourth-order Runge-Kutta can be realized in the DA framework in an equivalent way to the classic implementation. Furthermore, integrators which are based on differentiation and integration such as the Flow or fixed point Integrator, respectively, can be implemented very efficiently in the DA framework, which is due to its automatic differentiation and anti-differentiation operations. As a result, the DA based integrators yield a transfer map, which is an algebraic expression that yields the final state in terms of the initial state. Those maps can also be parameter-dependent, in contrast to regular numerical integrators that do not provide any algebraic expressions.

Furthermore, the DA structure was useful in the implemented DA Normal Form Algorithm, which transformed the transfer map into Normal Form coordinates to calculate the tunes. The tunes are the invariant quantities of the system and do not change along the phase space curve in Normal Form coordinates, which makes these coordinates uniquely 'natural' for the extraction of the tunes. The Normal Form Algorithm uses various transformations within the process, which always occurs together with their inverses. In this context, the property of the DA structure of only yielding an inverse for terms which contained a non-zero constant part became an issue for parameter-dependent maps. The original differential equation had to be transformed canonically to coordinates in which the linear part had a non-zero constant term. In the last step, the composition of the single transformations in the Normal Form Algorithm were used to express the tunes and their tune shifts in the original coordinates, to make the solution suitable for arbitrary initial conditions in the original coordinates.

In the comparison to the Lie Transform perturbation theory, the advantage of easily expressing

the solution in the original coordinates became apparent. Additionally, the tracking pictures illustrated the limitations of perturbation theory in general to the chosen reference system. Even though the COSY tracking could reveal the adjacent fixed points, the Normal Form Algorithm was only able to transform the phase space curves around the origin into circular motions with amplitude-dependent tune shifts. In contrast to the Lie Transform ansatz, a simple coordinate transformation to another fixed point allowed to use the Normal Form method equivalently to determine the tune shifts of oscillations around the new reference point.

As a result of the overall investigation, the program `perhamosc.fox` was written to generally solve parameter-dependent perturbed harmonic oscillators, with the ability to change the reference point of the perturbation. For this thesis all procedures used were either already implemented in `COSY INFINITY` or were programmed on the `USER` level since computing time was no relevant factor. An implementation of certain procedures in the underlying `FORTRAN` code as internal procedures would make those drastically more efficient.

APPENDIX

APPENDIX

COSY COEFFICIENTS

Table A.1 COSY coefficients of $r^2(q_1, p_1)$ up to order 10 in (q_1, p_1) for the Pendulum calculation.

Order	Factor	Coefficient	Order	Factor	Coefficient
2	q_1^2	1.000000000000000E+00	11	$q_1^2 p_1^6 a^3$	1.52587890584416E-03
2	p_1^2	1.000000000000000E+00	11	$q_1 p_1^7 a^3$	-6.23130019805629E-14
5	$q_1^4 a$	-5.208333333333330E-02	11	$p_1^8 a^3$	3.81469726555902E-04
5	$q_1^2 p_1^2 a$	6.24999999999983E-02	14	$q_1^{10} a^4$	-3.11449487795811E-07
5	$p_1^4 a$	3.12500000000003E-02	14	$q_1^9 p_1 a^4$	2.60559018750832E-13
8	$q_1^6 a^2$	4.99131944441055E-04	14	$q_1^8 p_1^2 a^4$	1.73561143225385E-05
8	$q_1^4 p_1^2 a^2$	3.58072916659495E-03	14	$q_1^7 p_1^3 a^4$	-9.96226834659921E-13
8	$q_1^2 p_1^4 a^2$	8.78906250007309E-03	14	$q_1^6 p_1^4 a^4$	2.27069853202729E-04
8	$p_1^6 a^2$	2.92968750000307E-03	14	$q_1^5 p_1^5 a^4$	-2.30420448719341E-12
11	$q_1^8 a^3$	-9.93032304185488E-06	14	$q_1^4 p_1^6 a^4$	4.56968944165443E-04
11	$q_1^7 p_1 a^3$	2.15106795223296E-14	14	$q_1^3 p_1^7 a^4$	-5.42693199542332E-13
11	$q_1^6 p_1^2 a^3$	2.34646267818247E-04	14	$q_1^2 p_1^8 a^4$	2.92062760508722E-04
11	$q_1^5 p_1^3 a^3$	2.67750123288113E-13	14	$q_1 p_1^9 a^4$	5.23138307236752E-13
11	$q_1^4 p_1^4 a^3$	1.55639648441389E-03	14	$p_1^{10} a^4$	5.84125518994400E-05
11	$q_1^3 p_1^5 a^3$	1.33353180928330E-13			

Table A.2 COSY coefficients of $\omega_{i'}(q_1, p_1)$ up to order 10 in (q_1, p_1) for the Pendulum calculation.

Order	Factor	Coefficient	Order	Factor	Coefficient
0	1	9,99999999999990E-01	12	$q_1^4 p_1^4 a^4$	-5,03063201898618E-04
3	$q_1^2 a$	-6,24999999999962E-02	12	$q_1^2 p_1^6 a^4$	-4,47273254388907E-04
3	$p_1^2 a$	-6,24999999999963E-02	12	$p_1^8 a^4$	-1,11818313597672E-04
6	$q_1^4 a^2$	3,25520833332584E-04	15	$q_1^{10} a^5$	-1,47522023408260E-07
6	$q_1^2 p_1^2 a^2$	-9,76562500000149E-03	15	$q_1^8 p_1^2 a^5$	-1,56177887847264E-05
6	$p_1^4 a^2$	-4,88281250000031E-03	15	$q_1^7 p_1^3 a^5$	5,01368288248799E-15
9	$q_1^6 a^3$	-3,11957465283522E-05	15	$q_1^6 p_1^4 a^5$	-9,92635885946822E-05
9	$q_1^4 p_1^2 a^3$	-1,20035807291816E-03	15	$q_1^5 p_1^5 a^5$	6,26444222558972E-15
9	$q_1^2 p_1^4 a^3$	-2,01416015625245E-03	15	$q_1^4 p_1^6 a^5$	-1,68214241683875E-04
9	$p_1^6 a^3$	-6,71386718750670E-04	15	$q_1^3 p_1^7 a^5$	2,25888609846247E-15
12	$q_1^8 a^4$	-1,90659174731445E-06	15	$q_1^2 p_1^8 a^5$	-1,02743506444934E-04
12	$q_1^6 p_1^2 a^4$	-1,38706631128647E-04	15	$p_1^{10} a^5$	-2,05487012877491E-05

Table A.3 COSY coefficients of $\omega_{i'}(q, p)$ up to order 10 in (q, p) for the Pendulum calculation.

Order	Factor	Coefficient	Order	Factor	Coefficient
0	1	9,99999999999990E-01	12	$q^6 p^2 a^2$	-1,38706631128647E-04
3	q^2	-6,24999999999962E-02	12	$q^4 p^4 a^4$	-5,03063201898618E-04
3	$p^2 a^2$	-6,24999999999963E-02	12	$q^2 p^6 a^6$	-4,47273254388907E-04
6	q^4	3,25520833332584E-04	12	$p^8 a^8$	-1,11818313597672E-04
6	$q^2 p^2 a^2$	-9,76562500000149E-03	15	q^{10}	-1,47522023408260E-07
6	$p^4 a^4$	-4,88281250000031E-03	15	$q^8 p^2 a^2$	-1,56177887847264E-05
9	q^6	-3,11957465283522E-05	15	$q^6 p^4 a^4$	-9,92635885946822E-05
9	$q^4 p^2 a^2$	-1,20035807291816E-03	15	$q^4 p^6 a^6$	-1,68214241683875E-04
9	$q^2 p^4 a^4$	-2,01416015625245E-03	15	$q^2 p^8 a^8$	-1,02743506444934E-04
9	$p^6 a^6$	-6,71386718750670E-04	15	$p^{10} a^{10}$	-2,05487012877491E-05
12	q^8	-1,90659174731445E-06			

BIBLIOGRAPHY

BIBLIOGRAPHY

- [1] Vladimir I Arnold. *Mathematical methods of classical mechanics. Translated from the 1974 Russian original by K. Vogtmann and A. Weinstein. Corrected reprint of the second (1989) edition.* Springer-Verlag, 2nd edition edition, 1978.
- [2] Martin Berz. Private communication.
- [3] Martin Berz. The new method of TPSA algebra for the description of beam dynamics to high orders. *Technical Report AT-6: ATN-86-16, Los Alamos National Laboratory*, 1986.
- [4] Martin Berz. The method of power series tracking for the mathematical description of beam dynamics. *Nuclear Instruments and Methods in Physics Research Section A: Accelerators, Spectrometers, Detectors and Associated Equipment*, 258(3):431–436, 1987.
- [5] Martin Berz. Differential algebraic description of beam dynamics to very high orders. *Part. Accel.*, 24(SSC-152):109–124, 1988.
- [6] Martin Berz. *Modern Map Methods in Particle Beam Physics.* ACADEMIC PRESS A Harcourt Science and Technology Company, 1999.
- [7] Martin Berz, Kyoko Makino, Khodr Shamseddine, Georg H Hoffstätter, and Weishi Wan. 32. COSY INFINITY and its applications in nonlinear dynamics. 1996.
- [8] J. C. Butcher. Coefficients for the study of Runge-Kutta integration processes. *Journal of the Australian Mathematical Society*, 3:185–201, 5 1963.
- [9] John R Cary. Lie transform perturbation theory for Hamiltonian systems. *Physics Reports*, 79(2):129–159, 1981.
- [10] Chetvorno. Diagram of simple gravity pendulum, an ideal model of a pendulum. it consists of a massive bob suspended by a weightless rod from a frictionless pivot, without air friction. when given an initial impulse, it oscillates at constant amplitude, forever. https://commons.wikimedia.org/wiki/File:Simple_gravity_pendulum.svg, Dec 2008.
- [11] Samuel Daniel Conte and Carl W De Boor. *Elementary numerical analysis: an algorithmic approach.* McGraw-Hill Higher Education, 1980.
- [12] E.D Courant and H.S Snyder. Theory of the alternating-gradient synchrotron. *Annals of Physics*, 3(1):1 – 48, 1958.
- [13] Etienne Forest, John Irwin, and M Berz. Normal form methods for complicated periodic systems. *Part. Accel.*, 24:91–107, 1989.
- [14] David Goldberg. What every computer scientist should know about floating-point arithmetic. *ACM Comput. Surv.*, 23(1):5–48, March 1991.
- [15] E. Hairer and Gerhard Wanner. *Solving ordinary differential equations II.* Springer-Verlag, 1991.

- [16] Georg H Hoffstaetter and Martin Berz. Rigorous lower bounds on the survival time in particle accelerators. *Particle Accelerators*, 54(2):193–202, 1996.
- [17] Kyoko Makino and Martin Berz. COSY INFINITY version 8. *Nuclear Instruments and Methods in Physics Research Section A: Accelerators, Spectrometers, Detectors and Associated Equipment*, 427(1):338–343, 1999.
- [18] Kyoko Makino and Martin Berz. COSY INFINITY version 9. *Nuclear Instruments and Methods in Physics Research Section A: Accelerators, Spectrometers, Detectors and Associated Equipment*, 558(1):346 – 350, 2006. Proceedings of the 8th International Computational Accelerator Physics Conference ICAP 2004 8th International Computational Accelerator Physics Conference.
- [19] John H Mathews and Kurtis D Fink. *Numerical methods using MATLAB*, volume 31. Prentice hall Upper Saddle River, NJ, 1999.
- [20] Robert A Nelson and MG Olsson. The pendulum-rich physics from a simple system. *Am. J. Phys*, 54(2):112–121, 1986.
- [21] Institute of Electrical and Electronics Engineers. *IEEE Standard for Binary Floating-point Arithmetic*. IEEE, 1985.
- [22] GA Sardanashvily. *HANDBOOK OF INTEGRABLE HAMILTONIAN SYSTEMS*. URSS, 2015.